ROLE FOR LIPIDS IN THE CELLULAR TRANSMISSION OF α-SYNUCLEIN

APPROVED BY SUPERVISORY COMMITTEE

Philip J. Thomas, Ph.D.

Peter A. Michaely, Ph.D.

Russell A. Debose-Boyd, Ph.D.

Joseph P. Albanesi, Ph.D.

Nature is the source of all true knowledge. She has her own logic, her own laws, she has no effect without cause nor invention without necessity.

Leonardo da Vinci

For my Family

ROLE FOR LIPIDS IN THE CELLULAR TRANSMISSION OF α-SYNUCLEIN

By

Yair Peres

DISSERTATION

Presented to the Faculty of the Graduate School of Biomedical Sciences

The University of Texas Southwestern Medical Center at Dallas

In Partial Fulfillment of the Requirements

For the Degree of

DOCTOR OF PHILOSOPHY

The University of Texas Southwestern Medical Center at Dallas

Dallas, Texas

August, 2015

ROLE FOR LIPIDS IN THE CELLULAR TRANSMISSION OF α-SYNUCLEIN

YAIR PERES

The University of Texas Southwestern Medical Center at Dallas, 2015

Supervising Professor: Philip J. Thomas Ph.D.

The presynaptic protein α-Synuclein (α-Syn) abnormally aggregates in the brains of Parkinson's Disease patients. Evidence suggest a transcellular transfer of an oligomeric form of the protein (seed) in a prion-like fashion. The mechanism underlying cell entry is unclear, but studies have implicated the cell surface glycan HSPG followed by macropinocytosis, as a possible uptake route. Secretion and uptake of aggregated α-Syn was reported to be associated with lipid vesicles in cells. Monomeric α-Syn was found to tubulate membranes *in-vitro*. This work aims to study the significance of membrane association and tubulation by α-Syn to its effect on uptake by cells.

Uptake of lipid-associated α-Syn seeds was significantly more efficient than lipid-free uptake. Furthermore, seeds in the presence of monomers and lipids, which formed tubules *in-vitro,* were more readily internalized than seeds and lipids in the absence of monomers. Lipid associated α-Syn was internalized by cells in an HSPG dependent manner as evident from competitive inhibition and enzymatic digestion experiments. Tubule associated seeds may constitute an efficient mechanism of pathological propagation of synucleinopathies. This mechanism should be considered in any therapeutic approach targeting the inhibition of α-Syn intercellular transfer.

TABLE OF CONTENTS

PRIOR PUBLICATIONS

Zohar Tiran, Anat Oren, Chen Hermesh, Galit Rotman, Zurit Levine, Hagit Amitai, Tal Handelsman, Merav Beiman, Aviva Chen, Dalit Landesman-Milo, Liat Dassa, Yair Peres, Cynthia Koifman, Sarit Glezer, Rinat Vidal-Finkelstein, Kobi Bahat, Tania Pergam, Cylia Israel, Judith Horev, Ilan Tsarfaty and Michal Ayalon-Soffer, A novel recombinant soluble splice variant of Met is a potent antagonist of the hepatocyte growth factor/scatter factor-Met pathway. Clinical Cancer Research 14, 4612-4621 (2008)

LISIT OF FIGURES

LIST OF TABLES

LIST OF APPENDICES

APPENDIX A: MATERIALS AND METHODS

LIST OF ABBREVIATIONS

α-Syn - α-Synuclein

PD - Parkinson's Disease

AD - Alzheimer's Disease

ALS - Amyotrophic Lateral Sclerosis

DLB - Dementia with Lewy Bodies

MSA - Mutliple System Atrophy

LB - Lewy Bodies

LN- Lewy Neurites

SN - Substantia Nigra

CNS - Central Nervous System

NAC- Non A-β Component

SCF- Cerebrospinal Fluid

LRRK2 - Leucine Rich Repeat Kinase2

SNARE - Soluble NSF Attachment Protein Receptor

GlcNAc - N-Acetylglucosamine

GlcA - D-glucuronic Acid

HS - Heparan Sulfate

HSPG - Heparan Sulfate Proteoglycan

Hprn - Heparin

Hpnase - Heparinase III

TAT - Trans-Activator of Transcription

MVB- Multivesicular Bodies

ESCRT - Endosomal Sorting Complexes Required for Transport

PLD - Phospholipase D

PG - Phosphatidyl glycerol

POPG - 1-palmitoyl-2-oleoyl-sn-glycero-3-phospho-(1'-rac-glycerol)

PA - Phosphatidic Acid

PC - Phosphatidylcholine

FL - Full Length

MLV - Multilamellar Vesicles

SUV - Small Unilamellar Vesicles

GUV - Giant Unilamellar Vesicles

AH - Amphipathic Helix

BAR - Bin/Amphiphysin/Rvs

NMR - Nuclear Magnetic Resonance

CD - Circular Dichroism

EM - Electron Microscopy

ThT/S - Thioflavin T, Thioflavin

CHAPTER ONE: GENERAL INTRODUCTION

Synucleinopathies, neurodegenerative diseases involving the abnormal accumulation of α-Synuclein (α-Syn), are to date, incurable diseases. Parkinson's Disease (PD), the most prevalent among these diseases, is characterized by a late age onset of progressive neuronal cell death spanning over a decade. This, practically chronic disease, entails an enormous economic burden on society. These costs are projected to grow substantially over the next few decades as the size of the elderly population grows (Kowal et al., 2013). The mental and emotional cost on patients, families and friends cannot be quantified.

The past few decades have seen a major progress in understanding the biochemical pathways that play are role in the development of PD. Gene mutations, neurotoxins and postmortem analyses brought a general consensus about the mechanisms of cytotoxicity that contribute to neuronal loss in PD. Aging is still considered the single most important risk factor. Questions remain as to what is the sequence of events leading to cell death and to what extent are they similar between parts of the central nervous system (CNS) and across individuals. An emerging model suggests a non-cell autonomous propagation of Lewy pathology by transcellular mechanisms with seeding and subsequent permissive templating, in a prion-like fashion (Angot et al., 2010; Brundin et al., 2010). If proven valid, this model can have profound implications on current and future design of therapies. Cell therapy may prove inefficient, while attention should be given to treatments designed to block transmission of the pathogenic protein, increase its cellular and extracellular clearance and inhibit protein aggregation. Research can help shed light on the properties of α-Syn transmission as a prion-like factor. The study described here suggests a yet unappreciated mechanism potentially contributing the cellular transmission of α-Syn.

Chapter two of this document provides an overview of synucleinopathies and α-Syn, a central protein to the understanding of this group of diseases. It further focuses on the current knowledge of the pathological and physiological function of this enigmatic protein. Chapter three describes the prion hypothesis, an emerging theory aiming to explain the propagation of α-Syn pathology throughout the course of the disease. It provides an extensive overview of published evidence supporting this provocative theory and suggested mechanisms implicated in it. Membrane binding and bending are central features of α-Syn important to its physiological and possibly pathological function. Chapter four provides a general description of mechanisms and function of membrane bending in the cell and highlights on the α-Syn membrane curving mechanism. Chapter Five describes experiments performed towards defining a role for membrane binding and tubule formation by α-Syn in its cellular uptake. Chapter six describes preliminary data garnered to expand on the role of lipid tubules in the proposed α-Syn uptake model. Chapter seven proposes necessary future experiments which, upon completion, will reinforce the proposed model and investigate it in more detail.

CHAPTER TWO: SYNUCLEINOPATHIES AND α-SYNUCLEIN

Synucleinopathies

The British physician James Parkinson first described, in 1817, six individuals with “paralysis agitans", a disease which will later bear his name (Parkinson, 1817). In 1912 the German neurologist Friedrich Lewy observed a key neuropathological lesion later coined "Lewy Body" (LB) or “Lewy Neurite” (LN), corresponding to their cellular location (FH., 1912). Although reaching its 200 anniversary, and despite remarkable research progress, many aspects of the disease remain vague. The study of the etiology of PD was hampered by the genetic and biochemical complexity of the disease. Furthermore, parkinsonism represents a wide spectrum of diseases which appear clinically similar and an autopsy is required to distinguish between the different entities. PD is the second most common neurodegenerative disease, affecting approximately 1% of the population over age 65 and over 3% of those age 85 (de Lau et al., 2014). PD is typically slowly progressing, with 15 years mean span from recognition to death. In the course of the disease loss of dopaminergic neurons in the substantia-nigra (SN) pars compacta leads to dysfunction of the basal ganglia which is responsible for coordination of movement. The typical motor symptoms of PD, which include resting tremor, bradykinesia (slowed movements), rigidity (increased muscular tone), postural instability, and gait impairment are attributed to dopaminergic cell loss (Fahn, 2003). Indeed, these symptoms are alleviated by dopamine replacement which constitutes the main therapeutic approach for treatment since the 1960s. Deep brain stimulations of the subthalamic nucleus is applied at later disease stages. However, current treatments affect only disease symptoms and to date, no treatment is effective in stopping or delaying the neurodegeneration process (Fahn, 2003). At advanced stages of the disease dementia and neuropsychiatric symptoms arise which might be associated with spread of

the pathology to areas beyond the midbrain (Fahn, 2003). When clinical symptoms are apparent the majority of dopaminergic neurons are lost and dopamine levels are significantly decreased. This underlines the need for tools for early diagnosis (Fahn, 2003).

No single cause for PD was found and the disease probably represents a sequential and/or a convergence of genetic, cellular and environmental factors. These affect mitochondrial dysfunction and increased oxydative stress, and impairment of protein degradation resulting in protein aggregation (Obeso et al., 2010). Exposure to environmental toxins, such paraquat and rotenone, have been correlated with disease occurrence and cigarette smoking and caffeine intake also seem to affect (Shulman et al., 2011). The toxins were found to cause neuronal death in animals but do not recapitulate all the pathological features of the disease (Maries et al., 2003). Several genes have been associated with PD. Autosomal dominant mutations in Leucine Rich Repeat Kinase 2 (LRRK2) affect its kinase activity. LRRK2 has been suggested to impair autophagy leading to α-Syn accumulation, but the mechanisms associating this protein with PD are not clear (Shulman et al., 2011). The parkin protein has a ubiquitin E3-ligase activity. It ubiquitinates targets for ubiquitin-proteasome-system-mediated degradation, thus contributing to protein clearance. Cells from patients with parkin mutations exhibit decreased mitochondrial complex I activity and ATP production (Mortiboys et al., 2008). Mutations in the lysosomal ATPase ATP132A2 cause Kufor-Rakeb disease, characterized by parkinsonism and dementia (Pan et al., 2008). Another lysosoml enzyme, GBA, is associated with Gaucher's Disease. This enzyme is involved in lipid metabolism and heterozygous mutations in GBA gene could lead to lysosomal dysfunction (Mazzulli et al., 2011).

α-Syn is associated with PD both genetically and pathologically. Linkage analysis of families with an autosomal dominant inherited PD have identified three point mutations: A30P, E46K and A53T as well as gene duplication and triplication (Kruger et al., 1998; Spillantini et al., 1997). Patients carrying these mutations and multiplications suffer early age onset of the disease, a relatively rapid progression of LB pathology and dopaminergic cell loss in the SN (Kruger et al., 1998; Spillantini et al., 1997). Pathological analysis of tissue sections from idiopathic PD and from Dementia with Lewy Body (DLB) found that α-Syn is a major component of these intracellular inclusions (Figure 2-1) (Spillantini et al., 1997). α-Syn is a cytosolic protein concentrated in pre-synaptic terminals (Maroteaux et al., 1988). It is a member of a gene family that also includes β-Synuclein and γ-Synuclein. All family members share sequence similarity. α-Syn is 140 amino acid long protein sequence with seven imperfect repeats of 11 amino acids long, containing the sequence KXKEGV at the N-terminus and an acidic C-terminus. A central hydrophobic portion, between amino acids 61-95, termed the non A-β component (NAC) is important for aggregation of the protein (Figure 2-2) (Cookson, 2005). The acidic C-terminus tends to decrease the aggregation propensity of the protein. This was demonstrated by *in-vitro* aggregation studies of truncated α-Syn, missing portions of the C-tail (Li et al., 2005; Ritchie and Thomas, 2012). Structurally, α-Syn adopts multiple conformations. Monomeric α-Syn lacks structure in solution and is referred to as natively unfolded. Binding to negatively charged phospholipids increases the α-helical content of the protein, whereas aggregation increases formation of pleated beta sheet (Cookson, 2005).

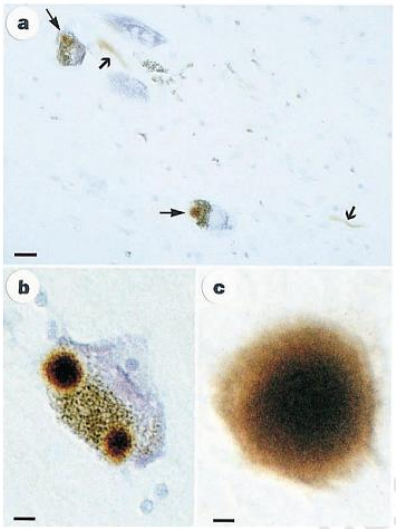

Figure 2-1. SN from patients with Parkinson's Disease stained for α-Syn. A) Two pigmented nerve cells, each containing an α-Syn-positive LB (thin arrows). LN (thick arrows). Scale bar, 20 mm. B) A pigmented nerve cell with two α-Syn-positive LB. Scale bar, 8 mm. C) α-Syn positive, extracellular LB. Scale bar, 4 mm.
From: Spillantini et al., 1997. Reprinted by permission from Nature Publishing.

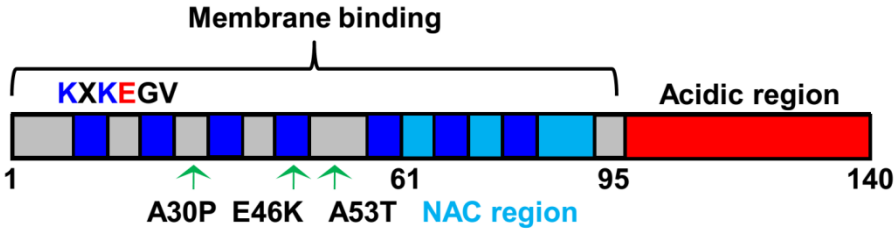

Figure 2-2. Main characteristics of sequence domains of α-Syn. Include a membrane binding, amphipathic region with seven imperfect 11 amino acid repeats. A central hydrophobic region required for aggregation termed "Non A-β Component" (NAC) and a highly acidic C-terminal region which inhibits aggregation. The three most studied PD causing mutations occur in the membrane binding region.
From: Pfefferkorn et al., 2012. Reprinted by permission from Elsevier.

PD belongs to a class of parkinsonian disorders, including progressive supranuclear palsy, corticobasal degeneration, and dementia pugilistica, all which share the clinical motor features of PD. Pathologically, PD is distinguished from these other disorders by the presence of

α-Syn inclusion of LB (Figure 2-1), which is different from the neurofibrillay tangles composed of the microtubule-binding protein Tau found in other parkinsonian disorders (Auluck et al., 2010). α -Syn accumulation is associated with a number of neurological diseases, collectively termed synucleinopathies; including DLB and multiple system atrophy (MSA). DLB patients suffer motor symptoms in addition to memory loss. Pathologically widespread Lewy pathology, staining similar to that of PD, appear in the cytoplasm of neurons throughout the brain stem area common in PD, in addition to cortical brain areas (Spillantini et al., 1998). MSA patients present with parkinsonism dementia, and/or ataxia. Pathologically MSA is distinct from PD and DLB in that α-Syn accumulation occurs predominantly within the cytoplasm of glial cells, but are also observed in the cytoplam of neurons. The inclusions are mostly immunoreactive for α-Syn filaments, but contain additional proteins (Grazia Spillantini et al., 1998). Thus, clinically and pathologically, LB disorders constitute a spectrum, with classical PD presenting major motor symptoms, minor cognitive impairment and minimal cortical pathology is at one end, and severe dementia, with or without motor symptoms and with a severe LB pathology, at the other end. LB contain other components, such as ubiquitin, cytoskeletal proteins and lipids (Cookson, 2005). This may suggest a role for these components as co-precipitants in the aggregation of α-Syn. However, α-Syn alone readily aggregates *in-vitro*, suggesting that no additional factors are required for the formation of amyloid fibrils. A twelve amino acid stretch between positions 71 and 82 is necessary and sufficient for aggregation *in-vitro* (Giasson et al., 2001). More recently, various post translational modifications have been detected in LB. These include phosphorylation, nitration, ubiquitination and truncation of the protein (Baba et al., 1998; Fujiwara et al., 2002; Giasson et al., 2000; Tofaris et al., 2003). Truncations of both C and N-terminal portions of α-Syn have been detected in patient samples (Lewis et al., 2010b; Liu et al.,

2003). As mentioned above, C-terminal truncations accelerate amyloid fibril formation *in-vitro*. Transgenic mice expressing C-terminally truncated α-Syn exhibited motor deficits and neuronal loss (Daher et al., 2009; Tofaris et al., 2006; Wakamatsu et al.). α-Syn protein degradation has been suggested to occur by either autophagy and the proteasome (Cuervo et al., 2004; Liu et al., 2003; Webb et al., 2003). Furthermore, α-Syn may be a substrate of cytoplasmic proteases (Miners et al., 2014). Thus, multiple mechanisms may be responsible for production of truncated variants in the cell.

It remains unclear if any of the α-Syn modifications elicit neurotoxicity in the context of disease, or whether they are merely a consequence of the toxic process.

Molecular Species Responsible for Toxicity

A key problem in the field is the lack of knowledge with respect to the definition of the structural properties that make α-Syn toxic and the molecular mechanism whereby toxicity is exerted. Most mechanisms ascribe neurotoxicity to a toxic gain-of-function associated with a pathological form of the protein. α-Syn tends to aggregate and the dynamic nature of this molecular form makes it difficult to study. The dynamic nature of this molecular form makes it difficult to study. Various conformations of α-Syn have been associated with synucleinopathies pathogenesis (Figure 2-3). Amyloid fibrils are a common constituent of LB (Spillantini et al., 1997). Fibrils are less dynamic and more stable structures thus may represent an attempt by cellular mechanisms to isolate and convert oligomers and/or protofibrils into a less toxic conformation. Supporting a role for oligomer toxicity, transgenic α-Syn flies display inverse correlation between the number of inclusion formed and toxicity (Chen and Feany, 2005). Rats expressing oligomers, rather than fibril forming mutants, displayed loss of dopaminergic neurons in the SN (Winner et al., 2011). Conformers, at a range of 2-150mers, that are SDS resistant have

been detected and isolated from diseased human brains and from those of transgenic animal models showing α-Syn pathology (Baba et al., 1998; Cremades et al., 2012; Danzer et al., 2007; Kahle et al., 2000; Kahle et al., 2001; Lee et al., 2002; Tsigelny et al., 2008). Oligomeric spheres (2–6 nm in diameter) have been observed *in-vivo* and exhibited abnormal calcium current and neuronal degeneration in primary cortical neuron culture (Danzer et al., 2007). Of note is that most *in-vivo* evidence represent an indirect detection of oligomers based on native and/or denaturing gel electrophoresis techniques.

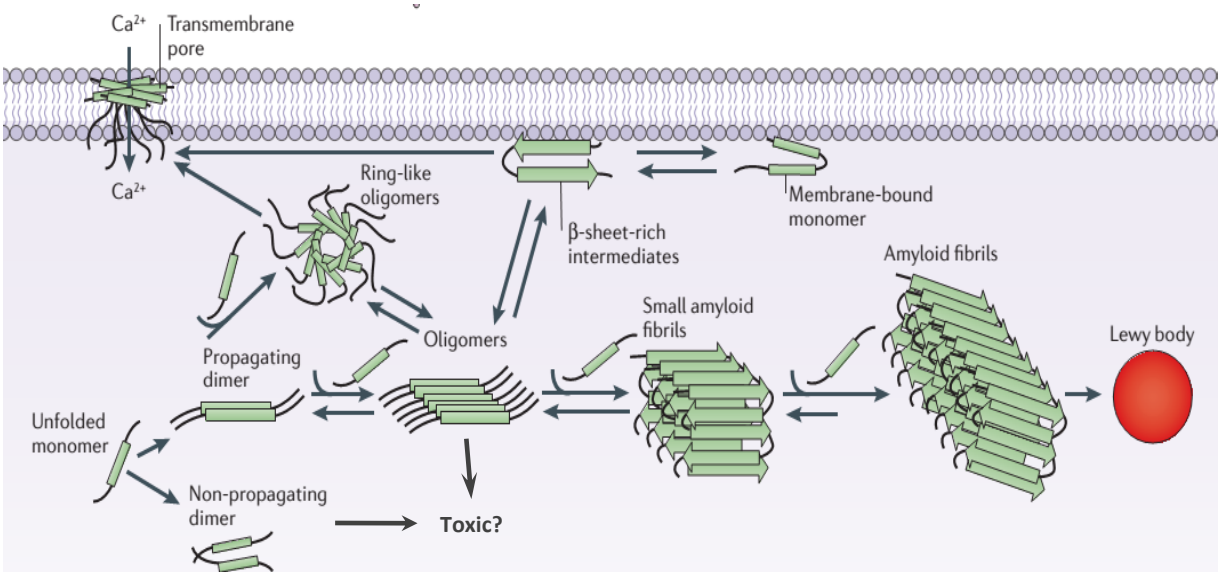

Figure 2-3. Propagating and/or toxic molecular forms of α-Syn. α-Syn aggregation can take place either in the cytoplasm or by association with membranes. Unfolded monomers slowly assemble into an oligomeric seed which may propagate further aggregation into an amyloid fibril and deposited into LB, or form potentially toxic annular structures. Toxicity may also arise from soluble oligomers on or off-amyloid aggregation pathway *via* interaction with membranes or by other mechanisms
From: Lashuel et al., 2013. Reprinted by permission from Nature Publishing.

In-vitro, various oligomeric species have been produced, which precede fibril formation. Oligomeric structures include spherical, chain-like and annular oligomers, which exist in equilibrium with monomers with slow conversion to fibrils (Figure 2-3) (Horvath et al., 2012).

The PD-associated mutations in the α-Syn protein sequence are thought to decrease intra-molecular interactions, expose more hydrophobic portions of the protein and increase inter-molecular interactions thereby enhancing oligomer formation (Auluck et al., 2010). Two of the mutants (E46K and A53T) accelerate both oligomerization and fibrillization phases *in-vitro* (Conway et al., 2000; Yonetani et al., 2009). Interestingly, A30P accelerate oligomerization but inhibit fibrillization *in-vitro*, while sections from A30P PD patients display extensive fibril containing LB pathology (Seidel et al., 2010; Yonetani et al., 2009). Conditions such as increased protein concentrations, increased temperature, addition of specific metal ions (Fe^{2+}, Cu^{2+} and Zn^{2+}), nitration or dopamine may be applied *in-vitro* to induce oligomer assembly (Conway et al., 2001; Hashimoto et al., 1999; Souza et al., 2000; Uversky et al., 2001). Resulting oligomers have various sizes and morphologies and some proceed to form amyloid fibrils. The relationships and the transition between these structures are not well understood and some (specifically some ring-like structures) are suggested to be off-pathway to amyloid formation (Figure 2-3). Post-translational modifications detected in LB including phosphorylation at serine residues 87 and 129, oxidative stress and truncation may confer toxicity to oligomers (Hashimoto et al., 1999; Luk et al., 2012c; Souza et al., 2000; Wakamatsu et al.).

Interaction with membranes *in-vitro* and in cells modify membrane permeability and increase calcium influx (Melachroinou et al., 2013; Volles and Lansbury, 2002). Furthermore, toxicity may be promoted by the interaction of α-Syn conformers with cellular organelles, including mitochondrial damage, lysosomal leakage and disruption of microtubules (Alim et al., 2004; Hashimoto et al., 2004; Hsu et al., 2000). All are malfunctioning cellular mechanisms observed in PD models (Maries et al., 2003; Shulman et al., 2011). Neuroinflammation is another culprit associated with PD (Appel, 2012). α-Syn has been has been suggested to induce

inclusions formation in astrocytes and to activate astrocytes and microglia cells eliciting an inflammatory response mediated through TLR receptor (Halliday and Stevens, 2011; Lee et al., 2010; Reynolds et al., 2008; Zhang et al., 2005).

It is likely that the aggregation process itself induces, or is associated with, toxicity *in-vivo*. Fibrillization promoting mutants expressed in transgenic animals enhance neuronal death and induce motor deficits (da Silveira et al., 2009; Gorbatyuk et al., 2008; Taschenberger et al., 2012). Moreover, fibrillar seeds that accelerate oligomerization *in-vitro*, were injected to wild type (WT) animal brains resulting in propagation of Lewy-like pathology motor deficits and cell death in the SN (Luk et al., 2012a).

While oligomers and aggregation dependent toxicity are being well investigated, other possible mechanisms, including an aggregation independent interaction with lipid membranes or other cellular factors leading to disruption of cellular processes may be possible (Lashuel et al., 2013).

Identification of the molecular nature of the primal pathologic seed, the biochemistry of its cytotoxicity and the pathways leading to its propagation are central to understanding how PD and other synucleinopathies.

Function of α-Syn

The role α-Syn play in pathology is considered a toxic gain of function of the protein and its physiological function remains unclear. α-Syn knockout mice are viable with intact synaptic structure and brain morphology (Abeliovich et al., 2000). Over-expression in transgenic animals present an inherent problem for physiological function studies, since high levels of the protein may lead to aggregation as evident from patients with gene loci multiplications (Chartier-Harlin et al.). α-Syn is widely expressed in the brain, accounting to 1% of the cytosolic soluble protein

fraction (Iwai et al.). It is localized to pre-synaptic terminals, where a portion of it is membrane bound (Maroteaux et al., 1988). This area has high concentrations of synaptic vesicles, which are among the smallest vesicles in the cell. As α-Syn preferentially binds highly curved membranes it is possible that this preference, determines its localization to this vesicle rich area of the cell (Iwai et al.). Membrane association and pre-synaptic location in the cell suggests a role for α-Syn in synaptic transmission (Maroteaux et al., 1988). Knock-out mice exhibit altered dopamine release including faster recovery of dopamine release after stimulation and reduction of dopamine in storage pool (Abeliovich et al., 2000; Yavich et al., 2004). Decreased α-Syn expression by RNA knockdown of α-Syn in hippocampal cultures caused a 50% reduction in the synaptic vesicle pool size (Murphy et al., 2000). In contrast, transgenic rodents and cultured neurons over-expressing α-Syn, at levels that do not induce inclusion formation or measurable toxicity, exhibit decreased synaptic vesicle exocytosis but reduces synaptic vesicle recycling pool size (Nemani et al.). This suggests that α-Syn functions to regulate the transmitter vesicle pool at the presynaptic membrane. Recent studies from the Sudhof lab suggested α-Syn binds as a multimer to synaptic membranes and to synaptobrevin-2 thereby promoting SNARE-complex assembly *in-vitro* and *in-vivo* (Burré et al., 2014; Burré et al., 2010). The authors proposed a model where binding of both vesicles and synaptobrevin-2 by α-Syn promotes clustering of vesicles docked to the presynaptic plasma membrane ready for release (Diao et al., 2013). However others reported that α-Syn inhibits vesicle fusion directly through membrane binding and is independent of SNARE binding (DeWitt and Rhoades, 2013).

CHAPTER THREE: TRANSCELLULAR TRANSFER OF PROTEIN SEEDS

The Prion Hypothesis

Prion proteins can take an amyloid conformation, a cross beta-sheet rich structure, formed by oligomerization accompanied by structural conversion of the joining monomer (Brundin et al., 2010). Amyloid fibril formation is a three phase process, beginning in long nucleation phase (lag phase), followed by a rapid fibril growth phase and ending in a steady-state phase (Figure 3-1) (Brundin et al., 2010). During the lag phase a stable oligomer is formed from a small number of monomers. The lag phase can be eliminated by addition of a preformed seed. Once formed this seed can further elongate by addition of monomeric subunits. This seeding is the molecular basis of prion infectivity (Brundin et al., 2010). It is commonly found among proteins playing a key pathogenic role in various neurodegenerative diseases. On the cellular level a protheopatic protein seed is transmitted between neurons exiting its origin cell and entering a neighboring cell where it may template the conversion of host protein from its native conformation into a misfolded conformation, thereby seeding its aggregation into an amyloid fibril (Figure 3-2) (Angot et al., 2010; Guo and Lee, 2014). Mounting evidence support a prion-like propagation model of PD pathology throughout the CNS.

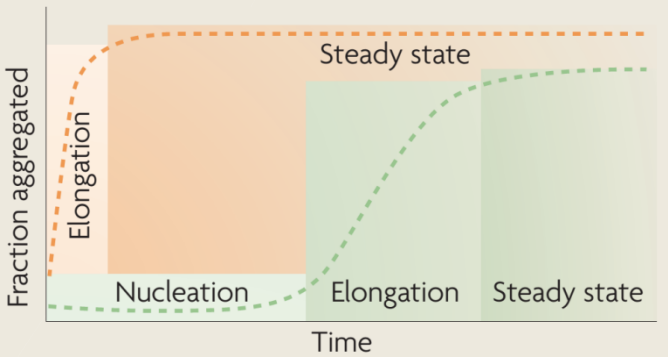

Figure 3-1. The typical in-vitro fibrillization process of an amyloid. Begins (green) in a nucleation step, where stable oligomer formation is thermodynamically unfavorable. Once formed the stable oligomers elongate in an exponential manner until equilibrium with soluble monomers is achieved. Nucleation step can be abolished (red) by addition of preformed seeds either externally or by sheering of the fibrils.
From: Brundin et al., 2010. Reprinted by permission from Nature Publishing.

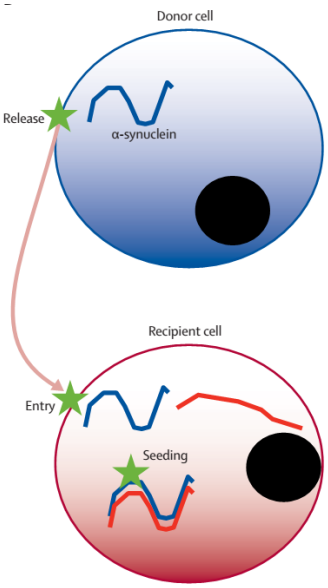

Figure 3-2. Propagation according to the prion hypothesis. A seed is released into the extracellular space and is taken-up by a neighboring cell, where it may convert host cell protein into the "diseased" form and aggregate to form an amyloid fibril
From: Angot et al., 2010. Reprinted by permission from Nature Publishing.

Braak et al. proposed an orderly appearance of Lewy pathology, along an interconnected network of neurons (Figure 3-3) (Braak et al., 2003). According to the Braak staging, pathology first appears in lower brainstem nuclei, olfactory nuclei, and peripheral neurons (stages 1 and 2). Next, the midbrain (including the SN) is affected (stages 3 and 4) . Last, pathology appears in the neocortical regions (stages 5 and 6). The stages of pathology are correlated with clinical disease symptoms. Thus, pathology begins several years before the SN is affected, which leads to the development of motor symptoms, while the last stages are correlated with dementia and hallucinations (Braak et al., 2003).

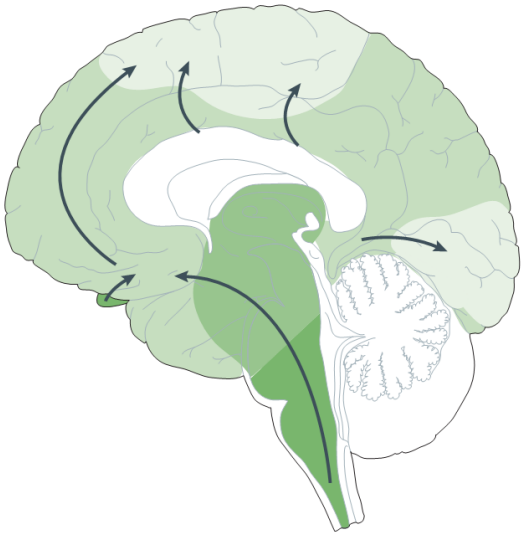

Figure 3-3. The Braak staging of neuropathological changes in PD. LB and LN are suggested to first appear in the dorsal motor nucleus of the vagal nerve in the brainstem and anterior olfactory structures (darkest green), and then to spread stereotypically to finally occupy large parts of the brain. Darker shading represent areas that are affected earlier.
From: Brundin et al., 2010. Reprinted by permission from Nature Publishing.

Several lines of evidence support a role for cell to cell transfer of a pathogenic form of the protein leading to propagation of pathology (Figure 3-2) (Kordower et al., 2008a; Kordower et al., 2008b; Li et al., 2008). First, although α-Syn is a cytoplasmic protein, lacking signal sequence, both monomeric and oligomeric forms are found in culture media and in human plasma and cerebrospinal fluids (CSF) of healthy and diseased individuals (Borghi et al., 2000; El-Agnaf et al., 2003; El-Agnaf et al., 2006; Emmanouilidou et al., 2011). This suggests secretion of the protein to the extracellular space under both physiological and pathological conditions. Evidence for secretion are further supported by cell culture studies reporting release of small amounts of α-Syn proteins to the culture media in the absence of membrane damage (Lee et al., 2014; Lee et al., 2005a). Second, patients that received transplanted fetal mesencephalic dopaminergic neurons eventually develop α-Syn positively stained LB in the grafted neurons, which are similar in characteristics to those of the patients' neurons (Kordower et al., 2008a; Kordower et al., 2008b; Li et al., 2008). Third, α-Syn protein seeds, produced from recombinant α-Syn, used in different models produce a transmissible phenotype (Danzer et al., 2009; Desplats et al., 2009; Lee et al., 2008; Luk et al., 2012a; Yonetani et al., 2009). In cell

culture models, using cell lines or primary neurons, seeds introduced to the growth media externally are later detected in the cytoplasm where it induces the formation of insoluble α-Syn aggregate inclusions. The inclusions stain by thioflavin S, indicating formation of amyloid fibrils, a key characteristics of LB, and are immunoreactive for ubiquitin. A donor-acceptor cell-line model, where cells over-expressing tagged α-Syn are co-cultured with non-transfected cells exhibits similar inclusion formation, on the acceptor side, demonstrating both cell release and uptake (Danzer et al., 2009; Desplats et al., 2009; Freundt et al., 2012; Hansen et al., 2011; Holmes et al., 2013; Lee et al., 2008; Luk et al., 2009; Volpicelli-Daley et al., 2011). In a rat model mimicking the host to graft phenomena observed in PD patients, animals over-expressing human α-Syn were grafted with dopaminergic neurons. The authors reported that the grafted cells developed inclusions composed of the transmitted human α-Syn core surrounded by rat α-Syn, supporting a role α-Syn transmission and seeding (Angot et al., 2012; Desplats et al., 2009; Hansen et al., 2011). Studies attempting to characterize the pathogenic species used healthy animals injected with brain homogenates prepared from human PD patients or symptomatic animals. The recipient animals develop LB-like inclusions progressing in a spatiotemporal fashion from the injection sites to other interconnected areas of the CNS, in addition to loss of dopaminergic neurons and motor deficits exhibited by the animals, a few months post injection (Luk et al., 2012a; Luk et al., 2012b). Further, WT or transgenic rodents injected with recombinant synthetic α-Syn sonicated fibrils develop similar patterns indicating that α-Syn protein alone is sufficient for inducing pathology (Luk et al., 2012a; Masuda-Suzukake et al., 2013; Sacino et al., 2014). Notably, α-Syn null mice did not develop pathology when injected with homogenates or seeds, demonstrating that the presence of host α-Syn is important for the development of pathology *via* seeding (Luk et al., 2012a; Mougenot et al., 2012).

Mechanisms Implicated in the Transmission of α-Syn

Although the cell-cell transmission of α-Syn has been well described, the mechanisms that underlay cell entry or exit remain unclear. Several mechanisms have been suggested. Supporting a role for the endocytic system as an entry route, in cell line model studies, the expression of dominant negative dynamin or Rab5A, or treatment with pharmacological endocytosis inhibitors, inhibit the internalization of α-Syn seeds (Desplats et al., 2009; Hansen et al., 2011; Lee et al., 2008; Sung et al., 2001). In a rat model, α-Syn transferred into grafted neurons co-localized with Early Endosome Antigen-1, a marker for early endosomes (Angot et al., 2012). Secretion of α-Syn was termed "unconventional exocytosis" as it was insensitive to brefeldin A, a blocker of Endoplasmic Reticulum-Golgi transport, in a neuronal cells line (Lee et al., 2005a). Factors that regulate autophagosome trafficking and pool size affected secretion of monomeric and aggregated α-Syn suggesting exophagy as a possible route of exit (Ejlerskov et al., 2013).

Proteoglycans have recently been demonstrated to function as receptors for internalization of amyloid seeds, including α-Syn (Holmes et al., 2013). Proteoglycans are a diverse family of macromolecules involved in multiple cellular processes and are found in multiple locations inside the cell, on the cell surface and in the extracellular matrix (Sarrazin et al., 2011b). They are classified based on location and molecular composition. The basic composition of these glycoproteins include linear sulfated polysaccharides, covalently attached to a core protein (Sarrazin et al., 2011b). One common group of polysacharide chains is heparan sulfate (HS), composed of a long polymer of repeating N-acetyl glucosamine (GlcNAc)-D-glucuronic acid (GlcA) disaccharide units, which may appear a single or multiple times on Heparan Sulfate Proteoglycan (HSPG) (van Horssen et al., 2003). HSPG are polyanionic, possessing exceptionally strong negative charge, due to their high level of sulfation, and may be found in

several cellular compartments, including the cell surface and endosomes (Esko JD, 2009). Sulfation patterns and other modifications are determined by the respective expressing cell type and dictate ligand binding. Structurally, sulfated residues are clustered in domains separated by non-sulfated regions (Esko JD, 2009). Heparin-binding ligands are diverse and include growth factors, cytokines, chemokines, enzymes, enzyme inhibitors, and extracellular matrix proteins (Varki A, 2009). Thus, there is no recognizable binding sequence or fold. Instead, HSPG binding sites occur as shallow grooves lined with positively charged amino acids or on the surface of proteins (Sarrazin et al., 2011a). Binding energy is mostly contributed by electrostatic interactions and the dissociation constants range at the millimolar to nanomolar values. The binding and activation mechanism may be diverse, as some low affinity ligands achieve high binding avidity through dimerization or by clustering (Sarrazin et al., 2011a).

Several lines of evidence implicate HSPG with neurodegenerative diseases. HSPG induce the conversion of α-Syn, tau and A-β from soluble into insoluble fibrillar conformation and may protect it against proteolytic degradation, therefore it may promote its deposition in cells (Liu et al., 2005; Papy-Garcia et al., 2011; van Horssen et al., 2003). It can bind to many types of amyloids and immunohistological studies reported HSPG is detected with various depositions, including tangles associated with progressive supranuclear palsy, Pick's disease, and other tauopathies (Papy-Garcia et al., 2011; van Horssen et al., 2003). Association with LB was not observed and the authors concluded that aggregation and deposition of α-Syn may occur independent of HSPG (van Horssen et al., 2004). The extracellular proteoglycan agrin was detected in LB from SN sections of PD brain (Liu et al., 2005). HSPG functions as an endocytic receptor for the uptake of macromolecules and undergo both constitutive and ligand induced endocytosis (Sarrazin et al., 2011a). The endocytic mechanism is unclear as evidence indicate

clathrin, caveolin and dynamin dependent and independent internalization, depending on the model system (Christianson and Belting, 2014; Sarrazin et al., 2011a). It also appears that lipid rafts play a role in the sorting of different HSPG receptors as well as cargo (Christianson and Belting, 2014; Sarrazin et al., 2011b). Following ligand uptake, some internalized HSPG were reported to be recycled, but most are degraded in lysosomes (Bernfield et al., 1999; Sarrazin et al., 2011a; Zimmermann et al., 2005). Pathogens exploit the promiscuity of HSPG in ligand binding to invade cells. Studies show that both viruses and bacteria invade cells in an HSPG dependent manner. Binding and cell uptake of HIV-transactivator of transcription (TAT) peptide (Tyagi et al., 2001), *Herpes simplex virus* (Shieh et al., 1992; Shukla et al., 1999) and *Neisseria gonorrhoeae* (Dehio et al., 1998) were inhibited by biochemical or genetic elimination of HSPG expression on the host cell surface. Following internalization TAT peptide is localized to endocytic vesicles (Kaplan et al., 2005). TAT peptide is rich in basic amino acid and it was demonstrated that polyarginine peptides display a membrane penetrating activity (Futaki et al., 2001). Infectious prions bind to and are internalized by cells in an HSPG-dependent manner. Enzymatic degradation, inhibition of HS sulfation and ligand binding by heparin, all inhibit prion internalization by neuroblastoma cells (Horonchik et al., 2005). Using similar techniques Holmes et al. reported that HSPG is required for tau and α-Syn seeds internalization. Co-localization with TAT and extensive actin filament rearrangement indicate that these seeds enter cells *via* macropinocytosis mechanism, independent of dynamin, caveolin and clathrin (Holmes et al., 2013).

Exosomes are emerging as a mechanism responsible for both cell exit and entry of α-Syn and other proteins involved in neurodegeneration (Bellingham et al., 2012). Exosomes are small (30–100 nm) vesicles released to the extracellular environment by diverse types of cells *in-vivo*

and *in-vitro* (Simons and Raposo, 2009; Thery et al., 2002). These bilayer membranous vesicles bud from the limiting membrane of late endosomes into their lumen in the process of their maturation into multi vesicular bodies (MVB). MVB fuse with either lysosomes or with the plasma membrane, resulting in degradation or extracellular release of their cargo, respectively (Simons and Raposo, 2009; Thery et al., 2002). The process of cargo sorting into exosomes is not clear and evidence suggests diverse mechanisms (Record et al., 2011). The endosomal sorting complex required for transport (ESCRT), which has an established role in sorting proteins to lysosomal degradation, was suggested by genetic and proteomic studies to be involved in the sorting of some proteins (Raiborg and Stenmark, 2009), however, examples of exosomal release, independent of ESCRT, also exist (Record et al., 2011; Simons and Raposo, 2009). The exosomal cargo includes proteins, lipids and nucleic acids, some of which are cell origin specific, but others are common and are therefore considered as "exosome markers" (Record et al., 2011; Thery et al., 2002). Implicating exsosomes with neurodegenerative diseases, normal and scrapie forms of prions, aggregates of A-β, tau and aggregates of super oxide dismutase 1 (SOD1) are secreted to the extracellular medium in association with exosomes and in some cases are internalized and are toxic to recipient cells (Fevrier et al., 2004; Gomes et al., 2007; Munch et al., 2011; Porto-Carreiro et al., 2005; Rajendran et al., 2006; Saman et al., 2012).

Mounting evidence suggests exosomes maybe involved in trans-cellular propagation of α-Syn aggregates. Aggregated α-Syn, released by cells into the media, is detected as both exosome-associated and free in the media (Danzer et al., 2012; Hasegawa et al., 2011; Melachroinou et al., 2013; Pan-Montojo et al., 2012). Notably, a portion of radio-labeled α-Syn injected into mouse brains was detected in exosomes and moved from the CSF to the plasma (Shi et al., 2014). This is consistent with reports of the protein levels being lower in the CSF of PD

patients compared to control subjects and higher in the serum of patients compared to controls (Hasegawa et al., 2011; Shi et al., 2014). Rotenone, a neurotoxin which acts to elicit mitochondrial dysfunction, associated with increased risk of PD, increases secretion of both exosomal and free α-Syn (Pan-Montojo et al., 2012). Lysosomal and proteasomal dysfunction, implicated in PD, lead to elevated secretion and transmission of exosomal α-Syn (Alvarez-Erviti et al., 2011; Danzer et al., 2012; Lee et al., 2005a). Sorting of α-Syn into undefined extracellular vesicles is regulated by sumolation (Kunadt et al., 2015). Vesicles are released from the cell in a calcium dependent manner (Emmanouilidou et al., 2010). Exosomes were reported to catalyze the aggregation of α-Syn by accelerating the formation of oligomers (Lee et al., 2005a). Moreover, only vesicles composed of gangliosides, but not other lipids detected in the composition of exoseomes, induced accelerated α-Syn fibrillization (Grey et al., 2015). Consistently, secreted oligomeric α-Syn associated with exososomes was more readily internalized and induces higher toxicity in recipient cells than free α-Syn protein (Danzer et al., 2012; Emmanouilidou et al., 2010). Conversely, a different study report that free, rather than vesicle associated α-Syn elicits toxicity in recipient cells by perturbation of calcium homeostasis (Melachroinou et al., 2013).

Membranous tubule structures, termed tunneling nanotubes connect neurons. Tunneling nanotubes hijacked by prion protein aggregates transferred them between cells, and can potentially be used by other protein aggregates (Gousset et al., 2009). *In-vivo* models have demonstrated the spreading of pathology along neuronal connections. This raises the idea that synaptic transmission maybe exploited by proteopathic entities to facilitate transmission of pathology (Luk et al., 2009; Volpicelli-Daley et al., 2011).

An important question that has not been thoroughly investigated is how do seeds, in internalized vesicles, gain access to endogenous endoplasmic α-Syn proteins. Evidence suggest a few potential routes: (1) Fusion of seeds containing endosomes with endogenous α-Syn containing autophagosomes. This is supported by evidence for degradation of α-Syn *via* autophagy (Webb et al., 2003). (2) Exogenous seeds reach the lysosome followed their endocytosis, while endogenous α-Syn is delivered to lysosomes *via* chaperone mediated autophagy (Cuervo et al., 2004). (3) Seeds rupture lysosomal membrane and escape into the cytoplasm gaining access directly to cytosolic α-Syn (Freeman et al., 2013). (4) Exosome containing seeds fuse with the plasma membrane thereby providing α-Syn seeds direct access to cytosolic α-Syn.

CHAPTER FOUR: INTERACTIONS OF α-SYN WITH LIPIDS

Cellular Functions of Membrane Curvature

The ability to form compartments by generating membrane curvature is essential for eukaryotic life. Organelles in the cell have boundaries defined by their membranes and the extent of the membranes' curvature defines the shape of organelle. The function of cellular organelles requires their shape to change dynamically, and sometimes dramatically, to satisfy the requirements of the cell (e.g. fission, maturation or fusion of endocytic vesicles)(McMahon and Boucrot, 2015).

Membrane shapes observed in the cell can be divided into flat, tubules, saddle-like and spherical (Figure 4-1). Uncoated plasma membranes have an almost flat shape while endocytic vesicles are spherical (Zimmerberg and Kozlov, 2006). Tubule structures connect the ER and the Golgi apparatus and budding vesicles have saddle-like shapes (Zimmerberg and Kozlov, 2006). Highly curved membrane structures, such as tubules and spheres, provide maximum surface area over minimum internal volume, which enables for fast and efficient transport across the membranes of these structures (Zimmerberg and Kozlov, 2006). The following examples define how curving membranes assist in performing cellular functions. Membrane fission is required in all trafficking and sorting events where a vesicle, or an organelle, separates from its membrane of origin. This process is assisted by the dynamin family proteins and the ESCRT protein complex in endosomes, by COPII in the ER, by COPI in the golgi and by clathrin in the plasma membrane. The proteins involved are recruited to the neck of the budding vesicle and increase curvature to create stress on the opposing membranes to favor fusion and session of the nascent vesicle (McMahon and Boucrot, 2015). Curvature sensing of incoming vesicles, by Golgin GMAP-210, is a primary step before engagement of SNARE proteins to ensure fidelity of vesicle

targeting (Drin et al., 2008). Membrane fusion between a vesicle and its target membrane allows delivery of cargo to target site. SNARE complex proteins assemble to bring target and vesicle membranes in close proximity before their fusion or session (Jahn and Scheller, 2006). Physical forces created in the curved membrane may create conditions that favor specific membrane proteins over others, thereby allowing the partitioning of transmembrane receptors or channels by a process of enrichment and exclusion into a bud or organelle. This may be the case for the enrichment of acetylcholine receptors at post-synaptic regions (Fertuck and Salpeter, 1974).

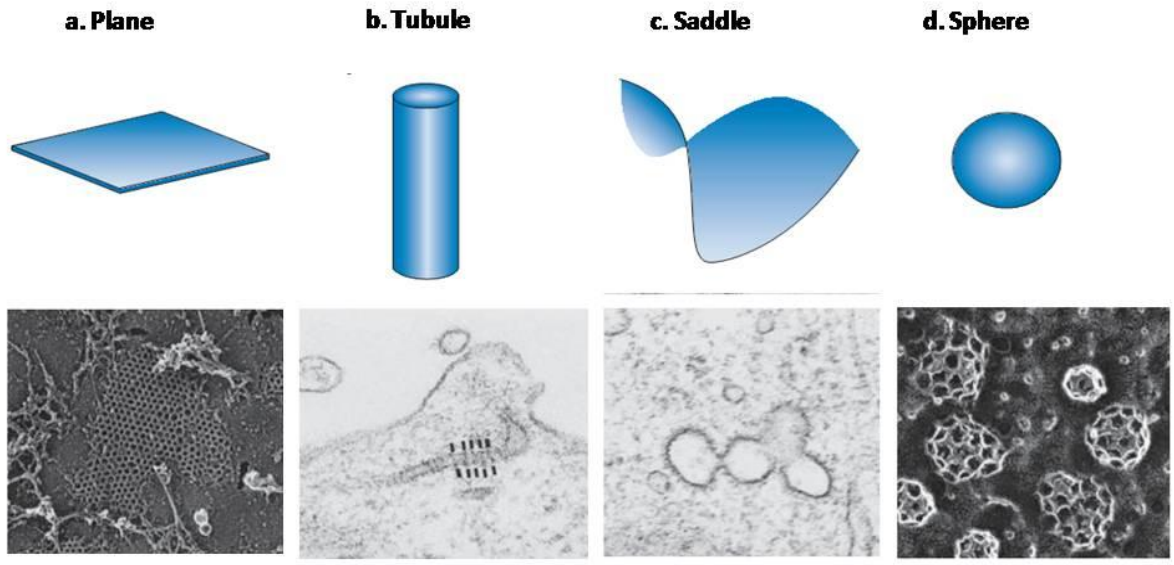

Figure 4-1. Membrane shapes in the cell. a) Flat membrane fragment under a clathrin lattice. b) Membrane tubule under dynamin coat c) The neck of a membrane bud. d) Assembly of pure clathrin cages *in-vitro*.
Modified from: Zimmerberg and Kozlov, 2006. Reprinted by permission from Nature Publishing.

Mechanisms of Membrane Curvature

Energetic considerations dictate that self-assembling lipid-bilayer membranes will have similar lipid composition on both monolayers. This symmetric lipid distribution allows no preference with respect to the curving direction of the membrane, resulting in a flat shape

adopted by the bilayer. The elastic properties of eukaryotic cell membranes makes them resistant to spontaneous bending. Thus, cells have to perform work in order to bend and shape membranes (Graham and Kozlov, 2010). Indeed, upon interaction with protein machinery, membranes of the cell undergo radical shape transformation. Cells use an interplay between lipids, proteins and mechanical forces applied to the membrane surface to generate curvature (Zimmerberg and Kozlov, 2006). In this process proteins can either modify the lipid composition of one monolayer with respect to the other to produce asymmetry, or apply direct physical forces to the membrane by serving as scaffolds or as wedges.

Changes in lipid composition: Enzymes can affect the symmetry of the membrane bilayer by modifying, either the concentrations of specific lipids within either monolayers, or the total amounts of specific lipid molecules in a monolayer. The curvature formed by a monolayer, referred to as its spontaneous curvature, is affected by the properties of the individual lipids composing it and by their concentrations in each leaflet. Since the spontaneous curvature of the bilayer is determined by the difference between the spontaneous curvatures of its outer and inner monolayers, imposing asymmetry can generate curvature (Graham and Kozlov, 2010). The phospholipid flippase Type IV P-type ATPases translocate phospholipids from the external to the internal leaflet of the plasma membrane in the process of vesicle budding (Graham and Kozlov, 2010). The lipid modifying enzyme phospholipase D (PLD) cleaves choline from the headgroup of phosphatidylcholine (PC) reducing its concentration and increasing the concentration of the product, phosphatidic acid (PA). This process facilitates formation of endocytic vesicles from the plasma membrane (Shen et al., 2001).

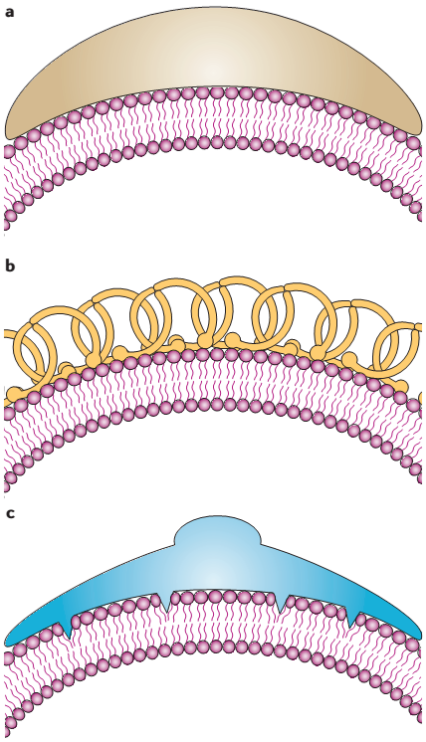

Figure 4-2. Mechanisms for membrane curvature generation a) A scaffold mechanism formed by proteins, such as the BAR protein dimer, with intrinsic curvature facing the membrane. b) Polymerized coat proteins, sometimes linked through an additional adaptor protein (not shown). c) Global curvature induced by a scaffold mechanism and local curvature induced by the insertion of amphipathic moieties of proteins between the polar headgroups of lipid molecules. Such mechanism is applied by a BAR protein.
Modified from: Zimmerberg and Kozlov, 2006. Reprinted by permission from Nature Publishing.

Induction of membrane bending by proteins (Figure 4-2): Many scaffold proteins have an exposed curvature formed either by their tertiary structure, or by forming a complex with other proteins. These scaffold possess intrinsic rigidity to counteract the tendency of the lipid bilayer to relax to its state of spontaneous curvature. The curvature of the scaffold is imposed on the lipid membrane by affinity for the lipid polar headgroups. The energy of the binding affinity has to exceed the membrane-bending energy (Farsad and De Camilli, 2003). Dynamin assembles into a polymeric spiral structure that binds to and wraps around the neck of a budding vesicle. Once in place, the structure constricts through GTP hydrolysis. The coil tightens around the vesicle neck to finally induces it pinching-off of the parent membrane (Hinshaw and Schmid, 1995). The cross section radius of free dynamin is similar to that of the lipid bound. Thus, the structure of dymanin is unaffected by membrane binding, indicating that the dynamin polymer rigidity is greater than that of the lipid bilayer allowing this scaffold mechanism to shape

membranes and induce their fission (Praefcke and McMahon, 2004). BAR (Bin, amphiphysin, Rvs)-domain-containing-proteins provide a banana-shape scaffold with positively charged residues positioned on its concave surface, which interact with phospholipid head-group of the lipid. A tetrameric BAR domain structure that induces membrane tubule have similar radii in the presence or absence of membrane implying greater rigidity of the protein scaffold with respect to the membrane bilayer (Peter et al., 2004).

Proteins inducing local spontaneous curvature: These proteins insert an amphipathic helix (AH) into one leaflet of the bilayer. Amphipathicity is acquired by segregation of polar and hydrophobic residues to opposing faces of the α-helix. Hydrophobic residues insert between the phospholipid acyl-chains, of a single leaflet, typically penetrating shallow into the monolayer. Polar residues face the phospholipid headgroup and depending on their charge, sometimes form electrostatic interactions with the negatively charged phosphates. This orients membrane associated AH parallel to the membrane plane axis (Drin and Antonny, 2010a). Association of AH with membranes takes three principal steps: First, long range electrostatic interactions promote increased local concentration of the unfolded peptide sequence proximate to the negatively charged lipids. Then hydrophobic interactions drive residues to insert between acyl-chains, accompanied by release of water molecules. Last, conformational transition occur from a random coil to α-helix, this offsets the energetic penalty for the presence of peptide bonds in a hydrophobic environment (Drin and Antonny, 2010a). For example, in a key step in the vesicle budding process, Sar1 and Arf proteins bind GTP and expose an N-terminal amphipathic helix which inserts into the membrane, inducing its curvature (Beck et al., 2008; Lee et al., 2005b).

Proteins using the bilayer-couple mechanism: In this mechanism proteins increase the area of one membrane leaflet by inserting through the entire depth of the monolayer. The

membrane bends to compensate for the area asymmetry between the monolayers (Sheetz and Singer, 1974).

Interplay between different mechanisms: Many of the membrane curving mechanisms involve a combination of proteins operating *via* multiple principles. In the cell, dynamin proteins create a scaffold for membrane session, but function in coordination with amphiphysin and endophilin, which operate by the local curvature mechanism. The interplay between protein machineries and membrane bending principals ensure reliability and fidelity of membrane-neck formation and fission (Zimmerberg and Kozlov, 2006). The N-BAR domain containing proteins endophilin and amphiphysin play a role in endocytosis. These proteins display both a concave shape, serving as a rigid scaffold which bind and bend large surfaces of membranes, and an amphipathic helix, wedging into the membrane and induce local curvature (Figure 4-2) (Gallop et al., 2006; Masuda et al., 2006).

Structural Aspects of α-Syn Interaction with Lipids

Binding of α-Syn to lipids and membranes have long been established (Auluck et al., 2010). More recent evidence support a role for α-Syn in curving membranes (Jiang et al., 2013; Mizuno et al., 2012; Ouberai et al., 2013; Pandey et al., 2011; Perlmutter et al., 2009; Varkey et al., 2010b; Varkey et al., 2013a, b; Westphal and Chandra, 2013). Expression of proteins involved in membrane shaping, as indicated by proteomic studies, is elevated in brain cells from triple (α/β/γ) Synuclein knock-out mice. In particular, the N-BAR protein endophilin A1 is reciprocally regulated with Synucleins, suggesting compensatory functions for these proteins (Westphal and Chandra, 2013). Functionally, endophilin A1 is involved in clathrin mediated synaptic vesicle endocytosis (Masuda et al., 2006). *In-vitro*, both α-Syn and endophilin associate with liposomes and induce their tubulation (Ambroso et al., 2014; Westphal and Chandra, 2013).

Both proteins contain N-terminal AH which are inserted into the membrane and induce curvature (Figure 4-3) (Masuda et al., 2006). Binding of α-Syn to membranes *in-vitro,* increases membrane curvature and disrupts liposome structure (Jiang et al., 2013; Mizuno et al., 2012; Ouberai et al., 2013; Varkey et al., 2013b). Membrane binding by α-Syn involves the N-terminal repeats (described in chapter two) spanning amino acids positions 1-87 (Jo et al., 2000). Studies by circular dichroism (CD) suggest an extensive structural rearrangement in this region upon interaction with lipids, transitioning from a coiled-coil to an α-helix (Davidson et al., 1998). Structural studies using nuclear magnetic resonance (NMR) suggest two distinct conformations for lipid bound α-Syn (Figure 4-4): (1) The SDS micelle bound protein is described to adopt a horseshoe shape and encompass two curved anti-parallel helices (Val3-Val37 and Lys45-Thr92), connected by an extended linker (Ulmer et al., 2005). While this structure has been extensively studied, the vesicle bound conformation is less defined. (2) Membrane bound α-Syn is proposed to assume an extended helix conformation which involves about 100 residues from the N-terminus (Georgieva et al., 2008; Trexler and Rhoades, 2009). The interaction of α-Syn with lipids is affected by multiple factors including: protein polymerization state, protein:lipid ratio, phospholipid headgroup charge, geometric shape of the lipid, ionic-strength of the surrounding buffer, membrane composition and degree of curvature. Thus, reported results are inconsistent and, in some cases, even contradictory, likely due to varying conditions between the reported experimental systems (Middleton and Rhoades, 2010; Pfefferkorn et al., 2012; Pirc and Ulrih, 2011). Similar to other AH domains, the N-terminal portion of α-Syn has been proposed to insert between the lipid molecules of the corresponding monolayer. Upon membrane association the hydrophobic portion inserts between the acyl-chains perturbing their packing as a wedge, while the positive lysine residues are thought to interact with the negatively charged phospholipid

headgroups (Mizuno et al., 2012; Ouberai et al., 2013; Varkey et al., 2010b; Varkey et al., 2013a, b).

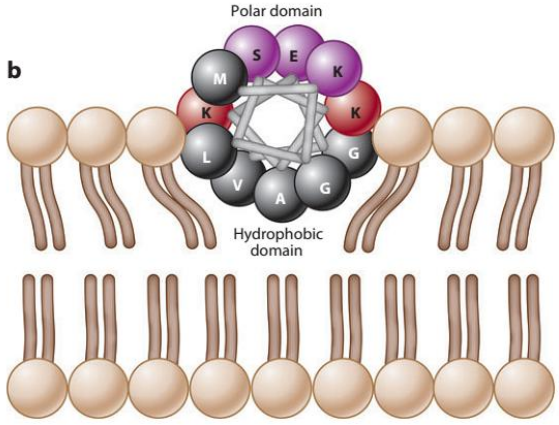

Figure 4-3. An axial view of α-Syn residues when displayed on Edmundson helix wheel. Polar residues (i.e., S, E, and K) face the hydrophilic environment of the cytosol, whereas hydrophobic residues are buried between the acyl-chains of the phospholipid bilayer. Positively charged lysine residues (K) separate the polar and hydrophobic domains and interact directly with the anionic surface of the phospholipid bilayer.
From: Auluck et al., 2010. Reprinted by permission from Annual Reviews.

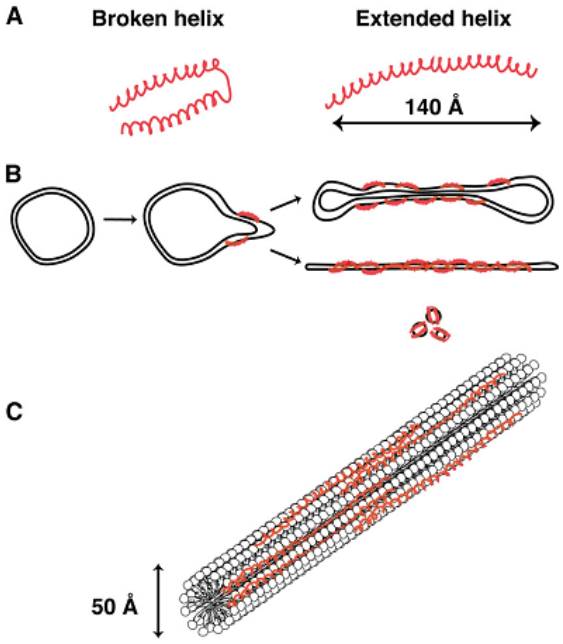

Figure 4-4. A model describing the interaction geometry of α-Syn with lipids. A) Two inferred α-helical conformations of α-Syn. α-Syn adopts an extended conformation (right) on vesicles remodeled into tubules. B) Possible arrangements of α-Syn on membrane surfaces. As

the cylindrical micelles are only 50 Å in diameter and the extended helical conformation is 140 Å long, α-Syn should be oriented nearly parallel to the tube axis. When the acyl chain of the lipids is bulkier (top right), the protein does not wedge to the same extent into the lipid surface, and the resulting tubes remain as bilayers. With shorter acyl-chains, α-Syn inserts deeper into the lipid phase, and cylindrical micelle formation occurs. At higher concentrations of the protein, the closing of the cylindrical micelles gets tighter (bottom right). C) Model of α-Syn attaching to cylindrical micelles.
From: Mizuno et al., 2012. Reprinted by permission from The American Society for Biochemistry and Molecular Biology.

This binding model involves both a hydrophobic interaction component and an electrostatic component. However, α-Syn binds small unilamellar vesicles (SUV) under high ionic-strength conditions (500mM NaCl), which disrupt electrostatic interactions, and tubulate larger liposomes composed of the zwitter-ionic lipid PC (Davidson et al., 1998; Jiang et al., 2013). This evidence supports a significant contribution for the hydrophobic interaction component in membrane binding. Evidence of binding to PC has a physiological significance as this lipid is enriched in cellular membranes. However, consistent with a role for negatively charged phospholipids in increased membrane association of α-Syn, tubule formation increases with elevated concentrations of anionic lipids in the membrane (Jiang et al., 2013; Pandey et al., 2011). Loose packing of the lipids in the membrane favors binding of α-Syn. Acyl-chain bulkiness and phospholipid headgroup size both affect tight lipid packing. Polyunsaturated acyl-chains are bulkier and increase packing disorder allowing easier peptide penetration and helix rearrangement (Middleton and Rhoades, 2010; Mizuno et al., 2012; Pfefferkorn et al., 2012; Pirc and Ulrih, 2011). Smaller headgroups, such as that of PA, provide more space at the membrane plane and requires less rearrangement to allow protein binding (Figure 4-5) (Middleton and Rhoades, 2010; Pfefferkorn et al., 2012; Pirc and Ulrih, 2011). Binding preference to smaller, over larger, vesicles is also reported, suggesting affinity for high over low plane curvature. This preference may also be due packing defects which may increase with curvature. However α-Syn

binds vesicles of a very wide size range, from Small Unilamellar Vesicles (SUV) to Giant Unilmellar Vesicles (GUV) (diameter ~50 nm to 10 μm, respectively) and even to flat planes (Figure 4-5) (Middleton and Rhoades, 2010; Pandey et al., 2011; Perlmutter et al., 2009; Pfefferkorn et al., 2012; Varkey et al., 2013b).

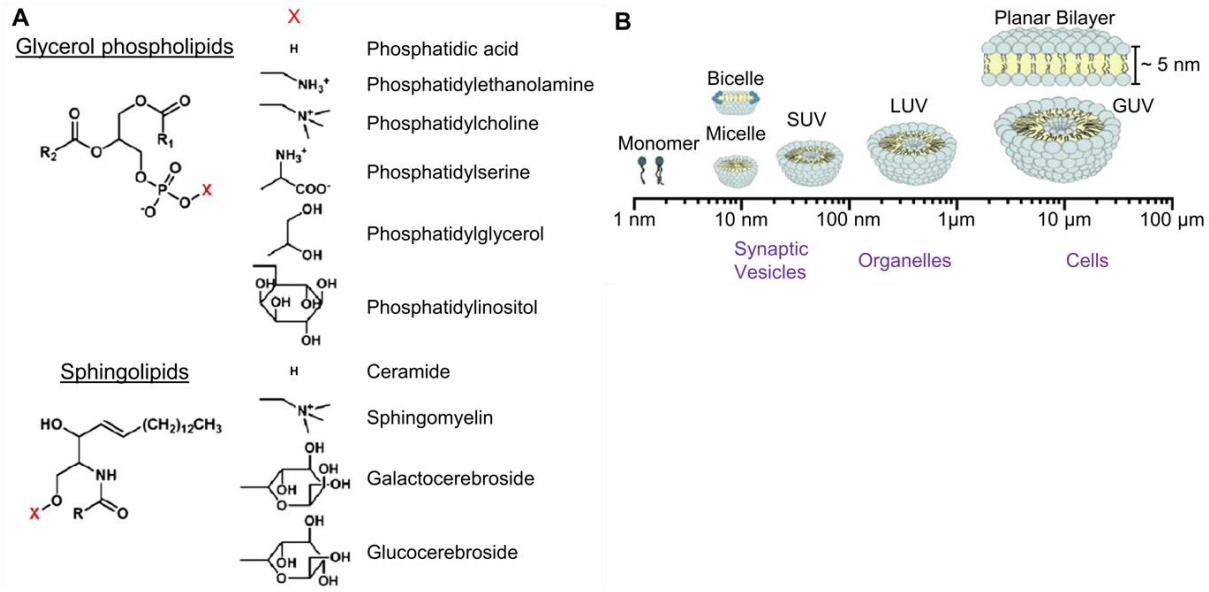

Figure 4-5. Lipid and membrane mimic structure. (A) Chemical structure of the glycerol phospholipid and sphingolipid backbone with different headgroups (X) and their corresponding names indicated. The R1, R2, and R designate fatty acid chains. (B) Schematic of the approximate size and organization of membrane mimics commonly used in biophysical research. Corresponding cellular compartments are provided for relative size reference.
From: Pfefferkorn et al., 2012. Reprinted by permission from Elsevier.

Increased α-Syn protein concentration, with respect to pure anionic lipids, induce higher level of tubule formation and affects their morphology (Jiang et al., 2013; Mizuno et al., 2012; Pandey et al., 2011). At a low protein to lipid ratio (<1/10) formation of discoid particles is observed (Figure 4-4) (Mizuno et al., 2012). Nanoparticles were also observed with α-Syn bound to oleic acid and to mitochondrial membranes. Interestingly the bound α-Syn is oligomeric (tri

and tetrameric). Particle morphology resembled that observed with apolipoprotein-bound lipids. These observations are consistent with a role for α-Syn in lipid transport and metabolism (Varkey et al., 2013b).

Although oligomeric α-Syn have been reported to remodel membranes (Lee et al., 2012) this property is more typically attributed to the monomeric form (Jiang et al., 2013; Pandey et al., 2011; Westphal and Chandra, 2013). Indeed, α-Syn protein membrane binding and oligomerization have been shown to be competing processes (Aisenbrey et al., 2008; Jiang et al., 2013; Lee et al., 2002; Narayanan and Scarlata, 2001; Zhu and Fink, 2003). However, in other cases, lipid association have been reported to both accelerate and inhibit protein aggregation (Aisenbrey et al., 2008; Lee et al., 2002; Narayanan and Scarlata, 2001; Zhu and Fink, 2003). The affects of lipid on α-Syn aggregation might be a function of relative concentrations: when protein concentration is higher membrane binding may serve to increase local molecular crowding and, over a critical concentration value, drive aggregation. At lower concentrations, the protein may be spaced far enough and bound in a non-amyloidogenic conformation, thereby protected from aggregation. In the latter case membrane binding also reduces protein concentration in the solution, decreasing soluble α-Syn and inhibiting aggregation in the solute phase (Dikiy and Eliezer, 2012).

Familial mutations in α-Syn all occur in the N-terminus, the portion involved in membrane binding, hence implicating an effect on membrane interaction. Although some inconsistencies between reported data exist, the general consensus for membrane binding affinity is: E46K>A53T≥WT>A30P (Auluck et al., 2010). Thus, membrane affinity does not correlate with the pathogenesis caused by these changes. The introduction of proline in the A30P disrupts the helical structure and weakens membrane binding relative to WT, as indicated by biochemical

studies, fluorescence correlation spectroscopy and liposome tubulation (Jensen et al., 1998; Jo et al., 2002; Middleton and Rhoades, 2010; Westphal and Chandra, 2013). The A53T mutation affects only side chain interactions and leaves the backbone conformation unchanged from that of WT (Ulmer and Bax, 2005). Its membrane interaction is stabilized by the hydrogen bonds that forms with the threonine, and is reported to have slightly increased or similar binding properties as WT (Jo et al., 2002; Middleton and Rhoades, 2010). The E46K mutation also gains a hydrogen bond leading to increased affinity with membranes and lipids (Choi et al., 2004; Middleton and Rhoades, 2010).

CHAPTER FIVE: CELLULAR UPTAKE OF LIPID-ASSOCIATED α-SYN SEEDS IS MORE EFFICIENT THAN UPTAKE OF LIPID-FREE SEEDS

Introduction

The presynaptic protein α-Syn is a key protein in many neurodegenerative diseases, collectively termed synucleinopathies, most known of which is PD. Although its involvement in neurodegenerative diseases has been well investigated, the physiological function of α-Syn is unclear. It is an unstructured amyloidogenic protein which abnormally accumulates in cytoplasmic inclusions termed LB, a hallmark of PD. α-Syn is also linked genetically to PD, through rare single point mutations and gene multiplications that cause early onset of the disease (Lashuel et al., 2013).

Mounting evidence support a prion-like progression of PD pathology throughout the CNS. According to this model a misfolded protein seed is transmitted from one cell to another, where it templates the conversion of host protein from an unstructured into a misfolded conformation, thereby seeding its aggregation into an amyloid fibril (Angot et al., 2010; Guo and Lee, 2014). Braak et al proposed an orderly appearance of Lewy pathology, along an interconnected network of neurons, ascending from the medulla oblongata to midbrain structures, including the SN, and finally to cortical areas (Braak et al., 2003). Thus, pathology begins several years before the SN is affected, which leads to the development of PD typical motor symptoms (Braak et al., 2003). Indeed, patients who received transplanted fetal mesencephalic dopaminergic neurons developed α-Syn positively stained LB in the grafted neurons, supporting a role for cell to cell transfer of a cytotoxic form of the protein (Kordower et al., 2008a; Kordower et al., 2008b; Li et al., 2008). The cytotoxic species is thought to be an oligomeric form of α-Syn which ,upon transfer, may directly or indirectly lead to damage of the affected cells (Danzer et al., 2009; Danzer et al., 2011; Winner et al., 2011). Such seeds were produced from recombinant α-Syn aggregated *in-*

vitro and used in different models to test their transmissibility (Danzer et al., 2009; Desplats et al., 2009; Lee et al., 2008; Luk et al., 2012a; Yonetani et al., 2009). In cell culture models, using cell lines or primary neurons, seeds, which were introduced to the growth media, were detected in the cytoplasm where it induced the formation of insoluble α-Syn aggregates (Desplats et al., 2009; Freundt et al., 2012; Holmes et al., 2013; Lee et al., 2008; Luk et al., 2009; Volpicelli-Daley et al., 2011). WT and transgenic rodents injected with seeds exhibited α-Syn LB-like inclusions progressing in a spatiotemporal fashion from the injection sites to anatomically connected areas of the CNS, in addition to loss of dopaminergic neurons and motor deficits exhibited by the animals (Luk et al., 2012a; Sacino et al., 2014).

Several mechanisms have been suggested to explain the cell to cell transmission of pathogenic α-Syn seeds. In a few cell-line model studies, the expression of dominant negative dynamin or Rab5A inhibited the internalization of α-Syn seeds, implicating the endocytic system as necessary for entry (Desplats et al., 2009; Lee et al., 2008; Sung et al., 2001). Accordingly, α-Syn aggregates were shown to induce lysosomal membrane rupture, following endocytosis, allowing them to escape lysosomes into the cytoplasm (Freeman et al., 2013). In a recent study, the cell surface HSPG was found to mediate binding and uptake of α-Syn, *via* macropinocytosis (Holmes et al., 2013). Inhibition of binding of externally added seeds to HSPG, or inhibition of expression of the proteoglycan, as well as its enzymatic digestion, all reduced cell uptake and aggregate formation. Exosomes have also been suggested as a potential mechanism accounting for both cell entry and exit of α-Syn aggregates. In cell culture studies, a portion of cellular α-Syn was found in the lumen of vesicles (which were not further characterized as exosomes), where it was more prone to aggregation and was secreted in an ER-golgi independent manner (Lee et al., 2005a). Sorting of α-Syn into undefined extracellular vesicles was regulated by

Sumoylation (Kunadt et al., 2015) and exosomal release was calcium dependent (Emmanouilidou et al., 2010). Induction of lysosomal dysfunction increased the exosomal content and the transmission of α-Syn (Alvarez-Erviti et al., 2011). In another study, oligomeric α-Syn expressed by cells in culture was found both associated with exosomes and free in the media, but exosome-associated α-Syn was internalized more efficiently than free α-Syn (Danzer et al., 2012). Moreover, several studies reported the requirement for commercial lipid reagents to drive α-Syn aggregates into cells (Luk et al., 2009; Nonaka et al., 2010). However, the mechanisms governing lipid-associated α-Syn internalization have not been described.

The interaction of α-Syn with membranes has also been implicated in its physiological role in membrane trafficking, where it is involved in the control of synaptic vesicle formation and maintenance (Burré et al., 2010). *In-vitro*, α-Syn induced membrane curvature and converted large vesicles into highly curved membrane tubules and vesicles (Mizuno et al., 2012; Varkey et al., 2010b). Mechanistically, α-Syn is suggested to adopt an extended amphipathic α-helical conformation, wedging into the outer leaflet of the bilayer, thereby partitioning the lipids and increasing surface curvature, leading to tube formation (Mizuno et al., 2012). At higher protein to lipid ratios, formation of lipoprotein particles was observed (Varkey et al., 2013b). This membrane binding and tubulation was attributed to the monomeric but not the tetrameric α-Syn conformation and competed with amyloid formation (Jiang et al., 2013; Westphal and Chandra, 2013).

Thus, α-Syn have been detected in the media and internalized by cells both as free seeds and membrane-associated. In this study, the efficiency of lipid-associated α-Syn internalization by cells was compared to that of free seeds. Furthermore, the significance of vesicle tubulation by monomeric α-Syn for its internalization was assessed.

This study suggests α-Syn seeds associated with monomer-induced lipid tubules are internalized by cells in culture more efficiently than free seeds. The requirement of HSPG for cellular internalization of this lipid-associated α-Syn was tested as it was previously reported to mediate free α-Syn seeds internalization (Holmes et al., 2013). Pharmacological and enzymatic techniques were used to show that lipid-associated α-Syn internalization employs the same cell entry route as free seeds. Altogether this study suggests that lipid-associated internalization of seeds is mediated by the HSPG pathway and is more efficient than internalization of seeds alone.

Results

The N-terminal portion of monomeric α-Syn induces tubulation of liposomes

α-Syn is a unique protein in its structural diversity. It is unstructured as a native monomer, has a beta sheet rich structure when aggregated into an amyloid fibril and assumes a α-helical structure when membrane bound (Auluck et al., 2010). Its binding to membranes affects not only its own structure but also that of the membrane. α-Syn was reported to curve membranes *in-vitro*, inducing various membrane structures depending on lipid composition and the protein to lipid ratio (Middleton and Rhoades, 2010; Mizuno et al., 2012; Varkey et al., 2010b; Varkey et al., 2013b).

First, tubulation was tested in the current system, as previous work demonstrated tubulation of large vesicles by monomeric full length α-Syn (FL α-Syn) (Mizuno et al., 2012; Varkey et al., 2010b). The negatively charged lipids 1-palmitoyl-2-oleoyl-sn-glycero-3-phospho-(1'-rac-glycerol) (POPG) were used to test two model liposomes: multilamellar vesicles (MLV), previously shown to form tubules when interacted with monomeric α-Syn (Mizuno et al., 2012; Varkey et al., 2010b) and small unilamellar vesicles (SUV) in which such tubulation was not observed (Varkey et al., 2013b). The protein was mixed with lipids at a molar ratio of 1:20 (P/L)

and was incubated for 30 minutes at room temperature. These conditions result in tubulation of MLV (Figure 5-1). MLV are typically large, but have variable size distribution. This can be noted by the large standard error of mean (SEM) (~10%) of MLV measured average diameter of 309.9±30.2 nm (Table 5-1). Consistent with previous reports, tubulation of MLV is observed when mixed with FL α-Syn (Figure 5-1A). The tubules have a diameter of 11.4±0.3 nm. In addition to the FL monomeric protein, two C-terminally truncated versions: α-Syn110 and α-Syn119 were included to assess their membrane tubulation efficiency. The truncated proteins have the membrane interacting sequence but lack 30 or 21 amino acids from the acidic C-terminus, respectively. These truncated versions were detected in the brains of patients with Diffuse Lewy Body Disease (DLBD), and Lewy Body Variant of Alzheimer's Disease (LBV) (Lewis et al.). Tubules were formed by incubating MLV with both α-Syn110 and α-Syn119. However, tubules induced by truncated monomeric α-Syn were both thinner than FL-induced tubules with measured average widths of 8.3±0.1 nm and 9.6±0.2 nm to tubules induced by α-Syn110 and α-Syn119, respectively (Table 5-1). The SUV were uniform in diameter at 45.2±1.1 nm (Figure 5-1B and Table 5-1). Interestingly, when mixed with monomeric FL α-Syn, a minority of SUV maintained a vesicular structure with measured average diameters of 30±1.3 nm, 33% smaller then SUV alone. The remaining lipid material appeared as deformed vesicles or thick tubules with a measured width of 17.1±1.0 nm. These structures are smaller than SUV alone (45.2±1.1 nm), but larger then tubules formed by MLV in the presence of monomeric FL α-Syn (11.4±0.3 nm) (Figure 5-1 and Table 5-1). SUV mixed with either truncated α-Syn maintained their vesicular structure and tubule formation was not observed. The measured diameters, 24.4±0.5 nm and 22.2±0.6 nm induced by α-Syn110 and α-Syn119, respectively, were smaller than the average measured diameters of SUV alone.

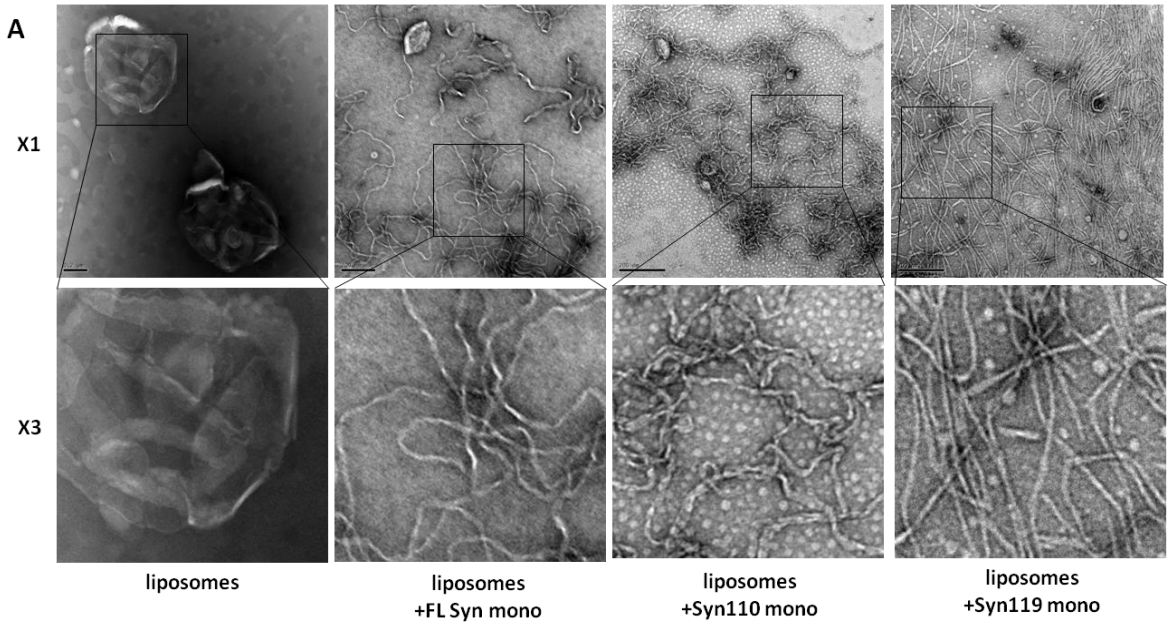
A
X1
X3
liposomes
liposomes
+FL Syn mono
liposomes
+Syn110 mono
liposomes
+Syn119 mono

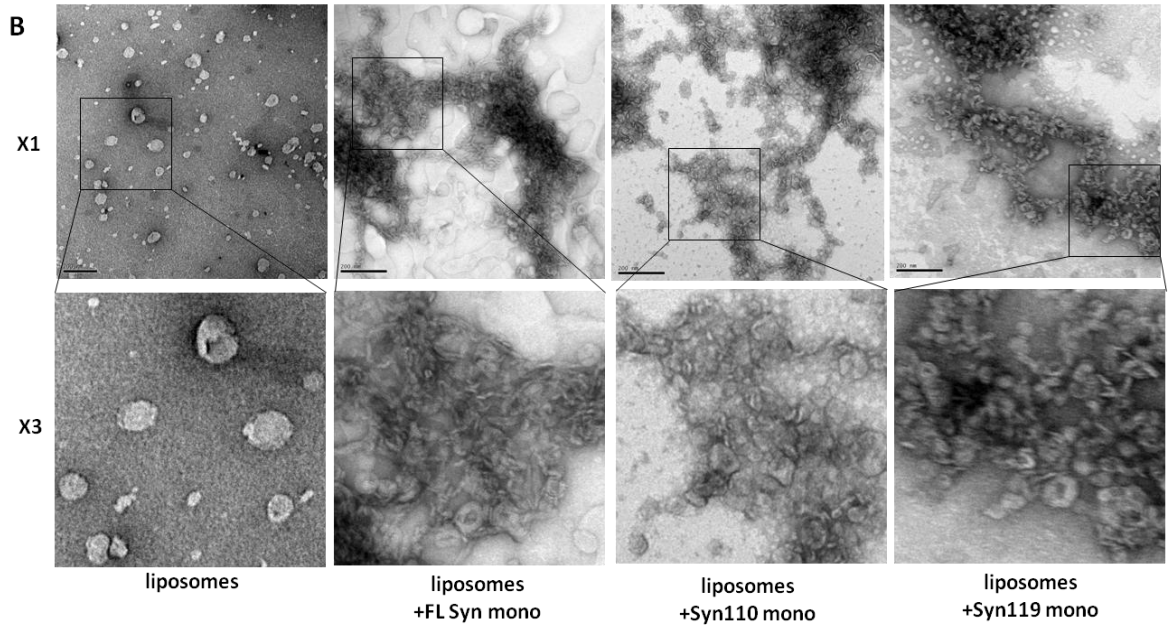
B
X1
X3
liposomes
liposomes
+FL Syn mono
liposomes
+Syn110 mono
liposomes
+Syn119 mono

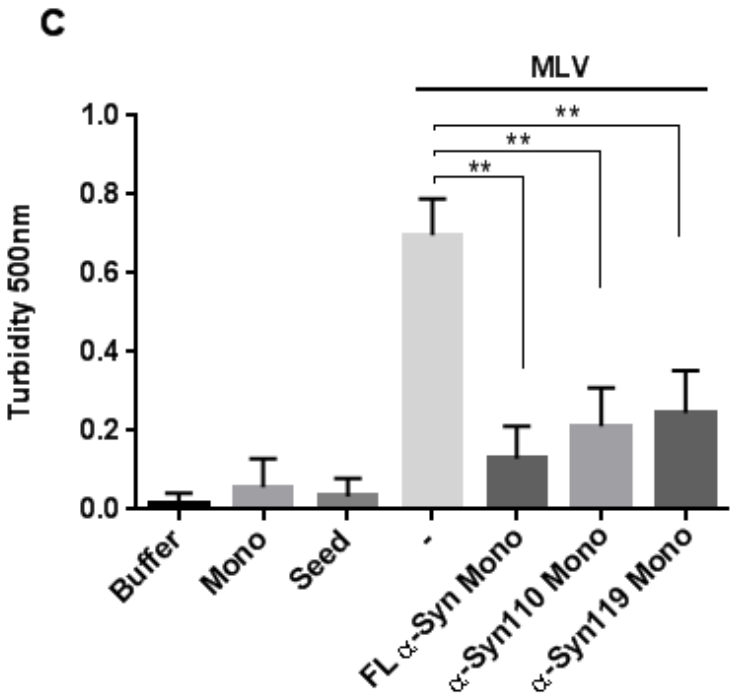

Figure 5-1. The Monomeric FL and truncated α-Syn induce tubulation of liposomes. EM images of (A) MLV and (B) SUV incubated with monomeric FL or C-terminally truncated α-Syn. Bar = 0.2um. The boxed areas at the top are magnified 3 fold and presented at the bottom panel, for better observation of small objects. Representative images were selected out of at least 5 fields per treatment, and at least 3 experimental repeats (N≥3). (C) Change in light scattering of liposomes and lipid tubes was measured to quantify the extent of MLV tubulation by full length and truncated monomeric α-Syn. Error bars represent standard error of mean (SEM), N=3. ** $p<0.05$.

To quantify reduction in the number of large vesicles, a simple turbidity assay was employed. This assay is based on the high degree of light scattering of large, but not small vesicles or tubules, as previously reported by Varkey et al. (Varkey et al., 2010b). Thus, the decrease in the light scattering intensity signal of a given liposome sample correlate with the number of liposomes that decrease in size and with the size decrease of individual liposomes. This assay was used to measure the change in light scattering of MLV incubated for 30 minutes in the presence or absence of monomeric α-Syn. The assay cannot be used for SUV

measurements as they do not scatter light at these wavelengths due to their small size (<50 nm) (Figure 5-3 and Table 5-1). Consistent with formation of tubules observed by the EM micrographs, all three variants of monomeric α-Syn reduced the turbidity of the MLV sample (Figure 5-1C). Specifically, after subtraction of the averaged background signal measured from FL α-Syn alone, FL α-Syn induced tubules reduced turbidity by 89% on average, compared to MLV, whereas α-Syn110 and α-Syn119 reduced it by 77 and 71%, respectively. Altogether, these data show that FL and truncated α-Syn tubulate large liposomes and deform the structure (FL α-Syn) or decrease the size of small liposomes (truncated α-Syn).

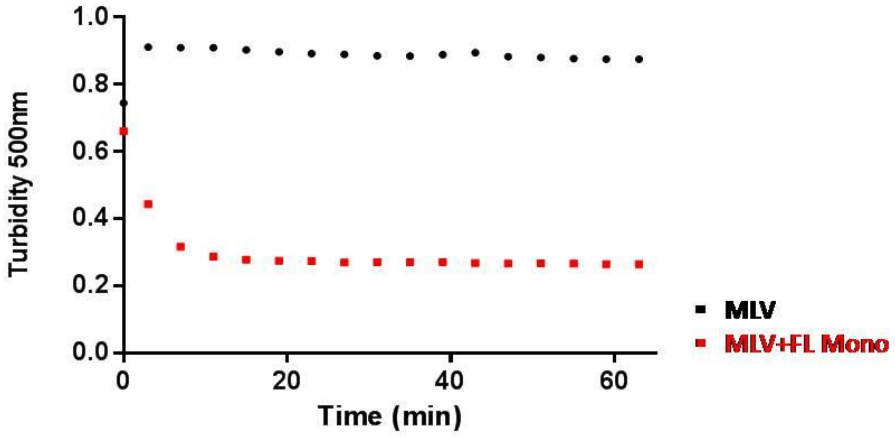

Figure 5-2. MLV turbidity is decreased when mixed with monomeric FL α-Syn. POPG-MLV were incubated with monomeric FL α-Syn at a ratio of 20/1, respectively, and turbidity at 500 nm was measured over 65 minutes.

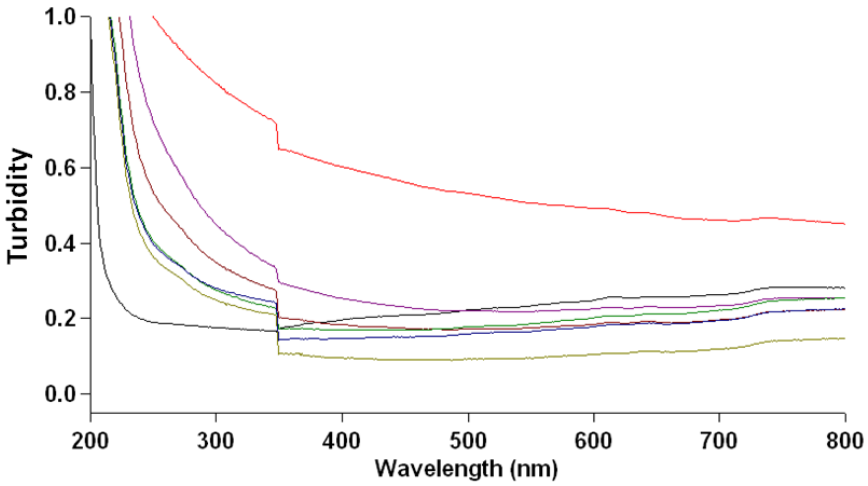

Figure 5-3. Liposomes turbidity decreased with size. MLV were sonicated for 10 minutes to produce SUV. Turbidity was measured across the spectrum 200-800 nm. MLV diluted x4 (red), 2 (purple), 4 (brown), 6 (green), 8 (olive green),10 min (blue), buffer (grey).

Seeds of FL α-Syn do not efficiently induce tubulation of liposomes

Oligomeric α-Syn was reported to be a cytotoxic agent in the pathology of PD, and oligomers were produced from fibrillar recombinant α-Syn and found efficient in seeding intracellular aggregation (Holmes et al., 2013; Lee et al., 2008; Luk et al., 2012a; Luk et al., 2009). To examine the effect of α-Syn oligomers on membranes FL α-Syn seeds were produced by briefly sonicating *in-vitro* aggregated amyloid fibrils, produced from FL α-Syn monomers. At the steady-state end-point of the *in-vitro* fibrillization reaction, measured by Thioflavin T incorporation into the β-sheet of the forming amyloid structure, the *in-vitro* reaction contains both amyloid fibrils as well as monomers. To solely observe the effect of the amyloid seeds on liposomes, seeds (insoluble protein) were separated from soluble monomers. When mixed with FL α-Syn seeds the majority of MLV and SUV retained their vesicular structure, however some minor tubule formation was observed and vesicle size decreased by 74.8% for MLV and 34.6% for SUV, to averaged diameters of 78.2±4.7 nm and 33.6±1.3 nm, respectively (Figure 5-4A and

5-4B, Table 5-1). Consistent with the EM micrographs, turbidity measurements of the FL α-Syn seeds+MLV (Figure 5-4C) showed only a slight reduction of 28% (after subtraction of background measured from seeds alone) suggesting only low tubulation of MLV takes place in the present of seeds. These data show minor tubulation of large and small liposomes by FL α-Syn.

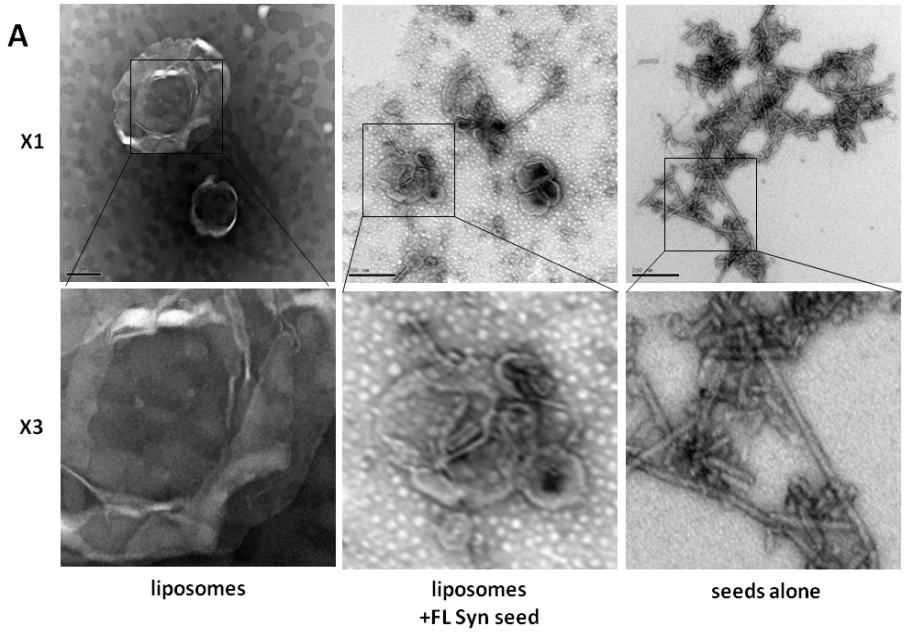

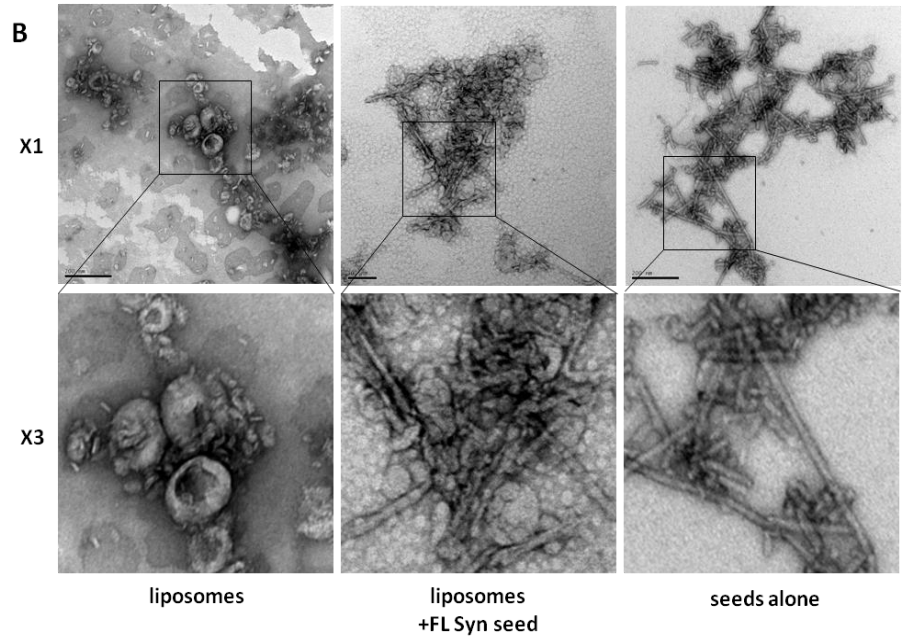

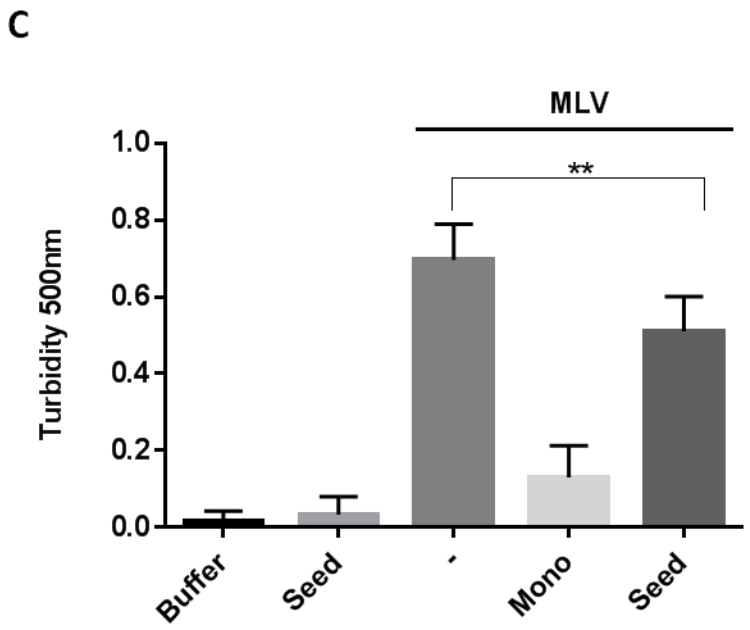

Figure 5-4. Seeds of FL α-Syn are inefficient in tubulation of liposomes. EM images of (A) MLV and (B) SUV incubated with FL α-Syn seeds. Seeds alone are shown, on the right panel, for reference. Bar = 0.2um. The boxed areas at the top are magnified 3 fold and presented at the bottom panel, for better observation of small objects. Seeds are distinguished from tubules by their straight and morphology and shorter length. Representative images were selected out of at least 5 fields per treatment, and at least 3 experimental repeats (N≥3). (C) Change in light scattering of liposomes and lipid tubes was measured to quantify the extent of MLV tubulation by seeds of α-Syn. Control sample are the same samples as in Figure 5-1C. Error bars represent SEM, N=3. ** $p<0.05$

Monomeric α-Syn induces tubulation of liposomes in the presence of seeds

As both α-Syn monomers and seeds likely present in the extracellular space at the same time, the combined effect of the FL of both forms on MLV was tested (Danzer et al., 2011; El-Agnaf et al., 2006; Lee et al., 2008; Lee et al., 2005a). Formation of tubules was measured using the *in-vitro* aggregation product, which includes both FL α-Syn monomers and seeds at approximately 60:40 ratio (based on BCA measurement of soluble protein). Seeds were produced by sonicating this preparation (termed "mix"), but monomers were not removed. The

EM images of the mix+MLV (Figure 5-5A) show tubules at an average width of 12.4±0.3 nm, similar to tubules formed by monomers alone, which had an average width of 11.4±0.3 nm (Table 5-1). Tubules and seeds have similar width (Table 5-1), but seeds may be distinguished from tubules by their straight morphology and uniform width, as oppose to the curvy morphology and more variable width of the tubules (Figure 5-4A). The tubules are in close proximity to seeds. Mix does not tubulate SUV but reduction of ~50% in average diameter of the vesicles (from 41.2±1.1 to 21.9±0.5 nm) is observed and the seeds are in close physical proximity to the vesicles. Turbidity measurement are consistent with tubule formation by the mix+MLV, exhibiting a reduction in turbidity to background level (Figure 5-5C). In addition an artificially mixed sample including purified monomers and seeds remixed at a 1:1 ratio (15μM each) was tested (Figure 5-5C). Reduction of 67% in lipid turbidity is observed in this sample. The smaller reduction in lipid turbidity with the artificial mixture, compared to the *in-vitro* mix sample suggests that monomer concentration in the mix sample is higher than estimated or that some oligomeric species, which are absent in the artificial mixture (composed of monomers and pelletable, high molecular weight species) but present in the mix, have an effect on tubulation.

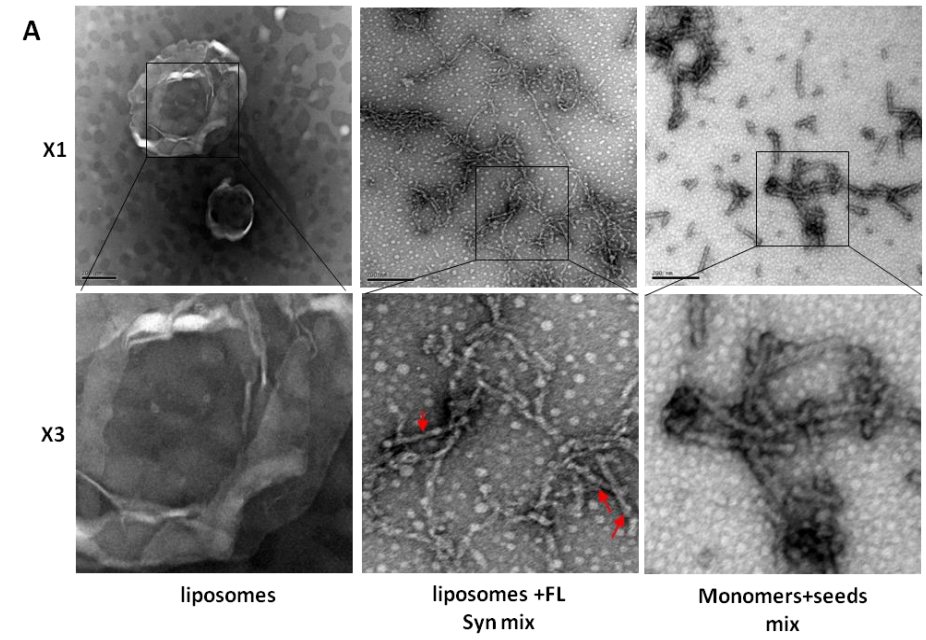
A
X1
X3
liposomes
liposomes +FL
Syn mix
Monomers+seeds
mix

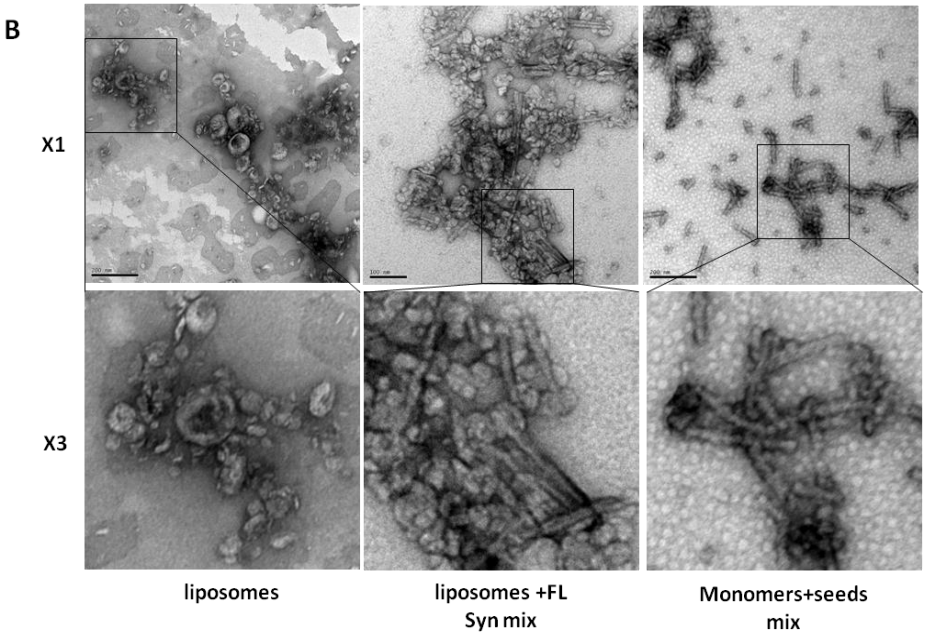
B
X1
X3
liposomes
liposomes +FL
Syn mix
Monomers+seeds
mix

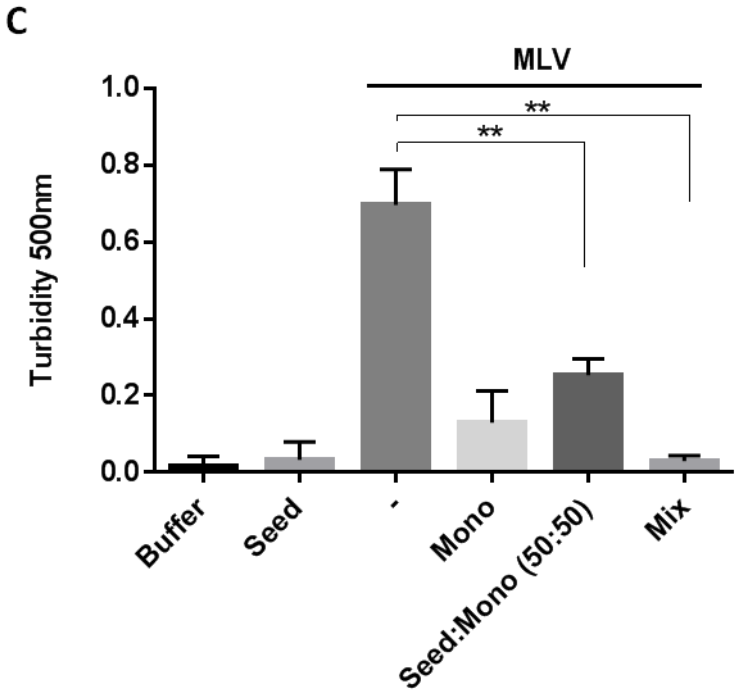

Figure 5-5. Monomers induce tubulation of liposomes in the presence of seeds. EM images of (A) MLV and (B) SUV incubated with seeds and monomers of FL α-Syn. Mix alone are shown, on the right panel, for reference and red arrows in the figure show seeds. Bar = 0.2um. The boxed areas at the top are magnified 3 fold and presented at the bottom panel, for better observation of small objects. Seeds (red arrows) are distinguished from tubules by their straight morphology and shorter length. Representative images were selected out of at least 5 fields per treatment, and at least 3 independent experimental repeats (N≥3). (C) Change in light scattering of liposomes and lipid tubes was measured to quantify the extent of MLV tubulation by mix of FL α-Syn. control sample are the same samples as in Figure 5-1C. Error bars represent SEM, N=3. ** $p<0.05$.

In summary, similar to the effects of monomers alone on liposomes (Figure 5-1), monomers in the presence seeds efficiently induce tubulation of MLV and decrease the size of SUV.

	Objects measured	Mean (nm)	SEM (nm)
MLV	Vesicles	310.0	30.2
FL α-Syn mono +MLV	Tubules	11.4	0.3
α-Syn110 mono +MLV	Tubules	8.3	0.1
α-Syn119 mono +MLV	Tubules	9.6	0.2
SUV	Vesicles	45.2	1.1
FL α-Syn mono +SUV	Vesicles	30.0	1.3
	Non-vesicular structures	17.1	11.0
α-Syn110 mono +SUV	Vesicles	24.4	0.5
α-Syn119 mono +SUV	Vesicles	22.2	0.6
Seeds	Filaments	13.3	0.2
FL α-Syn seed +MLV	Vesicles	78.2	4.7
FL α-Syn seed+SUV	Vesicles	33.6	1.3
FL α-Syn mix +MLV	Tubules	12.4	0.3
FL α-Syn mix+SUV	Vesicles	21.9	0.5

Table 5-1. Measurements of vesicles tubules and seeds. The measured object was the dominant object in selected representative images (N≥3). Expect in α-Syn FL mono +SUV, in which both vesicles and "non- vesicular structures" were dominant.

Seeds in the presence of monomer-induced lipid-tubules more efficiently induce intracellular aggregate formation than either seeds alone or seeds with MLV

Seeds of α-Syn were previously reported to be internalized by cells in culture in the absence or presence of lipids and to induce intracellular aggregation of endogenous protein (Desplats et al., 2009; Luk et al., 2009). To systematically compare the efficiency of α-Syn internalization in the absence or presence of lipids, the effect of the presence of lipid tubules on the efficiency of intra-cellular aggregate formation was determined. Intracellular aggregate formation of mix+MLV, a preparation which was observed to form tubules, was compared to mix+SUV, which did not form tubules. Mix+MLV was more efficient in tubules formation

(unpublished). Therefore, monomers, seeds or mix, were added in the presence or absence of MLV, into the culture media of differentiated SH-SY5Y cells. Aggregate formation in the cells was monitored by Western Blot (WB) and Immunocytochemistry (ICC) two days later. ICC (Figure 5-6A) revealed large aggregate formation in the cytoplasm of cells treated with mix+MLV while smaller aggregates formed in cells treated with seeds + MLV. Positive cells contained both single and multiple α-Syn staining aggregates. No staining was observed in cells that were treated with α-Syn (monomers, seeds or mix) without MLV, monomers+MLV or with MLV alone. The number α-Syn positive cells was quantified by counting α-Syn immuno-reactive puncta which overlapped with actin filaments (used as cell body marker) and divided by the number of counted nuclei (representing the number of cells). The number of puncta/cells treated with mix+MLV was 1.18, while 0.76 puntca/cells were counted for cells treated with seeds+MLV. The WB image (Figure 5-6B) represents triton-X insoluble, SDS soluble, fractions of cell lysates. Under these conditions the majority of aggregated α-Syn migrates at 15 kDa, representing the monomeric form, and a minority of the protein migrates at ~30 and ~45kDa representing dimers and trimers, respectively. Treating the cells with mix+MLV results in extensive aggregates formation. The WB data is consistent with the ICC data showing a 51 and 20 fold increase in insoluble protein for mix+MLV over buffer and over mix alone, respectively (3464 over 224 and 68, respectively) and more moderate increases of 11 and 2 for seeds+MLV over buffer and over seeds, respectively (770 over 373 and 68, respectively).

A

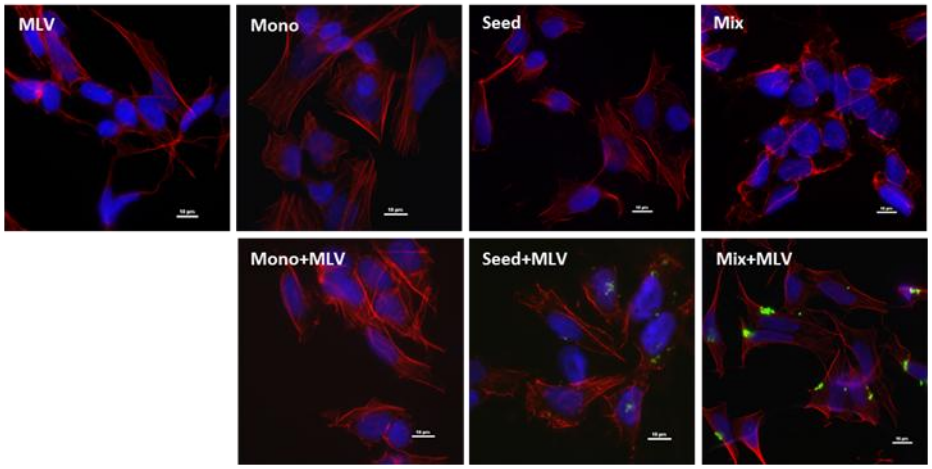
MLV
Mono
Seed
Mix
Mono+MLV
Seed+MLV
Mix+MLV

B

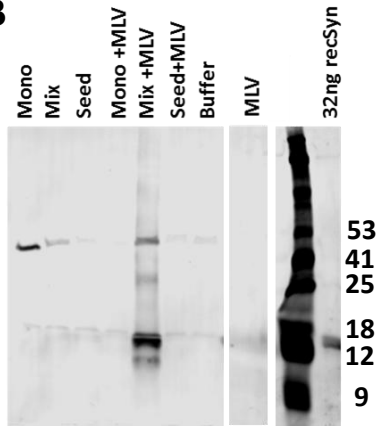
Mono
Mix
Seed
Mono +MLV
Mix +MLV
Seed+MLV
Buffer
MLV
32ng recSyn
53
41
25
18
12
9

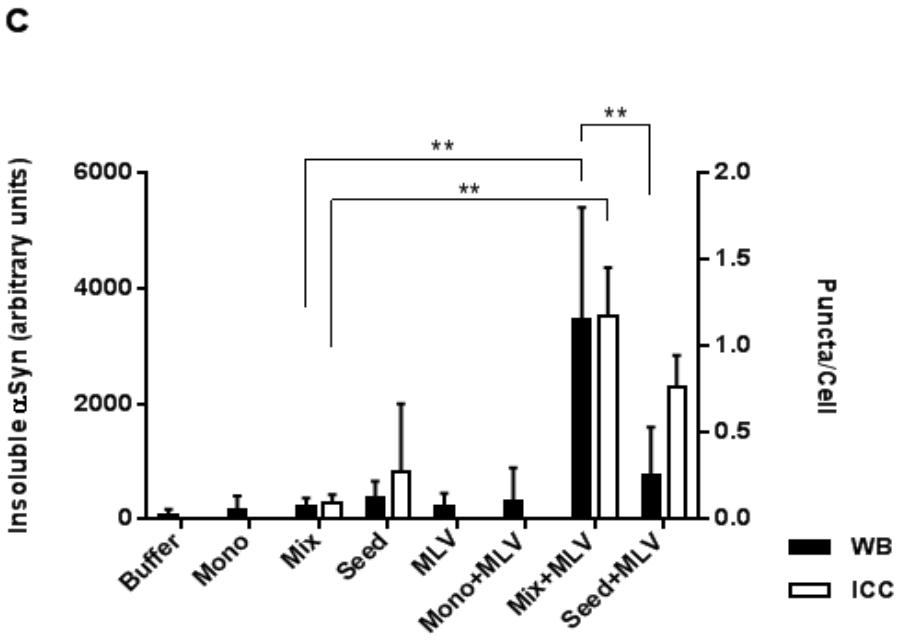

Figure 5-6. Seeds in the presence of tubules more efficiently induce intracellular aggregate formation than either seeds alone or seeds with MLV. Monomers, seeds or mix of FL α-Syn seeds were administered to the media of SH-SY5Y cells in the presence, or absence, of MLV. Aggregate formation was monitored by anti α-Syn (A) ICC or (B) WB. (C) WB quantification of insoluble α-Syn (N≥6) and ICC count of α-Syn positive puncta (green) overlapping with actin stain (red). DNA counter stain (blue). (N=3). At least 65 cells were counted for every treatment in each independent experiment. Error bars represent SEM. ** $p<0.05$.

The differences in the insoluble protein levels between mix+MLV and seeds+MLV cannot be explained by differences in the amounts of α-Syn introduced to the culture media, as those were comparable (Figure 5-7). These experiments shows that in the presence of MLV and monomers, seeds induce aggregate intra-cellular formation more efficiently than lipid free α-Syn.

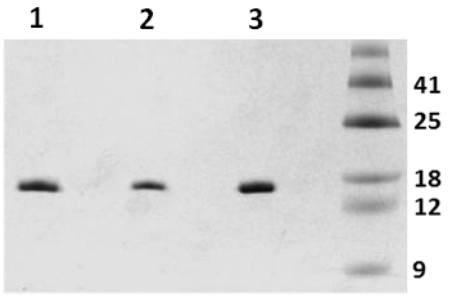

Figure 5-7. Analysis of FL α-Syn used for cellular internalization. Representing SDS/PAGE coomassie gel of (1) monomeric, (2) seeds and (3) mix. Equal volumes were loaded.

Heparin inhibits induction of intracellular aggregate formation mediated by tubule associated seeds

Previous studies determined that HSPG binding of proteopathic seeds and consequence macropinocytosis mediated their cellular uptake (Holmes et al., 2013; Horonchik et al., 2005). Next, the role of this pathway in internalization of seeds in the presence of lipids was tested. Heparin is a sulfated glycosaminoglycan previously shown to bind peptide sequences containing basic amino acids and structural domains in amyloids (Small et al., 1994; Warner et al., 2002; Watson et al., 1997). Heparin is predicted to compete for, and block, HSPG binding to α-Syn seeds. Mix+MLV was applied to SH-SY5Y culture media in the presence of increasing concentrations of Heparin and tested for aggregate formation by WB and ICC . Increasing concentrations of Heparin decreased the number of puncta formed in the cells in a dose response manner (Figure 5-8 A and 5-8B). The number of puncta observed per cell, decreased from 1.18, in the absence of Heparin, to 0.3 and 0.11 in the presence of 2 and 10µg/ml, respectively (Figure 5-8C). α-Syn was previously reported to be internalized by cells when administered to the media independent of lipids (Danzer et al., 2009; Desplats et al., 2009; Freundt et al., 2012; Holmes et al., 2013; Lee et al., 2008; Volpicelli-Daley et al., 2011). Therefore, the effect of Heparin on aggregate formation in cells treated with mix in the absence of MLV was also tested. In this model Heparin reduced aggregate formation from 0.09 to 0 aggregates per cell, though this change was not statistically significant (Figure 5-8A and 4-8C). WB analysis and quantification revealed a similar dose response trend. Insoluble α-Syn decreased 2 and 4 fold in the presence of 2 and 10µg/ml Heparin, respectively (Figure 5-8B and 5-8C). In the absence of lipids no changes were observed by the addition of Heparin. The lack of effect observed here may be explained by

the decreased sensitivity of the WB method, compared to the ICC, and also by relatively high background effect, seen with MLV alone.

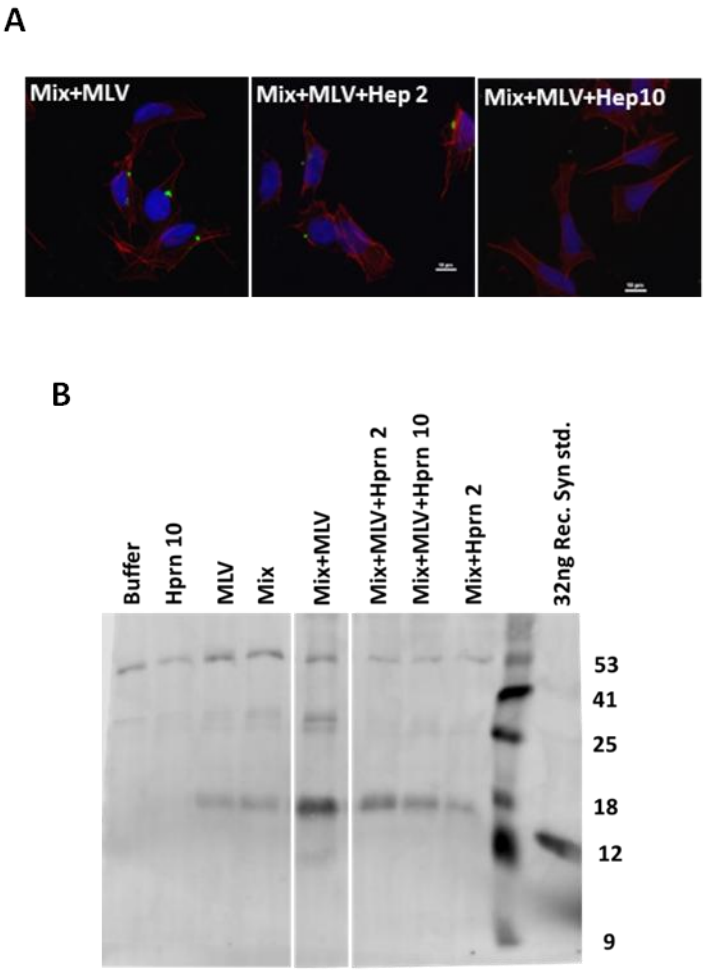

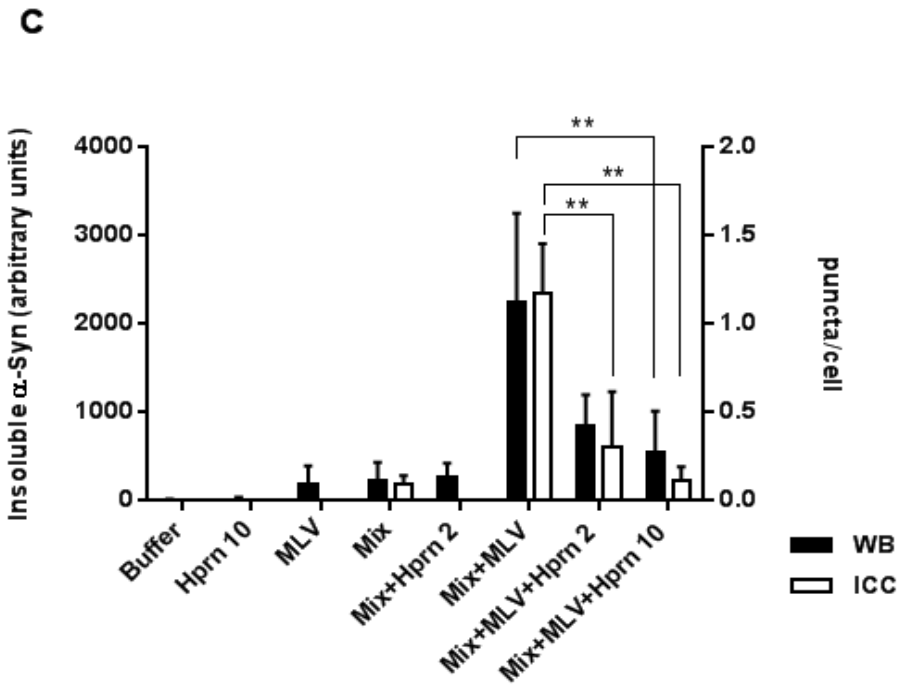

Figure 5-8. Heparin inhibits induction of intracellular aggregate formation mediated by seed-lipid tubules complexes. Monomers, seeds or mix of FL α-Syn seeds were administered to the media of SH-SY5Y cells in the presence, or absence, of MLV and with 0, 2 or 10µg/ml Heparin (Hprn2, Hprn10, respectively). Aggregate formation was monitored by anti α-Syn (A) ICC or (B) WB. (C) WB quantification of insoluble α-Syn (N≥3) and ICC count of α-Syn positive puncta (N=3) conducted as deacribed in Figure 5-6. At least 65 cells were counted for every treatment in each independent experiment. Error bars represent SEM. ** $p<0.05$.

These data show competitive inhibition of α-Syn mix uptake by Heparin applied in the presence of lipids and suggests a role for HSPG in the binding and uptake of lipid-associated seeds.

Heparinase III inhibits induction of intracellular aggregate formation mediated by tubules-associated seeds

As an additional, direct test of the requirement of the HSPG mechanism for α-Syn-lipid uptake, the effect of Heparinase III on internalization of the protein-lipid complex was evaluated. Heparinase III selectively cleaves, *via* an elimination mechanism, sulfated polysaccharide chains

containing 1-4 linkages between hexosamines and glucuronic acid residues from the cell surface. The activity of this enzyme was reported to inhibit cellular internalization of tau seeds in the absence of lipids (Holmes et al., 2013). SH-SY5Y cells were treated with increasing concentrations of Heparinase III, prior to applying mix+MLV. A dose dependent, inverse relationship, was observed between the enzyme concentration, used for treatment, and the number of cells with puncta (Figure 5-9A) or insoluble α-Syn band intensity (Figure 5-9B). The portion of cells with puncta decreased from 0.55 to 0.31, 0.13 and 0.07 in the presence of 0.001, 0.01 and 0.1 µg/ml Heprinase III, respectively (Figure 5-9C), represents an approximately 2-fold decrease in puncta formation for every 10 fold increase in enzyme concentration. The levels of insoluble α-Syn decreased in a similar manner by 2, 6 and 9-fold decrease in insoluble α-Syn from non-treated to 0.001, 0.01 and 0.1 µg/ml Heprinase III, respectively. Taken together, the Heparinase III experiments also support a critical role for HSPG in the internalization of lipid-associated α-Syn seeds.

A

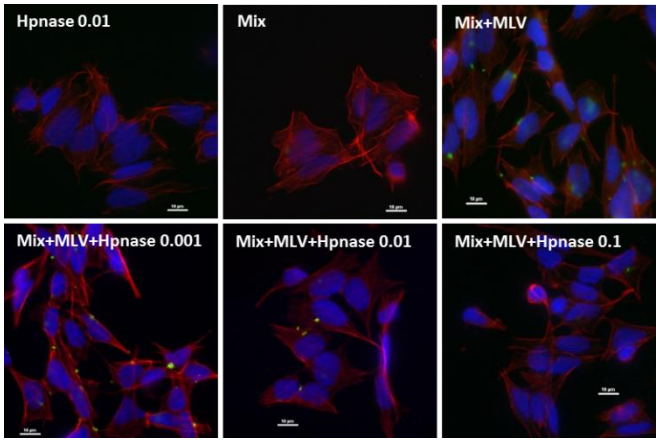

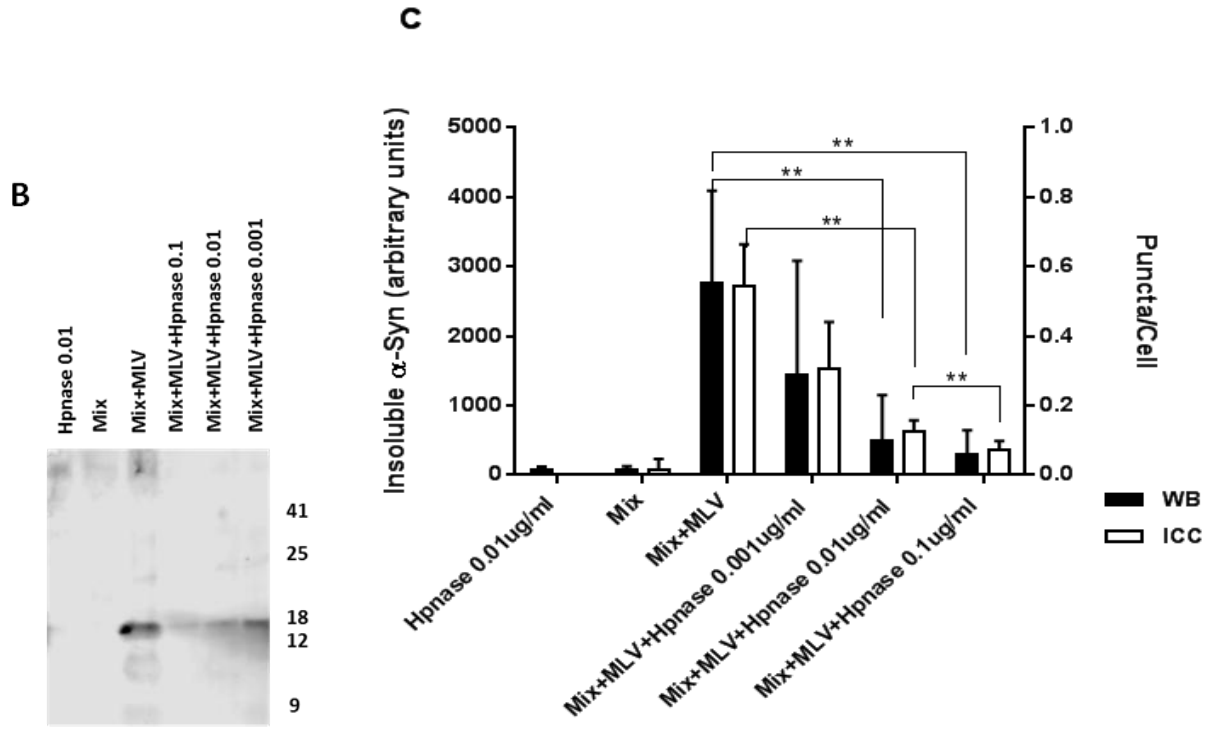

Figure 5-9. Heparinase III inhibits induction of intracellular aggregate formation mediated by seed-lipid tubules complexes. Monomers, seeds or mix of FL α-Syn seeds were administered to the media of SH-SY5Y cells, pretreated with 0.001, 0.01 and 0.1μg/ml P. heparinus Recombinant Heparinase III (Hpnase), in the presence of MLV. Internalization was monitored by anti α-Syn (A) WB (B) ICC. (C) WB (N≥3) quantification and ICC (N≥4) analysis were conducted as described in Figure 5-6. At least 130 cells were counted for every treatment in each independent experiment. Error bars represent SEM. ** $p<0.05$.

Discussion

PD and other synucleinopathies are, at present, only treated symptomatically. Evidence from recent studies suggests a prion-like model for the progression of Lewy pathology in PD, (Danzer et al., 2012; Danzer et al., 2009; Desplats et al., 2009; Freundt et al., 2012; Holmes et al., 2013; Kordower et al., 2008a; Lee et al., 2008; Luk et al., 2009; Volpicelli-Daley et al., 2011). A key feature of this model is the transmission of seeds between neurons in the (CNS). Thus, blocking such transmission by inhibiting either cell entry or exit may have promising therapeutic potential for slowing or even halting progression of the disease (Games et al., 2014;

Tran et al., 2014). In previous reports, using models recapitulating cell-cell transmission, α-Syn seeds were detected in the culture media both free and vesicle associated (Alvarez-Erviti et al., 2011; Danzer et al., 2012; Emmanouilidou et al., 2010). Furthermore, oligomeric α-Syn, thought to be a toxic agent, was more readily internalized and more toxic to recipient cells than free seeds (Freundt et al., 2012; Holmes et al., 2013; Lee et al., 2005a; Luk et al., 2009; Nonaka et al., 2010).

Important questions to be answered are whether both the lipid-associated and the free form of the protein are internalized by cells, which form is more efficiently internalized, and what mechanism is physiologically relevant. An interesting feature of α-Syn, a natively unstructured protein, is its ability to bend membranes into tubules structures while, by itself, assuming an α-helical structure in this process. In this study, the significance of membrane-tubules, induced by monomeric α-Syn, in the cellular uptake of α-Syn seeds was investigated.

EM and a novel turbidity assay, that allow structural characterization of lipid-associated monomeric α-Syn and seeds, indicate that monomers, but not seeds, efficiently induced tubulation of large liposomes (MLV). Seeds were observed in close proximity with both vesicles and tubules, but these methods are unable to support or rule out physical association. WB and cell staining were used to monitor and quantify the efficiency of each protein-lipid structure in inducing intracellular aggregate formation of α-Syn. Lipid-associated seeds induced aggregate formation much more efficiently than seeds alone. Moreover, adding seeds and lipids in the presence of monomers resulted in more aggregate formation than adding them in the absence of monomers. Intracellular aggregate formation was inhibited by blocking HSPG binding through competition and by an enzymatic digestion of HSPG.

Tubulation of MLV is consistent with previous reports demonstrating the ability of monomeric α-Syn to induce lipid tubulation of large liposomes (Jiang et al., 2013; Mizuno et al., 2012; Varkey et al., 2010a; Westphal and Chandra, 2013). The N-terminal AH of α-Syn penetrates into the monolayer, inducing curvature. The wedging of helices, from multiple monomers, all parallel to the same axis, forms the tubular structure (Jao et al., 2008; Mizuno et al., 2012; Varkey et al., 2010a). Tubulation of MLV, by C-terminally truncated α-Syn monomers, further supports this model by demonstrating that the C-terminal tail is not required for tubule formation. Monomeric α-Syn induced size decrease of SUV, consistent with previous reports (Varkey et al., 2013b). The differential effect of monomeric α-Syn on MLV *vs.* SUV might be due to differences in the curvature and the lipid packing of liposomes of different sizes. Insertion of AH into the better packed, low curvature MLV, pushes phospholipids apart and induces large structural rearrangement in the membrane, while insertion between the highly curved, more loosely packed SUV phospholipids merely stabilizes their structure by alleviating the tension between the two bilayers of the vesicle. Truncated α-Syn induced thinner tubules with MLV and smaller vesicles with SUV compared to FL α-Syn. This may be due to a larger number of truncated *vs.* FL α-Syn molecules bound to the lipids. The presence of the highly acidic C-termini may present an electrostatic repulsion to the negatively charged lipids leading to a spatial hindrance interfering with the binding of FL α-Syn to the liposomes.

Minimal tubulation of MLV with seeds was observed, consistent with a previous report showing lack of liposome tubulation by fibirls (Jiang et al., 2013). The lack of efficient tubulation may be explained, based on the "wedging helix" model, by the structural restraint on the protein, which when in a stable β-sheet amyloid form, cannot readily convert into the α-helical conformation and bend membranes. Indeed, aggregation and lipid binding were

previously demonstrated to be competitive processes (Zhu and Fink, 2003). The minimal tubulation observed may be attributed to "tubulation activity" of residual monomeric α-Syn present in the protein solution, a result of an equilibrium between fibrils and monomers (unpublished). Seeds were observed in close proximity to vesicles in the EM micrograph, but methods used in this study does not allow detection of direct interaction. Thus binding of seeds to membranes through some other mechanism, which does not induce tubulation, cannot be ruled out, in fact, disruption of membranes by fibrillar forms of the protein has been reported (Munishkina et al., 2003).

In the mix, the presence of higher monomer concentration (~60% of the α-Syn in the sample) induce maximal tubulation on MLV, to an extent similar to monomers alone. These data suggest that seeds do not interfere with the process of membrane tubulation by monomers. Furthermore, the data indicate that seeds may associate with tubules, as many of the seeds were observed in physical proximity to the monomer stabilized membrane tubules and had a "bundle-like" appearance, although direct interaction cannot be demonstrated with these techniques.

Significantly, intracellular aggregate formation is increased in the presence of lipids and is most efficient when both monomers and seeds are present with MLV. The increase in the total α-Syn level detected may be explained by the increased stability of the aggregates or their inhibition of protein turn-over systems previously described (Cook et al., 2012; Fonseca et al., 2015). Although seeds+MLV (in the absence of monomers) exhibited increased levels of aggregate formation over seeds alone these differences are not statistically significant. Preparation of "pure" seeds (compared to mix) requires an additional step to isolate insoluble seeds. This may have introduced variability to the product resulting in variable efficiencies of its

uptake between experiments, as indicated by the large error bars (seeds, seeds+MLV, Figure 5-6C). Additionally, no significant formation of aggregates was detected by seeds treatment in the absence of lipids, although such aggregation by similar treatments have been reported by others, using other detection methods (Danzer et al., 2009; Holmes et al., 2013; Volpicelli-Daley et al., 2011). This might be due to lower sensitivity of our detection methods or differences between the experimental systems. The structural differences between seeds+MLV and mix+MLV point to the presence of tubules in the latter preparation as a major difference (compare Figure 5-1A and 5-4A). Moreover the presence of tubules correlates with increased seeding efficiency implicating tubules in the cell entry mechanism. Further investigation is required to test this hypothesis. The model proposed here calls for the requirement of both monomer-induced tubules and seeds for efficient propagation of α-Syn pathology. This model may be tested *in-vivo* using mice over-expressing the human A30P α-Syn mutant on a triple Synuclein knock-out background. The A30P mutation accelerate seed formation but inhibits membrane binding and is thus predicted to be inefficient in liposome tubulation. In the lack of all Synuclein family members, previously shown to bind membranes, no lipid tubules will form and thus the model predicts that propagation α-Syn pathology in such mice would be inefficient (Varkey et al., 2010a). Indeed, α-Syn knock-out mice expressing two copies of human A30P α-Syn show no LB pathology and cell loss in the SN (Taylor et al., 2014).

Transcellular tubes termed tunneling nanotubes (TNTs) have been observed in neuronal cultures and shown to transfer prion-protein aggregates between cells. Though TNTs differ in size and structure from the tubules described in this work, the same principal of protein transfer may apply (Gousset and Zurzolo, 2009). Proteins with amphipathic helix domains, that induce curvature and form tubules *in-vitro*, participate in membrane trafficking in the cell (Drin and

Antonny, 2010b). Thus, the presence of extracellular tubules may increase the efficiency of α-Syn seeds uptake or their release from endocytic vesicles.

Inhibition of HSPG binding, or its removal from the cell surface by digetion, decreased intracellular aggregate formation in a dose dependent manner implicating HSPG in internalization of α-Syn seeds in the presence of lipids. HSPGs' requirement for binding and uptake of infectious prions was identified a decade ago (Horonchik et al., 2005). More recently, Holmes et al. reported their role in the uptake of α-Syn and tau seeds, which were introduced lipid-free to culture media of cell-lines (Holmes et al., 2013). The data presented here adds another mechanistic aspect to the HSPG-dependent internalization of proteopathic seeds, demonstrating its relevance for lipid-associated uptake of α-Syn seeds. In this system, lipid-associated uptake was far more efficient, as reflected by higher aggregate formation in the cells.

Increased uptake could be achieved by the formation of "packed bundles" of seeds and tubules, promoting an increased local concentration of seeds in the vicinity of HSPG, that allow the cells to engulf higher levels of seeds, in the previously described, macropinocytic process (Holmes et al., 2013). Association with tubules may also render seeds more accessible to interact with cell surface HSPG, thereby increasing the efficiency of their uptake, for example, by inducing receptor clustering or by other means of increasing receptor activation. Endocytosed seeds or monomers may interact with membranes of endocytic vesicles and rupture them or otherwise modify their structure to gain access into the cytoplasm.

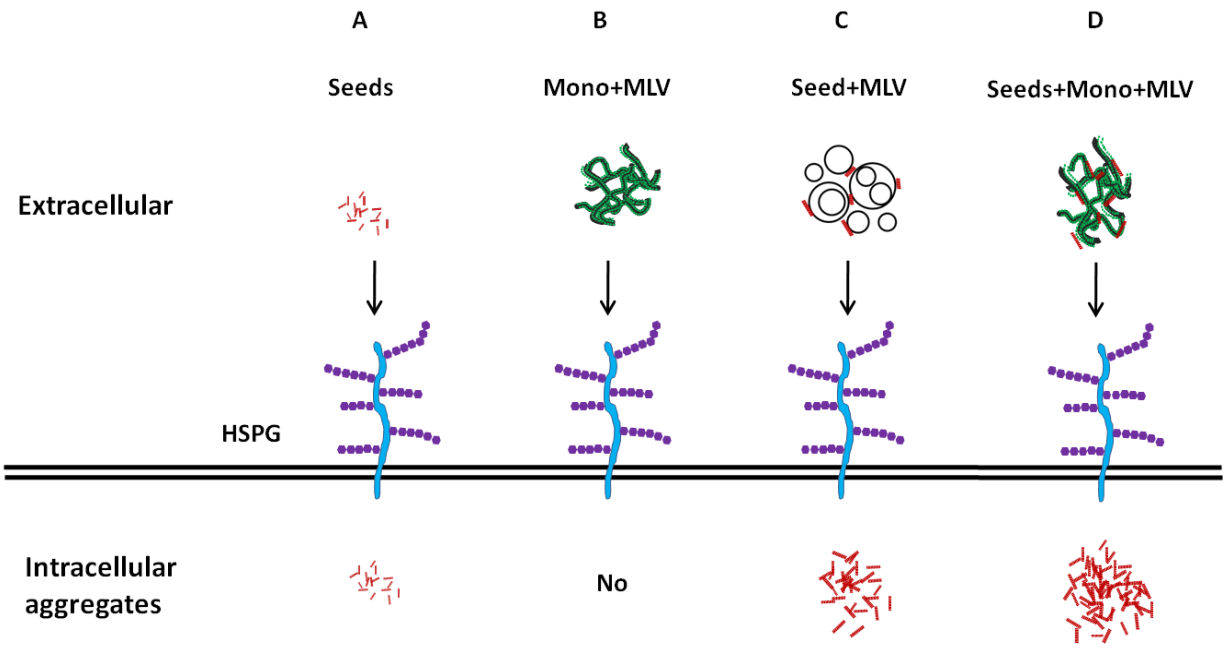

Figure 5-10. Suggested model for uptake of lipid-associated α-Syn. (A) Lipid free seeds are internalized by cells in an HSPG dependent uptake . (B) Monomeric α-Syn induce liposomes into tubules, *via* its N-terminal portion, but does not induce cellular aggregate formation. (C) Seeds are inefficient in inducing liposome tubulation but induce cellular aggregate formation. (D) Monomers induce tubules formation in the presence of seeds. Tubules associated seeds induce extensive aggregate formation in the cell in an HSPG dependent manner.

In conclusion, this work suggests a lipid-based model for uptake of α-Syn proteopathic seeds by cells. This mode of internalization is far more efficient, than internalization of lipid free seeds (Figure 5-10). Specifically, formation of lipid tubules, induced by the presence of monomeric α-Syn, increases the uptake of seeds. This model of transmission suggests novel approaches to interfering with intracellular transmission of α-Syn seeds.

CHAPTER SIX: EFFECT OF PD MUTATION A30P ON TUBULE MEDIATED UPTAKE OF SEEDS

This chapter discusses preliminary data obtained to examine additional aspects of the of the lipid-associated α-Syn seed uptake hypothesis. Data described here should be considered with caution as most experiments described here miss sufficient number of repeats to achieve statistical significance (and quantification) and some miss informative (though not critical) controls. Upon completion, the experiments described here will shed light on the contribution of α-Syn monomer-induced tubules for transmission of α-Syn seeds.

Results

A30P α-Syn mutant is known to have lower affinity for membranes compared to WT (Ulmer and Bax, 2005). The effect this mutation has on lipid tubulation was examined by a series of experiments to structurally characterize both protein and membranes in the complex. The effect of MLV liposome binding on monomeric A30P α-Syn secondary structure was assessed using circular dichroism (CD). A30P was mixed with MLV (1:20 molar ratio, respectively) or buffer (20mM phosphate) and incubated for 30 minutes prior to CD analysis. The CD spectra curves observed (Figure 6-1) represents a structural transition from a coiled-coil (unstructured), in the absence of MLV, to α-helix in its presence. Buffer and MLV alone had no contribution to the observed spectra.

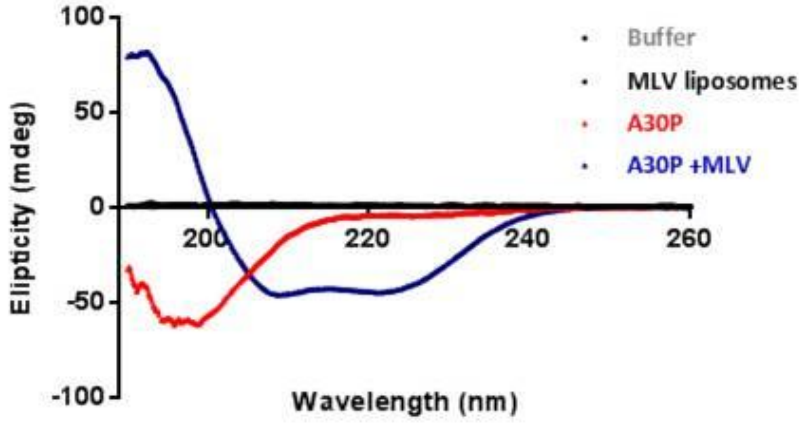

Figure 6-1. Monomeric A30P assumes α helical structure upon binding to POPG-MLV in the absence of salt. A30P α-Syn was mixed with MLV in 20mM phosphate (blue) or with buffer alone (red). Change in secondary structure was observed by CD. Buffer (grey) and MLV (black) controls are also represented.

Next, the effect of monomeric WT and A30P α-Syn on the structure of lipids in the presence of low and high ionic-strength was assessed. Salt was used as it is known to have an effect on membrane binding by α-Syn. To simulate physiological ionic-strength 150mM of sodium chloride were used. WT and A30P α-Syn were mixed with MLV and incubated for 30 minutes before observed by EM (Figure 6-2). Monomeric WT protein in the presence of low and high ionic-strength, and A30P at low ionic-strength, all induced tubule formation from MLV. Tubule morphology varied between these conditions. WT in buffer alone induced formation of thin tubes, with uniform structure and width, while WT in the presence of 150mM NaCl and A30P in buffer induced formation of thicker tubules, at varying width. Small vesicles are also induced by WT+NaCl and A30P in greater numbers than by WT alone.

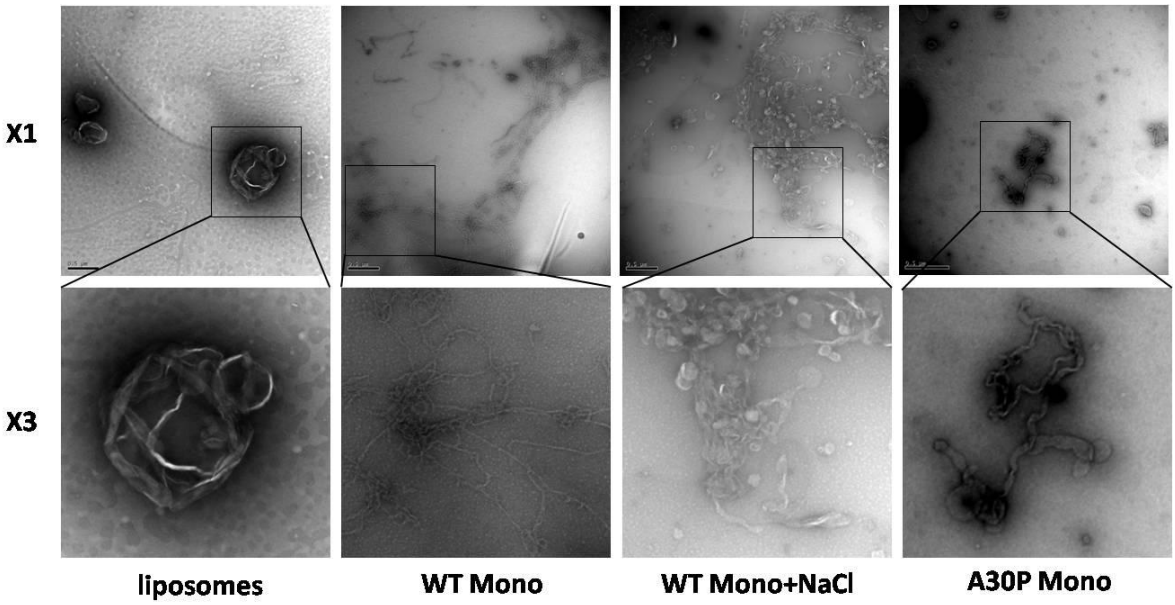

Figure 6-2. Monomeric WT and A30P α-Syn induce tubulation of liposomes under low ionic-strength. EM images of MLV incubated with monomeric WT or A30P α-Syn. Bar = 0.5μm. The boxed part of the top are magnified 3 fold at the bottom raw for better observation of small objects. Representative images were selected out of at least 5 fields per treatment, and at least 2 experimental repeats (N≥2).

To further investigate the effect of ionic-strength on membrane tubulation by the two α-Syn variants, lipid turbidity assay was employed. MLV were incubated with monomers and mix preparations of WT and A30P α-Syn and lipid turbidity was measured (Figure 6-3). Of note, in this experiment the plate format of this assay was employed (in contrast to the cuvette format, previously described). Due to the shorter wave-path in this format overall turbidty values span a narrower range, compared with the cuvette format.

Both monomeric WT and A30P decrease lipid turbidity by approximately 45% MLV. This reduction in turbidity is consistent with lipid binding and tubulation induction, as indicated by previous experiments (Figure 6-1 and 6-2). Interestingly, WT monomers induce turbidity decrease to the same extent in low or high ionic-strength, while A30P monomers have no affect on turbidity at high ionic-strength. Mix samples of either WT or A30P at low ionic-strength

decrease lipid turbidity by a smaller extent, 17% and 9%, respectively. At high ionic-strength neither WT nor A30P mix affect turbidity.

These results suggest that high ionic-strength have negative effect on liposome tubulation by mix of both variants. Strikingly, 150mM sodium chloride abolishes liposome tubulation by A30P monomers, while there is little effect on tubulation by monomeric WT.

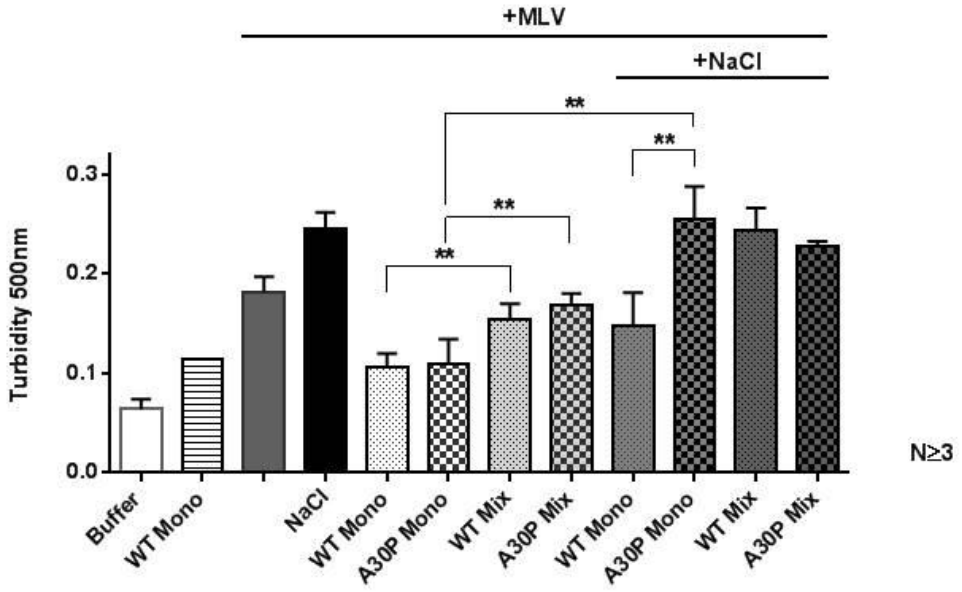

Figure 6-3. Change in light scattering of liposomes and lipid tubes. Light scattering measured to quantify the extent of MLV tubulation by WT and A30P α-Syn monomers and mix in the presence ,or absence of 150mM NaCl. Error bars represent SEM. N≥3. ** $p<0.05$.

The A30P mutation affects the aggregation propensity of α-Syn. *In-vitro* A30P forms oligomers, but fibril elongation is inhibited by this mutant (Yonetani et al., 2009). Next, the effect of WT and A30P α-Syn mix on intracellular aggregate formation was examined using the α-Syn uptake assay. For increased aggregate formation, differentiated SH-SY5Y cells stably transfected with human α-Syn (SH-SY5Y/hSyn) were used. These cells express higher levels of α-Syn resulting in more cytosolic protein susceptible to conversation and aggregation by internalized seeds. Mix α-Syn samples of either WT or A30P, pre-incubated in the presence or

absence of MLV and 150mM NaCl were introduced to the growth media. Aggregate formation was assessed 48 hours later by WB and ICC (Figure 6-4). For ICC, cells were co-stained with anti-pS129 recognizing phosphorylated serine 129 (green), a marker for LB deposited α-Syn (Fujiwara et al., 2002), and a second antibody, which recognizes a central sequence epitope (anti Syn, red). Aggregates, in the form of puncta in the cells, were observed only with WT mix+MLV. The other treatments show fade staining throughout the cytoplasm, representative of soluble protein. Blot data is partially consistent with ICC showing insoluble aggregate formation (lanes marked by P) in WT mix alone and WT mix+MLV. Both analyses exihibit no aggregate formation for A30P mix either in the presence or in the absence of MLV.

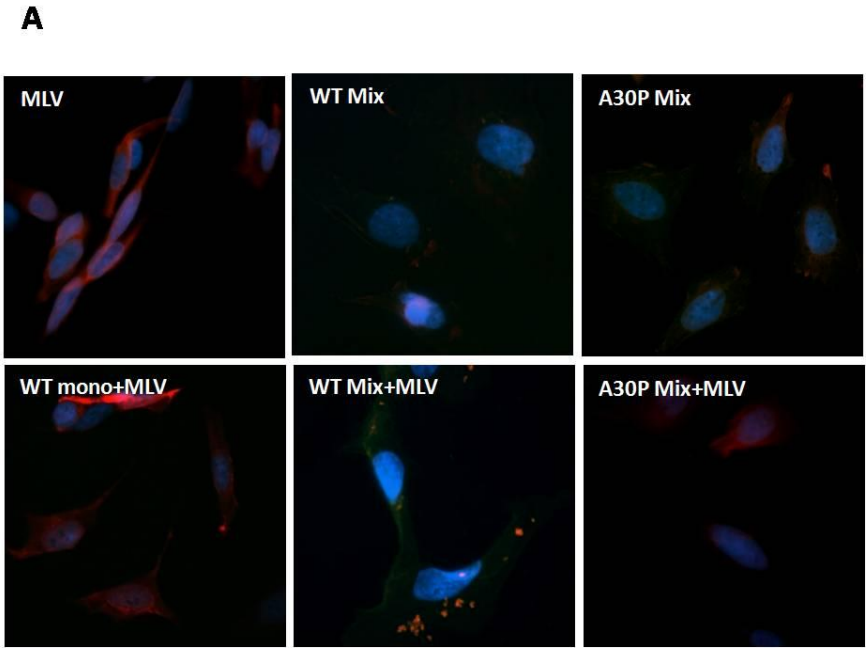

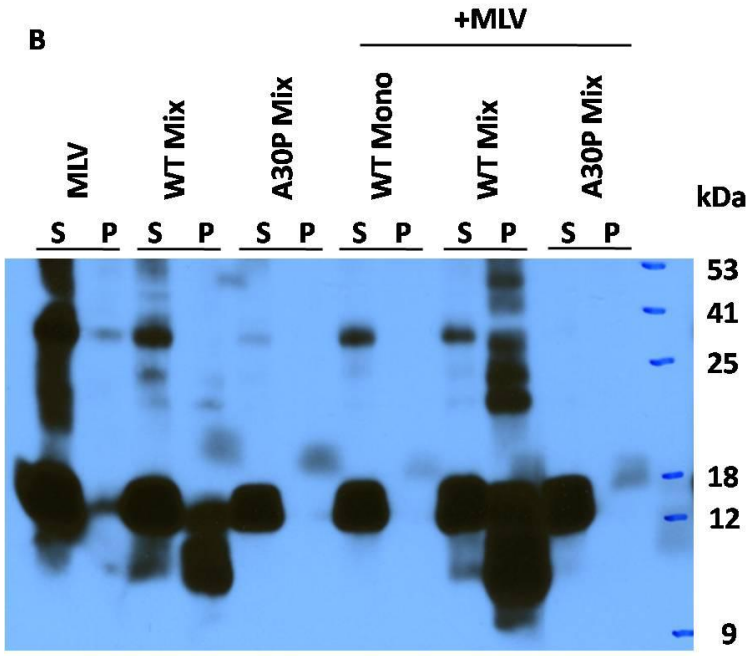

Figure 6-4. WT, but not A30P α-Syn mix, induce efficient intra-cellular aggregate formation in the presence of MLV. α-Syn WT and A30P mix were administered to the media of SH-SY5Y/hSyn cells in the presence, or absence, of MLV. (A) ICC or Aggregate formation was monitored by anti α-Syn (red) and anti pS129 (green) least 15 cells were counted for every treatment. (B) WB. Both triton-X soluble (S), and insoluble (P) fractions are presented.

Discussion

The structural data described here, suggests that ionic-strength affects the interactions of α-Syn with lipid membranes. This is consistent with previous data suggesting a two component interaction model of α-Syn with membranes: (1) Hydrophobic interaction component - facilitated by the insertion of the hydrophobic face of the α- helix between the lipid acyl chains in the monolayer. (2) Electrostatic component - facilitated by the interaction of lysine residues, lining the hydrophobic face, with the negatively charged phosphate headgroups (Jao et al., 2008). The A30P mutation introduces proline, an amino acid known as a helix breaker, in the region associated with helix formation. This is thought to disrupt secondary structure and weaken

membrane interaction (Ulmer and Bax, 2005). This change renders the protein more sensitive to salt, which is known to disrupt electrostatic interactions. Indeed, interaction of A30P mutant with phospholipids was reported as weaker and less tolerant to salt than that of WT (Jo et al., 2002; Stockl et al., 2008). However, in the current study no differences in tubulation induction are observed between monomeric WT and A30P at low ionic-strength. These contradictions can be explained by the differences in the membrane properties used here compared to previous reports. In previous reports mixtures of phosphatidyl choline (PC), a zwitter-ionic lipid, with anionic lipids were used which would result in a less negatively charged membrane. Here PG, a pure anionic lipid was used here, which may account for tighter interaction with the A30P making it less sensitive to disruption by salt ions.

The data presented here provides important clues about the interaction of A30P with lipids. However, it is partial and more experiments are required before clear conclusions can be drawn. Secondary structure analysis of monomeric A30P by CD is essential to study the interactions of this protein with MLV at high ionic-strength. There are inconsistencies between the turbidity data, obtained by the plate format, to that obtained by measuring turbidity in cuvettes (e.g. Figure 5-1C). Relative turbidity of monomeric WT+MLV and mix+MLV can be used as internal standards to compare the two measuring techniques. This comparison shows approximately 80% and 90% reduction in turbidity for monomers and seeds, respectively, when measured in cuvettes (Figure 5-1C), but only 40% and 17% when measured by using the plate format (Figure 6-3). These differences suggest that when using the plate format the measured effect is underrepresented.

Images of EM analysis of neither of the mix samples were obtained to assess tubule formation under any conditions and importantly, EM images of A30P interaction with MLV at high ionic-strength were not obtained, so definitive outcome of this interaction cannot be concluded.

The use of 150mM sodium chloride is both within the physiological realm and presents a condition by which monomeric α-Syn binding to membranes and the accompanying liposome tubulation, differ for WT and A30P. Thus using these conditions provides a simple system to test the tubules-associated uptake hypothesis.

The α-Syn uptake assay data suggests that lipid-associated WT α-Syn mix is more efficient than α-Syn mix alone, in inducing aggregate formation, while lipid-associated A30P mix is inefficient. Based on these observations a role for lipid tubulation may be considered, but for a number of reasons, it cannot be concluded based on the data presented here alone: First, due to missing structural data, specified above, it is difficult to draw a clear conclusion as to the structural outcome of either monomeric or A30P seeds interaction with MLV under high ionic-strength conditions. These data are critical for understanding the contribution of tubules in the uptake mechanism. Second, intra-cellular aggregate formation was induced by WT, but not by A30P, in the absence of MLV, suggesting that A30P may not be as potent aggregator or may not be transmitted as efficiently in the absence of lipids. Third, a simpler, and a probably more physiologically relevant experimental test to addressing the question in hand would be to use a mix of monomeric A30P with WT seeds. Such experiment will eliminate the potency question raised above and will solely address the question of tubule contribution for delivering seeds into the cell.

In summary, the data presented in this chapter provide clues to the role of lipid tubules in the transmission of α-Syn pathology and proposes a simple model to test this hypothesis.

CHAPTER SEVEN: PROSPECTUS FOR FUTURE WORK

This work proposes a novel model for the cellular internalization of α-Syn seeds. Further investigation of two aspects of this model will highlight its physiological relevance and provide a better understanding of the mechanistic aspects involved in it.

In order to test the physiological relevance of the proposed model it is important to assess the existence of α-Syn-associated lipids in the extracellular space and to examine their structure. As the work highlights a process involved in the pathological propagation of α-Syn seeds, a relevant source of specimen for such examination would be the body fluids of PD patients, animal model or media collected from a PD cell model. Monomers and aggregates of α-Syn have been detected in human body fluids and culture media (El-Agnaf et al., 2003; Lee et al., 2008). Antibody based separation and detection techniques will allow the detection and identification of α-Syn and co-precipitants from the sample. Lipid separation and analysis techniques will enable profiling of lipids. Electron and high-resolution microscopy can be used to identify particular protein-lipid structures. Finally, biochemical techniques, using specific enzymes and inhibitors will assess the requirement of lipids in the uptake α-Syn. Using these methods may allow to assess the presence of α-Syn associated lipids and their structure. It will further test the requirement of lipids for the internalization of α-Syn by cells.

The α-Syn-liposome complexes tested here were produced *in-vitro* using synthetic recombinant protein and pure liposomes. Liposomes were made pure from POPG, an anionic lipid, previously reported to be tubulated by α-Syn (Jiang et al., 2013; Mizuno et al., 2012; Varkey et al., 2010a). A key feature of the model is the formation of lipid tubules as a mean to increase uptake of seeds. In this study tubules and seeds were observed in close proximity but direct association could not be determined for two reasons: First, lipid tubules induced by

monomeric α-Syn have very similar morphology to that of seeds, which makes it difficult to distinguish the two entities by using EM (Table 5-1 and Figure 5-5). Second, unlike monomeric α-Syn, binding of seeds to liposomes (if such binding indeed takes place) result in no measurable change. Revealing the detailed structure of tubules associated with seeds including their morphological features and the stoichiometry involved would contribute to our understanding of the mechanism of uptake. These can be explored using Fluorescence resonance energy transfer (FRET) and fluorescence microscopy.

Receptor clustering play a role in endocytosis (Schwartz, 1995). Clustering of the syndican-4 HSPG by FGF2 has been suggested as a key step in its endocytosis (Tkachenko and Simons, 2002). Similarly, it is possible that tubules function as scaffolds that hold multiple α-Syn seeds thereby making an avid ligand for clustering of their respective HSPG. Cross-linking of seeds held by flexible linkers can test this hypothesis. If this hypothesis proves valid an increased efficiency of internalization would be expected with an increase in the number of cross-linked seeds, at least up to certain saturation level.

A second line of research should investigate the details of the internalization mechanism of lipid-based propagation. The relationship between lipids and proteins involved in the internalization and their contribution for uptake can be explored by titration experiments. Increased cytoplasmic aggregate formation can be an outcome of exposing the cells to higher concentration of external seeds. Alternatively, increasing tubules formation by higher lipid and/or monomer concentration may increase the efficiency of the uptake process and lead to the same result.

Multiple types of proteoglycans exist. Cell surface HSPG use different mechanisms to internalize bound ligands (Christianson and Belting, 2014). The identity of the proteoglycan

involved may provide clues as to the mechanism involved in the internalization of α-Syn seeds. For example: glypicans have a GPI anchored core protein, while syndicans' core protein have a trans-membrane cytoplasmic domain (Esko JD, 2009). Each of these structures may imply a different mechanism of ligand uptake, which may be triggered directly by the HSPG or involve additional surface receptors (Christianson and Belting, 2014). An experimental approach involving cross-linking and immuno-precipitation may identify the interacting entities and elucidate the mechanism that takes place in the initial steps of the uptake process. Genetic manipulations of identified factors will ascertain their role in the process.

An important question is whether the source of aggregates detected in the cells is endogenous α-Syn protein or is it the externally added seeds internalized by the cell. Distinguishing external seeds from cell expressed protein can help clarify this question. An effective source of external seeds for this purpose would be the use of C-terminally truncated α-Syn. These readily aggregate, making them easy to produce, and may effectively seed conversion of FL endogenous α-Syn into fibrils. Molecular weight differences and specific antibodies distinguish FL from truncated α-Syn proteins.

Seeds internalized through the HSPG pathway are suggested to use macropinocytosis, which later converges with the endo-lysosomal pathway (Holmes et al., 2013; Wittrup et al., 2009). Thus, induction of aggregation of intracellular α-Syn requires that seeds escape the lumen of endosomes to gain direct access into endogenous cytoplasmic α-Syn (routes seeds may use to gain direct access to cytoplasmic α-Syn are specified in chapter three). HSPG may co-internalize with their respective ligands and take place in the lumen of endocytic vesicles (Christianson et al., 2013). Studies show that HSPG bind amyloids and may protect them from proteolytic degradation (Gupta-Bansal et al., 1995). Together these findings suggest that HSPG bound seeds

may be protected from lysosomal degradation before escaping it. However, other escape routes may also be utilized (Kämper et al., 2006; Salomone et al., 2012; Turk et al., 2002). Genetic manipulation of key endocytic proteins and co-localization with endocytic markers can be used to determine how far down the endocytic route internalized seeds travel. The differences in the pH environment between the lumen of endocytic vesicles and the cytoplasm may be exploited to monitor escape of seeds into the cytoplasm.

In summary, the experimental approaches proposed in this chapter may help to determine the physiological relevance of lipids and their specific membrane structures involved in the cellular uptake of α-Syn. It will further highlight the details of the uptake and internalization mechanism mediating the transcellular aggregation of pathogenic α-Syn seeds. The knowledge gained can be used to target factors in this mechanism to interfere with, or halt, propagation of LB pathology in PD and other synucleinopathies.

APPENDIX A: MATERIALS AND METHODS

Materials

Phosphate inhibitors cocktail 2 and 3, Triton X100, Pen/Strep, Geneticin (G-418) Ammonium Sulfate, Thioflavin T, All-trans retinoic acid, Heparin sodium salt from porcine intestinal mucosa (Sigma, St Louis, MO, USA). Alexa Fluor 555 phalloidin, F-actin staining, Hoechst 33342-DNA staining, ProLong Gold Anti fade Mountant, GlutaMAX cell culture medium, Heat inactivated fetal Bovine Serum, BCAPRotein Assay, ECL substrate (Life technologies, Grand Island, NY). Milk powder (Sam's Club). Complete Protease inhibitor cocktail, ProSieve color protein markers (Roche-Lonza, San Francisco, CA). Bradford Protein Assay (BioRad).

Phenyl Sepharose 6 Fast Flow, DEAE -Sepharose Fast Flow (GE Healthcare, Pittsburgh, PA). P. heparinus Heparinase III Recombinant Protein (R&D Systems, Minneapolis, MN). Bradford assay regent (Bio-rad, Hercules, Ca). SH-SY5Y neuroblastoma cell line (ATCC, Manassas, VA). 1-hexadecanoyl-2-(9Z-octadecenoyl)-sn-glycero-3-phospho-(1'-rac-glycerol) sodium salt (POPG) (Avanti polar lipids, Alabaster, AL). Primary antibodies: monoclonal mouse anti Rat α-Syn IgG (BD Transduction Laboratories, San Jose, CA), mouse monoclonal anti α-Syn LB509 (Abcam Cambridge, MA). Secondary antibodies: goat anti mouse IgG 680RD conjugated (LiCOR, Lincoln, NE), goat anti mouse FITC conjugated (Jackson Immunoresearch, West Grove, PA).

SH-SY5Y/hSyn - were a kind gift from Dr. Harry Ischiropoulos (U. Penn)

α-Syn Expression and Purification

α-Syn was inserted into the pET28a vector using NcoI and HindIII restriction sites and expressed in the BL-21 line of E. coli. Large scale (1-4L) cultures were grown to OD600 of 0.5-

0.75, and expression of α-Syn was induced by adding IPTG to a final concentration of 500μM. After the addition of IPTG, growth of the cultures was continued at 37°C for 4 hours with shaking. After 4 hours, cells were harvested by centrifugation at 5000xg for 5 minutes at 4°C in a fixed-angle rotor (Beckman Coulter). Lysis was performed in 20mM Tris, pH=7.6 at, 20mM NaCl, Protease Inhibitor Cocktail Tablet at 4°C (10mL lysis buffer for each liter of culture). Cells were disrupted by sonication for 6 minutes in an ice water bath (Branson Sonifier 450). The cell lysate was spun at 40,000xg for 20 minutes at 4°C in a fixed-angle rotor and the supernatant was collected. The supernatant was heated to 90°C for 10 minutes, in a water bath, followed by centrifugation at 40,000xg for 20 minutes. The supernatant was brought to a final concentration of 1M $(NH_4)_2SO_4$, and 10mL of a 50% slurry of charged Phenyl Sepharose 6 Fast Flow beads in 20mM Tris, pH=7.6, 20mM NaCl, 1M $(NH_4)_2SO_4$ was added. The solution was allowed to incubate with the resin for 1 hour with rocking at 4°C, in a glass column (BioRad). The flowthrough was retrieved and the resin was washed with 10mL wash buffer (20mM Tris, pH=7.6, 20mM NaCl, 1M $(NH_4)_2SO_4$). The flowthrough and wash fractions were pooled, brought to a final concentration of 3M $(NH_4)_2SO_4$, and allowed to agitate for 1-2 hours at 4°C. The sample was then centrifuged at 40,000xg for 20 minutes at 4°C in a fixed angle rotor. The pellet was resuspended in 10mL of 20mM Tris, pH=7.6, 20mM NaCl, and dialyzed into 20mM Tris, pH=7.6 at 4°C, 20mM NaCl, 1mM EDTA with 3500 Dalton MW cut-off dialysis tubing (Spectra/Por). The protein was dialyzed by 3 cycles, against 2L buffer each, for over 36 hours. After dialysis, the protein was loaded onto a DEAE Sepharose Fast Flow anion exchange column and eluted with 8-25% gradient of 20mM Tris, pH=7.2, 1M NaCl. All fractions were analyzed by SDS-PAGE and fractions of desired purity were pooled and dialyzed into storage buffer (20mM sodium phosphate, pH=7.6) using 3500 Dalton MW cut-off dialysis tubing

(Spectra/Por). The purified α-Syn was, aliquoted, snap-frozen in liquid nitrogen, and stored at -80°C. 1% uranyl acetate solution (Electron Microscopy Sciences).

In-vitro Aggregation and Seed Preparation

Preparative samples containing 200μL α-Syn at 100-300μM, or analytical samples (for aggregation monitoring) containing α-Syn, with 20μM Thioflavin T (ThT) were prepared in a white 96 well assay plate (Costar). A 1/8" teflon bead was added to each well and the plates were sealed with an ABI-PRISM optical adhesive cover (Applied Biosystems). The plate was incubated at 37^{o}C in a fluorescence plate reader (Molecular Devices), and shaken for 5 minutes, in 10 minutes intervals, for at least 4 days. ThT fluorescence was monitored, at 450 nm excitation/482 nm emission. Formation of fibril was validated, structurally, by electron microscopy. *In-vitro* mix of monomers and seeds ("mix") was prepared by sonicating the prepared fibrils with 45 strokes, at level 3 output (Branson Sonifier 450). For pure seed preparation ("seed") insoluble α-Syn was separated from soluble by centrifuging at 150,000 xg for 20 min at 4^{o}C in TLA100 fixed rotor (Beckman Coulter OptimaTLX Ultracentrifuge). The concentration of seeds was determined by subtracting the concentration of soluble α-Syn, measured by BCA assay with a BSA standard (Life technologies), from the monomer concentration used for the fibril preparation. Formation of seeds was validated, structurally, by electron microscopy, and functionally by the efficiency of the seeds to nucleate fibril formation from monomers *in-vitro* as described above.

Liposomes Preparation

1-hexadecanoyl-2-(9Z-octadecenoyl)-sn-glycero-3-phospho-(1'-rac-glycerol) sodium salt (POPG) in chloroform was aliquoted into glass amber vials and dried under a gentle flow of Argon gas, then placed in a vacuum chamber, overnight, to remove chloroform residues. The

vials were filled with Argon gas, caped and stored in a desiccated container at -20^{o}C. MLV were prepared by suspending the lipid films in 20mM phosphate buffer pH 7.4 and vortexing on maximum speed for 4-5 minutes. Small unilamellar vesicles (SUV) were prepared by sonicating MLV on ice, for 4 cycles of 2 minutes each, at output level 3, with a 30 seconds break sonication, to allow cooling of the lipids. Formation of MLV and SUV was validated by electron microscopy. Length of sonication required for formation of SUV was determined by monitoring the decrease in light scattering of the sample at 500nm.

Electron microscopy of Lipid-α-Syn Complexes

Samples at a volume of 5 µl (~250ng protein) were deposited on a copper formvar grid 300 square mesh (Electron Microscopy Sciences), incubated for 1 minute and excess sample was drained using a filter paper. Staining was carried out with 1% uranyl acetate solution (Electron Microscopy Sciences) applied for 1 minute. Excess solution was removed with a filter paper. images were acquired using Tecnai G2 spirit transmission electron microscope (FEI) equipped with a LaB6 source using a voltage of 120 kV, equipped with Morada Soft Imaging System, side mount camera and iTEM FEI 5.0 software for acquiring images. Measurements of objects (vesicles, tubules or seeds) from EM images were performed using the measuring tool at Image J (v1.47). Representing objects with clear boundaries were selected for measurements. Long tubules with varied morphologies (as judged visually) were measured at a few places at fixed distances.

Lipid Turbidity Assay

α-Syn monomers, seeds or mix, were mixed with POPG MLV or SUV in 20mM phosphate buffer at a ratio of 1:20 (Protein:Lipid) and incubated for 30 minutes at RT. Light

scattering of the samples was measured at 500nm in a quartz cuvette (Cary 300 Bio UV-Vis spectrophotometer), or in a clear 96 well plate (Molecular Devices).

SH-SY5Y Cell Culture and Differentiation

SH-SY5Y neuroblastoma cell line was grown in DMEM/F-12, GlutaMAX with 10% heat inactivated fetal Bovine Serum and Pen/Strep, in 10 cm culture plates at 37oC, 5% CO2. If SH-SY5Y/hSyn cells were used the media was also supplemented with 300µM G-418. Upon confluence cells were split to into 6 well plates either with or without 12mm cover slides at the well bottom. Cells were differentiated by administration of 20µM retinoic acid (Sigma, Cat#R2625) every other day for 6 to 14 days. Differentiation was verified by observing morphological changes of the culture (namely, extension of neurites).

α-Syn Uptake Assay

Differentiated SH-SY5Y or SH-SY5Y/hSyn cells, at approximately 80% confluence, were treated with a total of 170ng FL α-Syn monomeric, seeds or a mix. The protein was added in the presence or absence of MLV and Heparin or Heparinase at the indicated concentrations. For Heparinase III treatments, cell were treated, with indicated concentrations of the enzyme for 3-4 hours prior to protein addition. The protein was incubated with lipids for 30 minutes before diluting it into growth media. Heparin was added after incubation with lipids. The media in the wells was replaced with lipid-protein complexes, supplemented media. The cells were incubated with the protein-lipid complexes or controls for 48 hours before being processed for analysis by western blot or immunocytochemistry.

Cell Lysis and Sample Preparation for Detection of α-Syn

Treated cells in a 6 well plate were placed on ice. The media was aspirated and the cells were washed 3 times in 2ml/well of cold PBS before adding 200µl lysis buffer (50mM Tris pH 7.4, 150mM NaCl, 1% triton, a tablet of mini complete EDTA-free protease inhibitors and a cocktails 2 and 3 of phosphate inhibitors. The cells were scraped from the bottom of the wells using a cell lifter (corning costar) and collected into pre-chilled microtubes. The harvested cells were lysed by sonication of 65 strokes on ice, at output level 3 (Branson Sonifier 450). The samples' total protein level was measured using the Bradford assay with a BSA standard, and protein level was normalized across the samples in a volume of 180µL. The samples were fractionated by centrifugation at 100,000 xg, for 30 minutes at 4^{o}C (TLA100 fixed rotor in a Beckman coulter OptimaTLX Ultracentrifuge). The supernatant were collected into pre-chilled microtubes and the centrifugation tubes were flipped upside-down on a kimwipe, to drain residual liquid before resuspending the pellet in 180µL of 2% SDS in water by trituration through a 200µL tip. All samples were mixed with 5X sample buffer to a final concentration of 1% SDS, and heated to 100^{o}C for 5 minutes. The samples were stored at -80^{o}C, until analyzed, or analyzed directly by Western blotting.

Western Blotting

30µL samples (~20µg) were loaded on 10% polyacrylamide tricine gel containing 0.12% SDS and run for approximately 60 minutes at 160 volts (BioRad). ProSieve color protein markers was (5 µL) used to follow the progression of the electrophoresis process on the gel. PVDF Immobilon-FL Membrane (Merck/Millipore) was activated by rinsing in methanol and the proteins were transferred to the membrane at 90 volts for 120 minutes at 4^{o}C (BioRad). The proteins were fixed by incubating the membranes in 0.4% paraformaldehyde, TBS, 0.05% tween

(TBS-T) at RT for 30 minutes with shaking. The membranes were blocked by 5% milk in TBS-T (blocking buffer) for 1 hour and then incubated overnight with mouse anti Rat α-Syn IgG diluted 1:4000 in TBS-T, 4^{o}C. The membrane was washed 3 times in TBS-T and incubated for 1 hour with fluorophore conjugated goat anti mouse IgG, diluted 1:10000 in blocking buffer, at RT. The membrane was washed 3 times and scanned by LiCOR Odyssey CLx to quantify band intensity. The intensity of the 15 kDa band of insoluble α-Syn was quantified from at least 3 independent experiments. Statistical significance was calculated by student t-test using MS-Excel. Alternatively, membranes were incubated with HRP-conjugted goat anti mouse antibodies diluted1:10000 in blocking buffer washed and developed with ECL substrate for 5 minutes, before film exposure and development using Fuji Developing Machine.

Cell Immunostaining and Microscopy

Treated cells were washed, fixed with 4% paraformaldehyde in PBS for 10 minutes and permeabilized with 0.5% triton X100 for 5 minutes. The cells were blocked with 1% BSA in PBS and incubated for 1 hour with mouse monoclonal anti α-Syn LB509. The cells were washed with PBS and incubated with FITC conjugated goat anti mouse IgG for 1 hour, followed by washing and counter staining with Alexa Fluor 555 phalloidin (F-actin staining) and Hoechst 33342 (DNA staining). The slides were washed twice with PBS, and once with water. ProLong Gold AntifadeMountant was applied and the slides were mounted on cover glasses. The stained cells were observed using a fluorescent microscope (Nikon Eclipse TE2000-U). The images were analyzed using Nikon Software (NIS Elements, BR4.20.02) Nuclei and anti α-Syn punctate with actin overlap were counted to assess intracellular aggregate formation.

Circular Dichroism Spectroscopy

30μM alphα-Syn was pre-incubated with MLV liposomes in 20mM sodium phosphate buffer, pH=7.4, at room temperature for 30 minutes. Internal temperature was set to 25°C on a Jasco model J-810 spectropolarimeter. Spectra were scanned from 260 to 195 nm at` 100nm/min with a 1 second averaging time. The background was automatically subtracted using the background correction algorithm of the JASCO Spectra Analysis program.

Statistical Analysis

All experiments were repeated at least 3 times. Values in the figures are expressed as mean ± SEM. Differences were considered significant if p-values were less than 0.05. Statistical significance of values was calculated by two tail, student t-test using MS-Excel.

REFERENCES

Abeliovich, A., Schmitz, Y., Fariñas, I., Choi-Lundberg, D., Ho, W.-H., Castillo, P.E., Shinsky, N., Verdugo, J.M.G., Armanini, M., Ryan, A., *et al.* (2000). Mice Lacking α-Synuclein Display Functional Deficits in the Nigrostriatal Dopamine System. Neuron *25*, 239-252.

Aisenbrey, C., Borowik, T., Byström, R., Bokvist, M., Lindström, F., Misiak, H., Sani, M.-A., and Gröbner, G. (2008). How is protein aggregation in amyloidogenic diseases modulated by biological membranes? European Biophysics Journal *37*, 247-255.

Alim, M.A., Ma, Q.-L., Takeda, K., Aizawa, T., Matsubara, M., Nakamura, v., Asada, A., Saito, T., xkaji, M., and Yoshii, M. (2004). Demonstration of a role for a-synuclein as a functional microtubule-associated protein. Journal of Alzheimer's disease *6*, 435-442.

Alvarez-Erviti, L., Seow, Y., Schapira, A.H., Gardiner, C., Sargent, I.L., Wood, M.J., and Cooper, J.M. (2011). Lysosomal dysfunction increases exosome-mediated alpha-synuclein release and transmission. Neurobiol Dis *42*, 360-367.

Ambroso, M.R., Hegde, B.G., and Langen, R. (2014). Endophilin A1 induces different membrane shapes using a conformational switch that is regulated by phosphorylation. Proceedings of the National Academy of Sciences *111*, 6982-6987.

Angot, E., Steiner, J.A., Hansen, C., Li, J.-Y., and Brundin, P. (2010). Are synucleinopathies prion-like disorders? The Lancet Neurology *9*, 1128-1138.

Angot, E., Steiner, J.A., Lema Tome, C.M., Ekstrom, P., Mattsson, B., Bjorklund, A., and Brundin, P. (2012). Alpha-synuclein cell-to-cell transfer and seeding in grafted dopaminergic neurons in vivo. PLoS One *7*, e39465.

Appel, S.H. (2012). Inflammation in Parkinson's disease: cause or consequence? Movement Disorders *27*, 1075-1077.

Auluck, P.K., Caraveo, G., and Lindquist, S. (2010). α-Synuclein: membrane interactions and toxicity in Parkinson's disease. Annual review of cell and developmental biology *26*, 211-233.

Baba, M., Nakajo, S., Tu, P.-H., Tomita, T., Nakaya, K., Lee, V., Trojanowski, J.Q., and Iwatsubo, T. (1998). Aggregation of alpha-synuclein in Lewy bodies of sporadic Parkinson's disease and dementia with Lewy bodies. The American journal of pathology *152*, 879.

Beck, R., Sun, Z., Adolf, F., Rutz, C., Bassler, J., Wild, K., Sinning, I., Hurt, E., Brügger, B., Béthune, J., *et al.* (2008). Membrane curvature induced by Arf1-GTP is essential for vesicle formation. Proceedings of the National Academy of Sciences of the United States of America *105*, 11731-11736.

Bellingham, S.A., Guo, B., Coleman, B., and Hill, A.F. (2012). Exosomes: vehicles for the transfer of toxic proteins associated with neurodegenerative diseases? Frontiers in Physiology *3*.

Bernfield, M., Gotte, M., Park, P.W., Reizes, O., Fitzgerald, M.L., Lincecum, J., and Zako, M. (1999). Functions of cell surface heparan sulfate proteoglycans. Annual review of biochemistry *68*, 729-777.

Borghi, R., Marchese, R., Negro, A., Marinelli, L., Forloni, G., Zaccheo, D., Abbruzzese, G., and Tabaton, M. (2000). Full length α-synuclein is present in cerebrospinal fluid from Parkinson's disease and normal subjects. Neuroscience Letters *287*, 65-67.

Braak, H., Tredici, K.D., Rüb, U., de Vos, R.A.I., Jansen Steur, E.N.H., and Braak, E. (2003). Staging of brain pathology related to sporadic Parkinson's disease. Neurobiology of Aging *24*, 197-211.

Brundin, P., Melki, R., and Kopito, R. (2010). Prion-like transmission of protein aggregates in neurodegenerative diseases. Nature Reviews Molecular Cell Biology *11*, 301-307.

Burré, J., Sharma, M., and Südhof, T.C. (2014). α-Synuclein assembles into higher-order multimers upon membrane binding to promote SNARE complex formation. Proceedings of the National Academy of Sciences *111*, E4274-E4283.

Burré, J., Sharma, M., Tsetsenis, T., Buchman, V., Etherton, M., and Südhof, T.C. (2010). α-Synuclein Promotes SNARE-Complex Assembly in vivo and in vitro. Science (New York, NY) *329*, 1663-1667.

Chartier-Harlin, M.-C., Kachergus, J., Roumier, C., Mouroux, V., Douay, X., Lincoln, S., Levecque, C., Larvor, L., Andrieux, J., Hulihan, M., *et al.* α-synuclein locus duplication as a cause of familial Parkinson's disease. The Lancet *364*, 1167-1169.

Chen, L., and Feany, M.B. (2005). Alpha-synuclein phosphorylation controls neurotoxicity and inclusion formation in a Drosophila model of Parkinson disease. Nat Neurosci *8*, 657-663.

Choi, W., Zibaee, S., Jakes, R., Serpell, L.C., Davletov, B., Crowther, R.A., and Goedert, M. (2004). Mutation E46K increases phospholipid binding and assembly into filaments of human α-synuclein. Febs Letters *576*, 363-368.

Christianson, H.C., and Belting, M. (2014). Heparan sulfate proteoglycan as a cell-surface endocytosis receptor. Matrix Biol *35*, 51-55.

Christianson, H.C., Svensson, K.J., van Kuppevelt, T.H., Li, J.-P., and Belting, M. (2013). Cancer cell exosomes depend on cell-surface heparan sulfate proteoglycans for their internalization and functional activity. Proceedings of the National Academy of Sciences *110*, 17380-17385.

Conway, K., LEE, S.J., ROCHET, J.C., Ding, T., Harper, J., Williamson, R., and Lansbury, P. (2000). Accelerated Oligomerization by Parkinson's Disease Linked α-Synuclein Mutants. Annals of the New York Academy of Sciences *920*, 42-45.

Conway, K.A., Rochet, J.-C., Bieganski, R.M., and Lansbury, P.T. (2001). Kinetic stabilization of the α-synuclein protofibril by a dopamine-α-synuclein adduct. Science *294*, 1346-1349.

Cook, C., Stetler, C., and Petrucelli, L. (2012). Disruption of Protein Quality Control in Parkinson's Disease. Cold Spring Harbor Perspectives in Medicine *2*, a009423.

Cookson, M.R. (2005). The biochemistry of Parkinson's disease*. Annu Rev Biochem *74*, 29-52.

Cremades, N., Cohen, S.I., Deas, E., Abramov, A.Y., Chen, A.Y., Orte, A., Sandal, M., Clarke, R.W., Dunne, P., and Aprile, F.A. (2012). Direct observation of the interconversion of normal and toxic forms of α-synuclein. Cell *149*, 1048-1059.

Cuervo, A.M., Stefanis, L., Fredenburg, R., Lansbury, P.T., and Sulzer, D. (2004). Impaired degradation of mutant alpha-synuclein by chaperone-mediated autophagy. Science *305*, 1292-1295.

da Silveira, S.A., Schneider, B.L., Cifuentes-Diaz, C., Sage, D., Abbas-Terki, T., Iwatsubo, T., Unser, M., and Aebischer, P. (2009). Phosphorylation does not prompt, nor prevent, the formation of α-synuclein toxic species in a rat model of Parkinson's disease. Human molecular genetics *18*, 872-887.

Daher, J.P., Ying, M., Banerjee, R., McDonald, R.S., Hahn, M.D., Yang, L., Beal, M.F., Thomas, B., Dawson, V.L., and Dawson, T.M. (2009). Conditional transgenic mice expressing C-terminally truncated human α-synuclein (αSyn119) exhibit reduced striatal dopamine without loss of nigrostriatal pathway dopaminergic neurons. Molecular neurodegeneration *4*, 34.

Danzer, K., Kranich, L., Ruf, W., Cagsal-Getkin, O., Winslow, A., Zhu, L., Vanderburg, C., and McLean, P. (2012). Exosomal cell-to-cell transmission of alpha synuclein oligomers. Molecular Neurodegeneration *7*, 42.

Danzer, K.M., Haasen, D., Karow, A.R., Moussaud, S., Habeck, M., Giese, A., Kretzschmar, H., Hengerer, B., and Kostka, M. (2007). Different species of α-synuclein oligomers induce calcium influx and seeding. The Journal of Neuroscience *27*, 9220-9232.

Danzer, K.M., Krebs, S.K., Wolff, M., Birk, G., and Hengerer, B. (2009). Seeding induced by α-synuclein oligomers provides evidence for spreading of α-synuclein pathology. Journal of Neurochemistry *111*, 192-203.

Danzer, K.M., Ruf, W.P., Putcha, P., Joyner, D., Hashimoto, T., Glabe, C., Hyman, B.T., and McLean, P.J. (2011). Heat-shock protein 70 modulates toxic extracellular α-synuclein oligomers and rescues trans-synaptic toxicity. The FASEB Journal *25*, 326-336.

Davidson, W.S., Jonas, A., Clayton, D.F., and George, J.M. (1998). Stabilization of α-Synuclein Secondary Structure upon Binding to Synthetic Membranes. Journal of Biological Chemistry *273*, 9443-9449.

de Lau, L.M., Verbaan, D., Marinus, J., and van Hilten, J.J. (2014). Survival in Parkinson's disease. Relation with motor and non-motor features. Parkinsonism & related disorders *20*, 613-616.

Dehio, C., Freissler, E., Lanz, C., Gomez-Duarte, O.G., David, G., and Meyer, T.F. (1998). Ligation of cell surface heparan sulfate proteoglycans by antibody-coated beads stimulates phagocytic uptake into epithelial cells: a model for cellular invasion by Neisseria gonorrhoeae. Exp Cell Res *242*, 528-539.

Desplats, P., Lee, H.J., Bae, E.J., Patrick, C., Rockenstein, E., Crews, L., Spencer, B., Masliah, E., and Lee, S.J. (2009). Inclusion formation and neuronal cell death through neuron-to-neuron transmission of alpha-synuclein. Proc Natl Acad Sci U S A *106*, 13010-13015.

DeWitt, D.C., and Rhoades, E. (2013). alpha-Synuclein can inhibit SNARE-mediated vesicle fusion through direct interactions with lipid bilayers. Biochemistry *52*, 2385-2387.

Diao, J., Burré, J., Vivona, S., Cipriano, D.J., Sharma, M., Kyoung, M., Südhof, T.C., and Brunger, A.T. (2013). Native α-synuclein induces clustering of synaptic-vesicle mimics via binding to phospholipids and synaptobrevin-2/VAMP2, Vol 2.

Dikiy, I., and Eliezer, D. (2012). Folding and misfolding of alpha-synuclein on membranes. Biochimica et Biophysica Acta (BBA)-Biomembranes *1818*, 1013-1018.

Drin, G., and Antonny, B. (2010a). Amphipathic helices and membrane curvature. FEBS Lett *584*, 1840-1847.

Drin, G., and Antonny, B. (2010b). Amphipathic helices and membrane curvature. FEBS Letters *584*, 1840-1847.

Drin, G., Morello, V., Casella, J.F., Gounon, P., and Antonny, B. (2008). Asymmetric tethering of flat and curved lipid membranes by a golgin. Science *320*, 670-673.

Ejlerskov, P., Rasmussen, I., Nielsen, T.T., Bergstrom, A.L., Tohyama, Y., Jensen, P.H., and Vilhardt, F. (2013). Tubulin polymerization-promoting protein (TPPP/p25alpha) promotes unconventional secretion of alpha-synuclein through exophagy by impairing autophagosome-lysosome fusion. J Biol Chem *288*, 17313-17335.

El-Agnaf, O.M., Salem, S.A., Paleologou, K.E., Cooper, L.J., Fullwood, N.J., Gibson, M.J., Curran, M.D., Court, J.A., Mann, D.M., Ikeda, S., *et al.* (2003). Alpha-synuclein implicated in Parkinson's disease is present in extracellular biological fluids, including human plasma. FASEB J *17*, 1945-1947.

El-Agnaf, O.M.A., Salem, S.A., Paleologou, K.E., Curran, M.D., Gibson, M.J., Court, J.A., Schlossmacher, M.G., and Allsop, D. (2006). Detection of oligomeric forms of α-synuclein protein in human plasma as a potential biomarker for Parkinson's disease. The FASEB Journal *20*, 419-425.

Emmanouilidou, E., Elenis, D., Papasilekas, T., Stranjalis, G., Gerozissis, K., Ioannou, P.C., and Vekrellis, K. (2011). Assessment of alpha-synuclein secretion in mouse and human brain parenchyma. PLoS One *6*, e22225.

Emmanouilidou, E., Melachroinou, K., Roumeliotis, T., Garbis, S.D., Ntzouni, M., Margaritis, L.H., Stefanis, L., and Vekrellis, K. (2010). Cell-produced alpha-synuclein is secreted in a calcium-dependent manner by exosomes and impacts neuronal survival. J Neurosci *30*, 6838-6851.

Esko JD, K.K., Lindahl U. (2009). Proteoglycans and Sulfated Glycosaminoglycans In Essentials of Glycobiology, C.R. Varki A, Esko JD, et al., ed. (Cold Spring Harbor (NY): Cold Spring Harbor Laboratory Press).

Fahn, S. (2003). Description of Parkinson's disease as a clinical syndrome. Annals of the New York Academy of Sciences *991*, 1-14.

Farsad, K., and De Camilli, P. (2003). Mechanisms of membrane deformation. Curr Opin Cell Biol *15*, 372-381.

Fertuck, H.C., and Salpeter, M.M. (1974). Localization of Acetylcholine Receptor by (125)I-Labeled α-Bungarotoxin Binding at Mouse Motor Endplates. Proceedings of the National Academy of Sciences of the United States of America *71*, 1376-1378.

Fevrier, B., Vilette, D., Archer, F., Loew, D., Faigle, W., Vidal, M., Laude, H., and Raposo, G. (2004). Cells release prions in association with exosomes. Proc Natl Acad Sci U S A *101*, 9683-9688.

FH., L. (1912). Paralysis agitans. I. Pathologische anatomie. In Handbuch der Neurologie (Berlin: Springer), pp. 920-933.

Fonseca, T.L., Villar-Pique, A., and Outeiro, T.F. (2015). The Interplay between Alpha-Synuclein Clearance and Spreading. Biomolecules *5*, 435-471.

Freeman, D., Cedillos, R., Choyke, S., Lukic, Z., McGuire, K., Marvin, S., Burrage, A.M., Sudholt, S., Rana, A., O'Connor, C., *et al.* (2013). Alpha-Synuclein Induces Lysosomal Rupture and Cathepsin Dependent Reactive Oxygen Species Following Endocytosis. PLoS ONE *8*, e62143.

Freundt, E.C., Maynard, N., Clancy, E.K., Roy, S., Bousset, L., Sourigues, Y., Covert, M., Melki, R., Kirkegaard, K., and Brahic, M. (2012). Neuron-to-neuron transmission of α-synuclein fibrils through axonal transport. Annals of Neurology *72*, 517-524.

Fujiwara, H., Hasegawa, M., Dohmae, N., Kawashima, A., Masliah, E., Goldberg, M.S., Shen, J., Takio, K., and Iwatsubo, T. (2002). α-Synuclein is phosphorylated in synucleinopathy lesions. Nature cell biology *4*, 160-164.

Futaki, S., Suzuki, T., Ohashi, W., Yagami, T., Tanaka, S., Ueda, K., and Sugiura, Y. (2001). Arginine-rich peptides. An abundant source of membrane-permeable peptides having potential as carriers for intracellular protein delivery. J Biol Chem *276*, 5836-5840.

Gallop, J.L., Jao, C.C., Kent, H.M., Butler, P.J.G., Evans, P.R., Langen, R., and McMahon, H.T. (2006). Mechanism of endophilin N-BAR domain-mediated membrane curvature, Vol 25.

Games, D., Valera, E., Spencer, B., Rockenstein, E., Mante, M., Adame, A., Patrick, C., Ubhi, K., Nuber, S., Sacayon, P., *et al.* (2014). Reducing C-Terminal-Truncated Alpha-Synuclein by Immunotherapy Attenuates Neurodegeneration and Propagation in Parkinson's Disease-Like Models. The Journal of Neuroscience *34*, 9441-9454.

Georgieva, E.R., Ramlall, T.F., Borbat, P.P., Freed, J.H., and Eliezer, D. (2008). Membrane-bound α-synuclein forms an extended helix: long-distance pulsed ESR measurements using vesicles, bicelles, and rodlike micelles. Journal of the American Chemical Society *130*, 12856-12857.

Giasson, B.I., Duda, J.E., Murray, I.V., Chen, Q., Souza, J.M., Hurtig, H.I., Ischiropoulos, H., Trojanowski, J.Q., and Lee, V.M.-Y. (2000). Oxidative damage linked to neurodegeneration by selective α-synuclein nitration in synucleinopathy lesions. Science *290*, 985-989.

Giasson, B.I., Murray, I.V.J., Trojanowski, J.Q., and Lee, V.M.-Y. (2001). A Hydrophobic Stretch of 12 Amino Acid Residues in the Middle of α-Synuclein Is Essential for Filament Assembly. Journal of Biological Chemistry *276*, 2380-2386.

Gomes, C., Keller, S., Altevogt, P., and Costa, J. (2007). Evidence for secretion of Cu,Zn superoxide dismutase via exosomes from a cell model of amyotrophic lateral sclerosis. Neurosci Lett *428*, 43-46.

Gorbatyuk, O.S., Li, S., Sullivan, L.F., Chen, W., Kondrikova, G., Manfredsson, F.P., Mandel, R.J., and Muzyczka, N. (2008). The phosphorylation state of Ser-129 in human α-synuclein determines neurodegeneration in a rat model of Parkinson disease. Proceedings of the National Academy of Sciences *105*, 763-768.

Gousset, K., Schiff, E., Langevin, C., Marijanovic, Z., Caputo, A., Browman, D.T., Chenouard, N., De Chaumont, F., Martino, A., and Enninga, J. (2009). Prions hijack tunnelling nanotubes for intercellular spread. nature cell biology *11*, 328-336.

Gousset, K., and Zurzolo, C. (2009). Tunnelling nanotubes: A highway for prion spreading? Prion *3*, 94-98.

Graham, T.R., and Kozlov, M.M. (2010). Interplay of proteins and lipids in generating membrane curvature. Curr Opin Cell Biol *22*, 430-436.

Grazia Spillantini, M., Anthony Crowther, R., Jakes, R., Cairns, N.J., Lantos, P.L., and Goedert, M. (1998). Filamentous α-synuclein inclusions link multiple system atrophy with Parkinson's disease and dementia with Lewy bodies. Neuroscience Letters *251*, 205-208.

Grey, M., Dunning, C.J., Gaspar, R., Grey, C., Brundin, P., Sparr, E., and Linse, S. (2015). Acceleration of alpha-synuclein aggregation by exosomes. J Biol Chem *290*, 2969-2982.

Guo, J.L., and Lee, V.M.Y. (2014). Cell-to-cell transmission of pathogenic proteins in neurodegenerative diseases. Nat Med *20*, 130-138.

Gupta-Bansal, R., Frederickson, R.C., and Brunden, K.R. (1995). Proteoglycan-mediated inhibition of A beta proteolysis. A potential cause of senile plaque accumulation. J Biol Chem *270*, 18666-18671.

Halliday, G.M., and Stevens, C.H. (2011). Glia: initiators and progressors of pathology in Parkinson's disease. Mov Disord *26*, 6-17.

Hansen, C., Angot, E., Bergstr, xF, m, A.-L., Steiner, J.A., Pieri, L., Paul, G., Outeiro, T.F., Melki, R., *et al.* (2011). α-Synuclein propagates from mouse brain to grafted dopaminergic neurons and seeds aggregation in cultured human cells. The Journal of Clinical Investigation *121*, 715-725.

Hasegawa, T., Konno, M., Baba, T., Sugeno, N., Kikuchi, A., Kobayashi, M., Miura, E., Tanaka, N., Tamai, K., Furukawa, K., *et al.* (2011). The AAA-ATPase VPS4 Regulates Extracellular Secretion and Lysosomal Targeting of alpha-Synuclein. PLoS One *6*, e29460.

Hashimoto, M., Hsu, L.J., Xia, Y., Takeda, A., Sisk, A., Sundsmo, M., and Masliah, E. (1999). Oxidative stress induces amyloid-like aggregate formation of NACP/α-synuclein in vitro. Neuroreport *10*, 717-721.

Hashimoto, M., Kawahara, K., Bar-On, P., Rockenstein, E., Crews, L., and Masliah, E. (2004). The role of α-synuclein assembly and metabolism in the pathogenesis of Lewy body disease. Journal of Molecular Neuroscience *24*, 343-352.

Hinshaw, J.E., and Schmid, S.L. (1995). Dynamin self-assembles into rings suggesting a mechanism for coated vesicle budding. Nature *374*, 190-192.

Holmes, B.B., DeVos, S.L., Kfoury, N., Li, M., Jacks, R., Yanamandra, K., Ouidja, M.O., Brodsky, F.M., Marasa, J., Bagchi, D.P., *et al.* (2013). Heparan sulfate proteoglycans mediate internalization and propagation of specific proteopathic seeds. Proceedings of the National Academy of Sciences *110*, E3138-E3147.

Horonchik, L., Tzaban, S., Ben-Zaken, O., Yedidia, Y., Rouvinski, A., Papy-Garcia, D., Barritault, D., Vlodavsky, I., and Taraboulos, A. (2005). Heparan Sulfate Is a Cellular Receptor for Purified Infectious Prions. Journal of Biological Chemistry *280*, 17062-17067.

Horvath, I., Weise, C.F., Andersson, E.K., Chorell, E., Sellstedt, M., Bengtsson, C., Olofsson, A., Hultgren, S.J., Chapman, M., and Wolf-Watz, M. (2012). Mechanisms of protein oligomerization: inhibitor of functional amyloids templates α-synuclein fibrillation. Journal of the American Chemical Society *134*, 3439-3444.

Hsu, L.J., Sagara, Y., Arroyo, A., Rockenstein, E., Sisk, A., Mallory, M., Wong, J., Takenouchi, T., Hashimoto, M., and Masliah, E. (2000). α-Synuclein promotes mitochondrial deficit and oxidative stress. The American journal of pathology *157*, 401-410.

Iwai, A., Masliah, E., Yoshimoto, M., Ge, N., Flanagan, L., Rohan de Silva, H.A., Kittel, A., and Saitoh, T. The precursor protein of non-Aβ component of Alzheimer's disease amyloid is a presynaptic protein of the central nervous system. Neuron *14*, 467-475.

Jahn, R., and Scheller, R.H. (2006). SNAREs--engines for membrane fusion. Nat Rev Mol Cell Biol *7*, 631-643.

Jao, C.C., Hegde, B.G., Chen, J., Haworth, I.S., and Langen, R. (2008). Structure of membrane-bound α-synuclein from site-directed spin labeling and computational refinement. Proceedings of the National Academy of Sciences *105*, 19666-19671.

Jensen, P.H., Nielsen, M.S., Jakes, R., Dotti, C.G., and Goedert, M. (1998). Binding of α-Synuclein to Brain Vesicles Is Abolished by Familial Parkinson's Disease Mutation. Journal of Biological Chemistry *273*, 26292-26294.

Jiang, Z., de Messieres, M., and Lee, J.C. (2013). Membrane Remodeling by α-Synuclein and Effects on Amyloid Formation. Journal of the American Chemical Society *135*, 15970-15973.

Jo, E., Fuller, N., Rand, R.P., St George-Hyslop, P., and Fraser, P.E. (2002). Defective membrane interactions of familial Parkinson's disease mutant A30P α-synuclein1. Journal of Molecular Biology *315*, 799-807.

Jo, E., McLaurin, J., Yip, C.M., St. George-Hyslop, P., and Fraser, P.E. (2000). α-Synuclein Membrane Interactions and Lipid Specificity. Journal of Biological Chemistry *275*, 34328-34334.

Kahle, P.J., Neumann, M., Ozmen, L., Müller, V., Jacobsen, H., Schindzielorz, A., Okochi, M., Leimer, U., van der Putten, H., and Probst, A. (2000). Subcellular localization of wild-type and Parkinson's disease-associated mutant α-synuclein in human and transgenic mouse brain. The Journal of Neuroscience *20*, 6365-6373.

Kahle, P.J., Neumann, M., Ozmen, L., Müller, V., Odoy, S., Okamoto, N., Jacobsen, H., Iwatsubo, T., Trojanowski, J.Q., and Takahashi, H. (2001). Selective insolubility of α-synuclein in human Lewy body diseases is recapitulated in a transgenic mouse model. The American journal of pathology *159*, 2215-2225.

Kämper, N., Day, P.M., Nowak, T., Selinka, H.-C., Florin, L., Bolscher, J., Hilbig, L., Schiller, J.T., and Sapp, M. (2006). A Membrane-Destabilizing Peptide in Capsid Protein L2 Is Required for Egress of Papillomavirus Genomes from Endosomes. Journal of Virology *80*, 759-768.

Kaplan, I.M., Wadia, J.S., and Dowdy, S.F. (2005). Cationic TAT peptide transduction domain enters cells by macropinocytosis. Journal of Controlled Release *102*, 247-253.

Kordower, J.H., Chu, Y., Hauser, R.A., Freeman, T.B., and Olanow, C.W. (2008a). Lewy body-like pathology in long-term embryonic nigral transplants in Parkinson's disease. Nat Med *14*, 504-506.

Kordower, J.H., Chu, Y., Hauser, R.A., Olanow, C.W., and Freeman, T.B. (2008b). Transplanted dopaminergic neurons develop PD pathologic changes: A second case report. Movement Disorders *23*, 2303-2306.

Kowal, S.L., Dall, T.M., Chakrabarti, R., Storm, M.V., and Jain, A. (2013). The current and projected economic burden of Parkinson's disease in the United States. Mov Disord *28*, 311-318.

Kruger, R., Kuhn, W., Muller, T., Woitalla, D., Graeber, M., Kosel, S., Przuntek, H., Epplen, J.T., Schols, L., and Riess, O. (1998). Ala30Pro mutation in the gene encoding alpha-synuclein in Parkinson's disease. Nat Genet *18*, 106-108.

Kunadt, M., Eckermann, K., Stuendl, A., Gong, J., Russo, B., Strauss, K., Rai, S., Kügler, S., Falomir Lockhart, L., Schwalbe, M., *et al.* (2015). Extracellular vesicle sorting of α-Synuclein is regulated by sumoylation. Acta Neuropathol *129*, 695-713.

Lashuel, H.A., Overk, C.R., Oueslati, A., and Masliah, E. (2013). The many faces of [alpha]-synuclein: from structure and toxicity to therapeutic target. Nat Rev Neurosci *14*, 38-48.

Lee, H.-J., Bae, E.-J., and Lee, S.-J. (2014). Extracellular [alpha]-synuclein[mdash]a novel and crucial factor in Lewy body diseases. Nat Rev Neurol *10*, 92-98.

Lee, H.-J., Suk, J.-E., Bae, E.-J., Lee, J.-H., Paik, S.R., and Lee, S.-J. (2008). Assembly-dependent endocytosis and clearance of extracellular a-synuclein. The International Journal of Biochemistry & Cell Biology *40*, 1835-1849.

Lee, H.J., Patel, S., and Lee, S.J. (2005a). Intravesicular localization and exocytosis of alpha-synuclein and its aggregates. J Neurosci *25*, 6016-6024.

Lee, H.J., Suk, J.E., Patrick, C., Bae, E.J., Cho, J.H., Rho, S., Hwang, D., Masliah, E., and Lee, S.J. (2010). Direct transfer of alpha-synuclein from neuron to astroglia causes inflammatory responses in synucleinopathies. J Biol Chem *285*, 9262-9272.

Lee, J.-H., Hong, C.-S., Lee, S., Yang, J.-E., Park, Y.I., Lee, D., Hyeon, T., Jung, S., and Paik, S.R. (2012). Radiating Amyloid Fibril Formation on the Surface of Lipid Membranes through Unit-Assembly of Oligomeric Species of α-Synuclein. PLoS ONE *7*, e47580.

Lee, M.C., Orci, L., Hamamoto, S., Futai, E., Ravazzola, M., and Schekman, R. (2005b). Sar1p N-terminal helix initiates membrane curvature and completes the fission of a COPII vesicle. Cell *122*, 605-617.

Lee, M.K., Stirling, W., Xu, Y., Xu, X., Qui, D., Mandir, A.S., Dawson, T.M., Copeland, N.G., Jenkins, N.A., and Price, D.L. (2002). Human α-synuclein-harboring familial Parkinson's disease-linked Ala-53→ Thr mutation causes neurodegenerative disease with α-synuclein aggregation in transgenic mice. Proceedings of the National Academy of Sciences *99*, 8968-8973.

Lewis, K.A., Su, Y., Jou, O., Ritchie, C., Foong, C., Hynan, L.S., White, C.L., Thomas, P.J., and Hatanpaa, K.J. (2010a). Abnormal Neurites Containing C-Terminally Truncated α-Synuclein Are Present in Alzheimer's Disease without Conventional Lewy Body Pathology. The American Journal of Pathology *177*, 3037-3050.

Lewis, K.A., Yaeger, A., DeMartino, G.N., and Thomas, P.J. (2010b). Accelerated formation of α-synuclein oligomers by concerted action of the 20S proteasome and familial Parkinson mutations. Journal of Bioenergetics and Biomembranes *42*, 85-95.

Li, J.-Y., Englund, E., Holton, J.L., Soulet, D., Hagell, P., Lees, A.J., Lashley, T., Quinn, N.P., Rehncrona, S., Bjorklund, A., *et al.* (2008). Lewy bodies in grafted neurons in subjects with Parkinson's disease suggest host-to-graft disease propagation. Nat Med *14*, 501-503.

Li, W., West, N., Colla, E., Pletnikova, O., Troncoso, J.C., Marsh, L., Dawson, T.M., Jäkälä, P., Hartmann, T., Price, D.L., *et al.* (2005). Aggregation promoting C-terminal truncation of α-synuclein is a normal cellular process and is enhanced by the familial Parkinson's disease-linked mutations. Proceedings of the National Academy of Sciences of the United States of America *102*, 2162-2167.

Liu, C.W., Corboy, M.J., DeMartino, G.N., and Thomas, P.J. (2003). Endoproteolytic activity of the proteasome. Science *299*, 408-411.

Liu, I.H., Uversky, V.N., Munishkina, L.A., Fink, A.L., Halfter, W., and Cole, G.J. (2005). Agrin binds alpha-synuclein and modulates alpha-synuclein fibrillation. Glycobiology *15*, 1320-1331.

Luk, K.C., Kehm, V., Carroll, J., Zhang, B., O'Brien, P., Trojanowski, J.Q., and Lee, V.M.Y. (2012a). Pathological α-Synuclein Transmission Initiates Parkinson-like Neurodegeneration in Non-transgenic Mice. Science (New York, NY) *338*, 949-953.

Luk, K.C., Kehm, V.M., Zhang, B., O'Brien, P., Trojanowski, J.Q., and Lee, V.M. (2012b). Intracerebral inoculation of pathological alpha-synuclein initiates a rapidly progressive neurodegenerative alpha-synucleinopathy in mice. J Exp Med *209*, 975-986.

Luk, K.C., Kehm, V.M., Zhang, B., O'Brien, P., Trojanowski, J.Q., and Lee, V.M. (2012c). Intracerebral inoculation of pathological α-synuclein initiates a rapidly progressive neurodegenerative α-synucleinopathy in mice. The Journal of experimental medicine *209*, 975-986.

Luk, K.C., Song, C., O'Brien, P., Stieber, A., Branch, J.R., Brunden, K.R., Trojanowski, J.Q., and Lee, V.M. (2009). Exogenous alpha-synuclein fibrils seed the formation of Lewy body-like intracellular inclusions in cultured cells. Proc Natl Acad Sci U S A *106*, 20051-20056.

Maries, E., Dass, B., Collier, T.J., Kordower, J.H., and Steece-Collier, K. (2003). The role of α-synuclein in Parkinson's disease: insights from animal models. Nature Reviews Neuroscience *4*, 727-738.

Maroteaux, L., Campanelli, J.T., and Scheller, R.H. (1988). Synuclein: a neuron-specific protein localized to the nucleus and presynaptic nerve terminal. J Neurosci *8*, 2804-2815.

Masuda-Suzukake, M., Nonaka, T., Hosokawa, M., Oikawa, T., Arai, T., Akiyama, H., Mann, D.M.A., and Hasegawa, M. (2013). Prion-like spreading of pathological α-synuclein in brain, Vol 136.

Masuda, M., Takeda, S., Sone, M., Ohki, T., Mori, H., Kamioka, Y., and Mochizuki, N. (2006). Endophilin BAR domain drives membrane curvature by two newly identified structure-based mechanisms, Vol 25.

Mazzulli, J.R., Xu, Y.-H., Sun, Y., Knight, A.L., McLean, P.J., Caldwell, G.A., Sidransky, E., Grabowski, G.A., and Krainc, D. (2011). Gaucher disease glucocerebrosidase and α-synuclein form a bidirectional pathogenic loop in synucleinopathies. Cell *146*, 37-52.

McMahon, H.T., and Boucrot, E. (2015). Membrane curvature at a glance. Journal of Cell Science *128*, 1065-1070.

Melachroinou, K., Xilouri, M., Emmanouilidou, E., Masgrau, R., Papazafiri, P., Stefanis, L., and Vekrellis, K. (2013). Deregulation of calcium homeostasis mediates secreted alpha-synuclein-induced neurotoxicity. Neurobiol Aging *34*, 2853-2865.

Middleton, E.R., and Rhoades, E. (2010). Effects of curvature and composition on α-synuclein binding to lipid vesicles. Biophysical journal *99*, 2279-2288.

Miners, J.S., Renfrew, R., Swirski, M., and Love, S. (2014). Accumulation of alpha-synuclein in dementia with Lewy bodies is associated with decline in the alpha-synuclein-degrading enzymes kallikrein-6 and calpain-1. Acta Neuropathol Commun *2*, 164.

Mizuno, N., Varkey, J., Kegulian, N.C., Hegde, B.G., Cheng, N., Langen, R., and Steven, A.C. (2012). Remodeling of Lipid Vesicles into Cylindrical Micelles by α-Synuclein in an Extended α-Helical Conformation. Journal of Biological Chemistry *287*, 29301-29311.

Mortiboys, H., Thomas, K.J., Koopman, W.J., Klaffke, S., Abou-Sleiman, P., Olpin, S., Wood, N.W., Willems, P.H., Smeitink, J.A., and Cookson, M.R. (2008). Mitochondrial function and morphology are impaired in parkin-mutant fibroblasts. Annals of neurology *64*, 555-565.

Mougenot, A.L., Nicot, S., Bencsik, A., Morignat, E., Verchere, J., Lakhdar, L., Legastelois, S., and Baron, T. (2012). Prion-like acceleration of a synucleinopathy in a transgenic mouse model. Neurobiol Aging *33*, 2225-2228.

Munch, C., O'Brien, J., and Bertolotti, A. (2011). Prion-like propagation of mutant superoxide dismutase-1 misfolding in neuronal cells. Proc Natl Acad Sci U S A *108*, 3548-3553.

Munishkina, L.A., Phelan, C., Uversky, V.N., and Fink, A.L. (2003). Conformational Behavior and Aggregation of α-Synuclein in Organic Solvents: Modeling the Effects of Membranes†. Biochemistry *42*, 2720-2730.

Murphy, D.D., Rueter, S.M., Trojanowski, J.Q., and Lee, V.M. (2000). Synucleins are developmentally expressed, and alpha-synuclein regulates the size of the presynaptic vesicular pool in primary hippocampal neurons. J Neurosci *20*, 3214-3220.

Narayanan, V., and Scarlata, S. (2001). Membrane binding and self-association of α-synucleins. Biochemistry *40*, 9927-9934.

Nemani, V.M., Lu, W., Berge, V., Nakamura, K., Onoa, B., Lee, M.K., Chaudhry, F.A., Nicoll, R.A., and Edwards, R.H. Increased Expression of α-Synuclein Reduces Neurotransmitter Release by Inhibiting Synaptic Vesicle Reclustering after Endocytosis. Neuron *65*, 66-79.

Nonaka, T., Watanabe, S.T., Iwatsubo, T., and Hasegawa, M. (2010). Seeded Aggregation and Toxicity of α-Synuclein and Tau: CELLULAR MODELS OF NEURODEGENERATIVE DISEASES. Journal of Biological Chemistry *285*, 34885-34898.

Obeso, J.A., Rodriguez-Oroz, M.C., Goetz, C.G., Marin, C., Kordower, J.H., Rodriguez, M., Hirsch, E.C., Farrer, M., Schapira, A.H., and Halliday, G. (2010). Missing pieces in the Parkinson's disease puzzle. Nature medicine *16*, 653-661.

Ouberai, M.M., Wang, J., Swann, M.J., Galvagnion, C., Guilliams, T., Dobson, C.M., and Welland, M.E. (2013). alpha-Synuclein senses lipid packing defects and induces lateral expansion of lipids leading to membrane remodeling. J Biol Chem *288*, 20883-20895.

Pan-Montojo, F., Schwarz, M., Winkler, C., Arnhold, M., O'Sullivan, G.A., Pal, A., Said, J., Marsico, G., Verbavatz, J.M., Rodrigo-Angulo, M., *et al.* (2012). Environmental toxins trigger PD-like progression via increased alpha-synuclein release from enteric neurons in mice. Sci Rep *2*, 898.

Pan, T., Kondo, S., Le, W., and Jankovic, J. (2008). The role of autophagy-lysosome pathway in neurodegeneration associated with Parkinson's disease. Brain *131*, 1969-1978.

Pandey, A.P., Haque, F., Rochet, J.C., and Hovis, J.S. (2011). alpha-Synuclein-induced tubule formation in lipid bilayers. J Phys Chem B *115*, 5886-5893.

Papy-Garcia, D., Christophe, M., Huynh, M.B., Fernando, S., Ludmilla, S., Sepulveda-Diaz, J.E., and Raisman-Vozari, R. (2011). Glycosaminoglycans, protein aggregation and neurodegeneration. Curr Protein Pept Sci *12*, 258-268.

Parkinson, J. (1817). An Essay on the Shaking Palsy. In (London: Whittingham & Rowland).

Perlmutter, J.D., Braun, A.R., and Sachs, J.N. (2009). Curvature dynamics of alpha-synuclein familial Parkinson disease mutants: molecular simulations of the micelle- and bilayer-bound forms. J Biol Chem *284*, 7177-7189.

Peter, B.J., Kent, H.M., Mills, I.G., Vallis, Y., Butler, P.J.G., Evans, P.R., and McMahon, H.T. (2004). BAR Domains as Sensors of Membrane Curvature: The Amphiphysin BAR Structure. Science *303*, 495-499.

Pfefferkorn, C.M., Jiang, Z., and Lee, J.C. (2012). Biophysics of α-synuclein membrane interactions. Biochimica et Biophysica Acta (BBA)-Biomembranes *1818*, 162-171.

Pirc, K., and Ulrih, N.P. (2011). Alpha-Synuclein Interactions with Membranes (INTECH Open Access Publisher).

Porto-Carreiro, I., Fevrier, B., Paquet, S., Vilette, D., and Raposo, G. (2005). Prions and exosomes: from PrPc trafficking to PrPsc propagation. Blood Cells Mol Dis *35*, 143-148.

Praefcke, G.J.K., and McMahon, H.T. (2004). The dynamin superfamily: universal membrane tubulation and fission molecules? Nat Rev Mol Cell Biol *5*, 133-147.

Raiborg, C., and Stenmark, H. (2009). The ESCRT machinery in endosomal sorting of ubiquitylated membrane proteins. Nature *458*, 445-452.

Rajendran, L., Honsho, M., Zahn, T.R., Keller, P., Geiger, K.D., Verkade, P., and Simons, K. (2006). Alzheimer's disease beta-amyloid peptides are released in association with exosomes. Proc Natl Acad Sci U S A *103*, 11172-11177.

Record, M., Subra, C., Silvente-Poirot, S., and Poirot, M. (2011). Exosomes as intercellular signalosomes and pharmacological effectors. Biochemical Pharmacology *81*, 1171-1182.

Reynolds, A.D., Glanzer, J.G., Kadiu, I., Ricardo-Dukelow, M., Chaudhuri, A., Ciborowski, P., Cerny, R., Gelman, B., Thomas, M.P., Mosley, R.L., *et al.* (2008). Nitrated alpha-synuclein-activated microglial profiling for Parkinson's disease. J Neurochem *104*, 1504-1525.

Ritchie, C.M., and Thomas, P.J. (2012). Alpha-synuclein truncation and disease.

Sacino, A.N., Brooks, M., Thomas, M.A., McKinney, A.B., Lee, S., Regenhardt, R.W., McGarvey, N.H., Ayers, J.I., Notterpek, L., Borchelt, D.R., *et al.* (2014). Intramuscular injection of α-synuclein induces CNS α-synuclein pathology and a rapid-onset motor phenotype in transgenic mice. Proceedings of the National Academy of Sciences *111*, 10732-10737.

Salomone, F., Cardarelli, F., Di Luca, M., Boccardi, C., Nifosì, R., Bardi, G., Di Bari, L., Serresi, M., and Beltram, F. (2012). A novel chimeric cell-penetrating peptide with membrane-disruptive properties for efficient endosomal escape. Journal of Controlled Release *163*, 293-303.

Saman, S., Kim, W., Raya, M., Visnick, Y., Miro, S., Saman, S., Jackson, B., McKee, A.C., Alvarez, V.E., Lee, N.C.Y., *et al.* (2012). Exosome-associated Tau Is Secreted in Tauopathy Models and Is Selectively Phosphorylated in Cerebrospinal Fluid in Early Alzheimer Disease. Journal of Biological Chemistry *287*, 3842-3849.

Sarrazin, S., Lamanna, W.C., and Esko, J.D. (2011a). Heparan Sulfate Proteoglycans. Cold Spring Harbor Perspectives in Biology *3*.

Sarrazin, S., Lamanna, W.C., and Esko, J.D. (2011b). Heparan Sulfate Proteoglycans. Cold Spring Harbor Perspectives in Biology *3*, a004952.

Schwartz, A.L. (1995). Receptor cell biology: receptor-mediated endocytosis. Pediatr Res *38*, 835-843.

Seidel, K., Schöls, L., Nuber, S., Petrasch-Parwez, E., Gierga, K., Wszolek, Z., Dickson, D., Gai, W.P., Bornemann, A., and Riess, O. (2010). First appraisal of brain pathology owing to A30P mutant alpha-synuclein. Annals of neurology *67*, 684-689.

Sheetz, M.P., and Singer, S.J. (1974). Biological Membranes as Bilayer Couples. A Molecular Mechanism of Drug-Erythrocyte Interactions. Proceedings of the National Academy of Sciences *71*, 4457-4461.

Shen, Y., Xu, L., and Foster, D.A. (2001). Role for Phospholipase D in Receptor-Mediated Endocytosis. Molecular and Cellular Biology *21*, 595-602.

Shi, M., Liu, C., Cook, T.J., Bullock, K.M., Zhao, Y., Ginghina, C., Li, Y., Aro, P., Dator, R., He, C., *et al.* (2014). Plasma exosomal alpha-synuclein is likely CNS-derived and increased in Parkinson's disease. Acta Neuropathol *128*, 639-650.

Shieh, M.T., WuDunn, D., Montgomery, R.I., Esko, J.D., and Spear, P.G. (1992). Cell surface receptors for herpes simplex virus are heparan sulfate proteoglycans. J Cell Biol *116*, 1273-1281.

Shukla, D., Liu, J., Blaiklock, P., Shworak, N.W., Bai, X., Esko, J.D., Cohen, G.H., Eisenberg, R.J., Rosenberg, R.D., and Spear, P.G. (1999). A novel role for 3-O-sulfated heparan sulfate in herpes simplex virus 1 entry. Cell *99*, 13-22.

Shulman, J.M., De Jager, P.L., and Feany, M.B. (2011). Parkinson's disease: genetics and pathogenesis. Annual Review of Pathology: Mechanisms of Disease *6*, 193-222.

Simons, M., and Raposo, G. (2009). Exosomes--vesicular carriers for intercellular communication. Curr Opin Cell Biol *21*, 575-581.

Small, D.H., Nurcombe, V., Reed, G., Clarris, H., Moir, R., Beyreuther, K., and Masters, C.L. (1994). A heparin-binding domain in the amyloid protein precursor of Alzheimer's disease is involved in the regulation of neurite outgrowth. J Neurosci *14*, 2117-2127.

Souza, J.M., Giasson, B.I., Chen, Q., Lee, V.M.-Y., and Ischiropoulos, H. (2000). Dityrosine Cross-linking Promotes Formation of Stable α-Synuclein Polymers IMPLICATION OF NITRATIVE AND OXIDATIVE STRESS IN THE PATHOGENESIS OF NEURODEGENERATIVE SYNUCLEINOPATHIES. Journal of Biological Chemistry *275*, 18344-18349.

Spillantini, M.G., Crowther, R.A., Jakes, R., Hasegawa, M., and Goedert, M. (1998). α-Synuclein in filamentous inclusions of Lewy bodies from Parkinson's disease and dementia with Lewy bodies. Proceedings of the National Academy of Sciences *95*, 6469-6473.

Spillantini, M.G., Schmidt, M.L., Lee, V.M., Trojanowski, J.Q., Jakes, R., and Goedert, M. (1997). Alpha-synuclein in Lewy bodies. Nature *388*, 839-840.

Stockl, M., Fischer, P., Wanker, E., and Herrmann, A. (2008). Alpha-synuclein selectively binds to anionic phospholipids embedded in liquid-disordered domains. J Mol Biol *375*, 1394-1404.

Sung, J.Y., Kim, J., Paik, S.R., Park, J.H., Ahn, Y.S., and Chung, K.C. (2001). Induction of neuronal cell death by Rab5A-dependent endocytosis of alpha-synuclein. J Biol Chem *276*, 27441-27448.

Taschenberger, G., Garrido, M., Tereshchenko, Y., Bahr, M., Zweckstetter, M., and Kugler, S. (2012). Aggregation of alphaSynuclein promotes progressive in vivo neurotoxicity in adult rat dopaminergic neurons. Acta Neuropathol *123*, 671-683.

Taylor, T.N., Potgieter, D., Anwar, S., Senior, S.L., Janezic, S., Threlfell, S., Ryan, B., Parkkinen, L., Deltheil, T., Cioroch, M., *et al.* (2014). Region-specific deficits in dopamine, but not norepinephrine, signaling in a novel A30P alpha-synuclein BAC transgenic mouse. Neurobiol Dis *62*, 193-207.

Thery, C., Zitvogel, L., and Amigorena, S. (2002). Exosomes: composition, biogenesis and function. Nat Rev Immunol *2*, 569-579.

Tkachenko, E., and Simons, M. (2002). Clustering Induces Redistribution of Syndecan-4 Core Protein into Raft Membrane Domains. Journal of Biological Chemistry *277*, 19946-19951.

Tofaris, G.K., Razzaq, A., Ghetti, B., Lilley, K.S., and Spillantini, M.G. (2003). Ubiquitination of α-synuclein in Lewy bodies is a pathological event not associated with impairment of proteasome function. Journal of Biological Chemistry *278*, 44405-44411.

Tofaris, G.K., Reitböck, P.G., Humby, T., Lambourne, S.L., O'Connell, M., Ghetti, B., Gossage, H., Emson, P.C., Wilkinson, L.S., and Goedert, M. (2006). Pathological changes in dopaminergic nerve cells of the substantia nigra and olfactory bulb in mice transgenic for truncated human α-synuclein (1–120): implications for Lewy body disorders. The Journal of neuroscience *26*, 3942-3950.

Tran, Hien T., Chung, Charlotte H.-Y., Iba, M., Zhang, B., Trojanowski, John Q., Luk, Kelvin C., and Lee, Virginia M.Y. (2014). α-Synuclein Immunotherapy Blocks Uptake and Templated Propagation of Misfolded α-Synuclein and Neurodegeneration. Cell Reports *7*, 2054-2065.

Trexler, A.J., and Rhoades, E. (2009). α-Synuclein Binds Large Unilamellar Vesicles as an Extended Helix†. Biochemistry *48*, 2304-2306.

Tsigelny, I.F., Crews, L., Desplats, P., Shaked, G.M., Sharikov, Y., Mizuno, H., Spencer, B., Rockenstein, E., Trejo, M., Platoshyn, O., *et al.* (2008). Mechanisms of hybrid oligomer formation in the pathogenesis of combined Alzheimer's and Parkinson's diseases. PLoS One *3*, e3135.

Turk, M.J., Reddy, J.A., Chmielewski, J.A., and Low, P.S. (2002). Characterization of a novel pH-sensitive peptide that enhances drug release from folate-targeted liposomes at endosomal pHs. Biochimica et Biophysica Acta (BBA) - Biomembranes *1559*, 56-68.

Tyagi, M., Rusnati, M., Presta, M., and Giacca, M. (2001). Internalization of HIV-1 Tat Requires Cell Surface Heparan Sulfate Proteoglycans. Journal of Biological Chemistry *276*, 3254-3261.

Ulmer, T.S., and Bax, A. (2005). Comparison of structure and dynamics of micelle-bound human α-synuclein and Parkinson disease variants. Journal of Biological Chemistry *280*, 43179-43187.

Ulmer, T.S., Bax, A., Cole, N.B., and Nussbaum, R.L. (2005). Structure and dynamics of micelle-bound human alpha-synuclein. J Biol Chem *280*, 9595-9603.

Uversky, V.N., Li, J., and Fink, A.L. (2001). Metal-triggered Structural Transformations, Aggregation, and Fibrillation of Human α-Synuclein A POSSIBLE MOLECULAR LINK BETWEEN PARKINSON′ S DISEASE AND HEAVY METAL EXPOSURE. Journal of Biological Chemistry *276*, 44284-44296.

van Horssen, J., de Vos, R.A., Steur, E.N., David, G., Wesseling, P., de Waal, R.M., and Verbeek, M.M. (2004). Absence of heparan sulfate proteoglycans in Lewy bodies and Lewy neurites in Parkinson's disease brains. J Alzheimers Dis *6*, 469-474.

van Horssen, J., Wesseling, P., van den Heuvel, L.P., de Waal, R.M., and Verbeek, M.M. (2003). Heparan sulphate proteoglycans in Alzheimer's disease and amyloid-related disorders. Lancet Neurol *2*, 482-492.

Varkey, J., Isas, J.M., Mizuno, N., Jensen, M.B., Bhatia, V.K., Jao, C.C., Petrlova, J., Voss, J.C., Stamou, D.G., and Steven, A.C. (2010a). Membrane curvature induction and tubulation are common features of synucleins and apolipoproteins. Journal of Biological Chemistry *285*, 32486-32493.

Varkey, J., Isas, J.M., Mizuno, N., Jensen, M.B., Bhatia, V.K., Jao, C.C., Petrlova, J., Voss, J.C., Stamou, D.G., Steven, A.C., *et al.* (2010b). Membrane Curvature Induction and Tubulation Are Common Features of Synucleins and Apolipoproteins. Journal of Biological Chemistry *285*, 32486-32493.

Varkey, J., Mizuno, N., Hegde, B.G., Cheng, N., Steven, A.C., and Langen, R. (2013a). α-Synuclein Oligomers with Broken Helical Conformation Form Lipoprotein Nanoparticles. The Journal of Biological Chemistry *288*, 17620-17630.

Varkey, J., Mizuno, N., Hegde, B.G., Cheng, N., Steven, A.C., and Langen, R. (2013b). α-Synuclein Oligomers with Broken Helical Conformation Form Lipoprotein Nanoparticles. Journal of Biological Chemistry *288*, 17620-17630.

Varki A, E.M., Cummings RD, et al. (2009). Discovery and Classification of Glycan-Binding Proteins. In Essentials of Glycobiology, C.R. Varki A, Esko JD, et al., ed. (Cold Spring Harbor (NY): Cold Spring Harbor Laboratory Press).

Volles, M.J., and Lansbury, P.T. (2002). Vesicle Permeabilization by Protofibrillar α-Synuclein Is Sensitive to Parkinson's Disease-Linked Mutations and Occurs by a Pore-like Mechanism†. Biochemistry *41*, 4595-4602.

Volpicelli-Daley, L.A., Luk, K.C., Patel, T.P., Tanik, S.A., Riddle, D.M., Stieber, A., Meaney, D.F., Trojanowski, J.Q., and Lee, V.M. (2011). Exogenous alpha-synuclein fibrils induce Lewy body pathology leading to synaptic dysfunction and neuron death. Neuron *72*, 57-71.

Wakamatsu, M., Ishii, A., Iwata, S., Sakagami, J., Ukai, Y., Ono, M., Kanbe, D., Muramatsu, S.-i., Kobayashi, K., Iwatsubo, T., *et al.* Selective loss of nigral dopamine neurons induced by overexpression of truncated human α-synuclein in mice. Neurobiology of Aging *29*, 574-585.

Warner, R.G., Hundt, C., Weiss, S., and Turnbull, J.E. (2002). Identification of the Heparan Sulfate Binding Sites in the Cellular Prion Protein. Journal of Biological Chemistry *277*, 18421-18430.

Watson, D.J., Lander, A.D., and Selkoe, D.J. (1997). Heparin-binding Properties of the Amyloidogenic Peptides Aβ and Amylin: DEPENDENCE ON AGGREGATION STATE AND INHIBITION BY CONGO RED. Journal of Biological Chemistry *272*, 31617-31624.

Webb, J.L., Ravikumar, B., Atkins, J., Skepper, J.N., and Rubinsztein, D.C. (2003). Alpha-Synuclein is degraded by both autophagy and the proteasome. J Biol Chem *278*, 25009-25013.

Westphal, C.H., and Chandra, S.S. (2013). Monomeric Synucleins Generate Membrane Curvature. Journal of Biological Chemistry *288*, 1829-1840.

Winner, B., Jappelli, R., Maji, S.K., Desplats, P.A., Boyer, L., Aigner, S., Hetzer, C., Loher, T., Vilar, M., Campioni, S., *et al.* (2011). In vivo demonstration that alpha-synuclein oligomers are toxic. Proc Natl Acad Sci U S A *108*, 4194-4199.

Wittrup, A., Zhang, S.H., ten Dam, G.B., van Kuppevelt, T.H., Bengtson, P., Johansson, M., Welch, J., Morgelin, M., and Belting, M. (2009). ScFv antibody-induced translocation of cell-surface heparan sulfate proteoglycan to endocytic vesicles: evidence for heparan sulfate epitope specificity and role of both syndecan and glypican. J Biol Chem *284*, 32959-32967.

Yavich, L., Tanila, H., Vepsalainen, S., and Jakala, P. (2004). Role of alpha-synuclein in presynaptic dopamine recruitment. J Neurosci *24*, 11165-11170.

Yonetani, M., Nonaka, T., Masuda, M., Inukai, Y., Oikawa, T., Hisanaga, S., and Hasegawa, M. (2009). Conversion of wild-type alpha-synuclein into mutant-type fibrils and its propagation in the presence of A30P mutant. J Biol Chem *284*, 7940-7950.

Zhang, W., Wang, T., Pei, Z., Miller, D.S., Wu, X., Block, M.L., Wilson, B., Zhang, W., Zhou, Y., Hong, J.S., *et al.* (2005). Aggregated alpha-synuclein activates microglia: a process leading to disease progression in Parkinson's disease. FASEB J *19*, 533-542.

Zhu, M., and Fink, A.L. (2003). Lipid Binding Inhibits α-Synuclein Fibril Formation. Journal of Biological Chemistry *278*, 16873-16877.

Zimmerberg, J., and Kozlov, M.M. (2006). How proteins produce cellular membrane curvature. Nat Rev Mol Cell Biol *7*, 9-19.

Zimmermann, P., Zhang, Z., Degeest, G., Mortier, E., Leenaerts, I., Coomans, C., Schulz, J., N'Kuli, F., Courtoy, P.J., and David, G. (2005). Syndecan Recyling Is Controlled by Syntenin-PIP2 Interaction and Arf6. Developmental Cell *9*, 377-388.